HIG-74-11

PRESSURE AND TEMPERATURE STUDIES OF GLASS PROPERTIES RELATED TO VIBRATIONAL SPECTRA

By

MURLI H. MANGHNANI

Contract N00014-67-A-0387-0012, NR 032-527

FINAL REPORT

Scientific Officer: Dr. A. M. Diness
Office of Naval Research

DECEMBER 1974

Prepared for

OFFICE OF NAVAL RESEARCH
DEPARTMENT OF THE NAVY (CODE 471)
METALLURGY PROGRAM
800 N. QUINCY STREET
ARLINGTON, VIRGINIA 22217

HAWAII INSTITUTE OF GEOPHYSICS
UNIVERSITY OF HAWAII

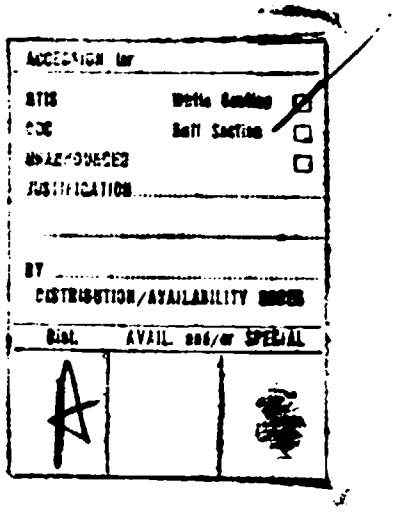
ACCESSION for
NTIS
DDC
UNANNOUNCED
JUSTIFICATION
BY
DISTRIBUTION/AVAILABILITY
Dist.
AVAIL and/or SPECIAL
A

HIG-74-11

PRESSURE AND TEMPERATURE STUDIES OF GLASS PROPERTIES RELATED TO VIBRATIONAL SPECTRA

By

Murli H. Manghnani
Hawaii Institute of Geophysics
University of Hawaii
Honolulu, Hawaii 96822

Contract N00014-67-A-0387-0012, NR-032-527

FINAL REPORT

Period covered: 1 Feb 1971 — 31 Dec 1974

Dec 1974

Contract Monitor: Arthur M. Diness
Office of Naval Research

Prepared for
Office of Naval Research
Department of the Navy (Code 471)
Metallurgy Program
800 N. Quincy Street
Arlington, Virginia 22217

Approved by Director

George D. Woodland

Date: 1 December 1974

TABLE OF CONTENTS

ACKNOWLEDGMENTS

The generous cooperation of Messrs. Given W. Cleek and W. Capps, of the National Bureau of Standards, and of Dr. Peter Schultz, of the Corning Glass Works, in making the glass specimens available for research is gratefully acknowledged.

Appreciation is expressed to Dr. Arthur M. Diness, Office of Naval Research, for stimulating scientific discussions, and for the introduction to glass science.

Participating in the laboratory measurements were: Messrs. Teruyuki Matsui, B.K. Singh, Keith Katahara, C.S. Rai, and J. Balogh. Mr. J. Balogh also expertly maintained the pressure and temperature equipment.

Thanks are due Prof. Robert Doremus and Mr. John Kay at Rensselear Polytechnic Institute, and Dr. J. Ferraro at Argonne National Laboratory, for cooperation in some of the experiments conducted for this research; Mrs. Ethel McAfee for her invaluable help in editing and supervision of this report; Mrs. Rita Pujalet for reprographic help; Miss Kehau Lee for drafting; and Mrs. Jean Taga, for stenographic services.

SECTION I

ULTRASONIC ATTENUATION IN ALKALI SILICATE GLASSES BETWEEN 80 and 300°K

Introduction

The acoustic loss spectra for almost all glasses having tetrahedral structure exhibit very interesting features at low temperatures [1-8]. For instance, a large attenuation peak is observed for fused silica at 48°K. Anderson and Bommel [1] suggested that the observed attenuation in the low temperature region is related to the transverse motion of oxygen atoms in the Si-O-Si bridge. The oxygen atom can assume any of two or more equivalent positions around the straight angle. The displaced oxygen atom requires a small activation energy (1340 cal/mole) to return to its original position, thereby causing ultrasonic loss. Based on the same structural concept but assuming longitudinal rather than transverse motion of the oxygen atom in the Si-O-Si bridge, Strakana [2,3] developed a theory to explain the loss peaks for SiO_2, GeO_2, B_2O_3, and As_2O_3 glasses. Although both of the theories offer a good explanation for acoustic loss they do not explain any of the other anomalous properties of fused silica such as negative thermal expansion, positive temperature derivatives of elastic moduli, negative pressure derivatives of elastic moduli, and excess specific heat. Moreover, neither theory is compatible with the X-ray data on oxygen angle distribution [9]. Recently, Vukcevich [9] has developed a new 'two minima potential' model to explain most

of the anomalous properties of fused silica including anomalous acoustical properties, the model being in agreement with the X-ray data. According to this model, the vitreous network has a tendency to assume certain values of the Si-O-Si angle. These angles are grouped around two crystalline phases, namely α and β phases, separated by a potential barrier. The activation energy required for a rotation from α to β phase is very close to the activation energy calculated for dielectric and acoustic loss. The Vukcevich theory thus offers very good explanation for the relaxation mechanism.

A review of the work on glasses shows that not much attenuation work has been done in alkali silicate glasses at ultrasonic frequencies. The results of ultrasonic attenuation at 30 MHz in M_2O-SiO_2 glasses (where M is lithium, sodium, or potassium) are presented here in the temperature range of 80 to 300°K. Three relaxation mechanisms are possible for alkali silicate glasses--the low temperature structural relaxation involving a small activation energy caused by oxygen atom vibration in the Si-O-Si bridge [1,2], the alkali ion-migration-type relaxation occurring at relatively higher temperature [4,10,11,15], and the relaxation caused by phase transformation near the phase transition temperature, T_g [12,15]. However, in the present temperature range and frequency, only structural relaxation and some part of the alkali-migration is observed.

Experimental Methods

Alkali silicate glasses, synthesized at the National Bureau

of Standards, Washington, D. C., and fused silica (Corning Glass Works code 7940) were used in this study. Table 1 contains the chemical composition of the glasses along with their annealing temperatures. Right circular cylinders of 1.9-cm diameter and $\sim$ 1.2-cm length were cored, and the end faces of these specimens were polished so that they were parallel to within 1 part in 10^4 and flat to $\pm$ 1/2 wavelength of sodium light.

A modified pulse-echo-overlap method developed by Chung et al. [13] was used for measuring ultrasonic attenuation at low temperatures. The block diagram of the experimental setup is shown in Figure 1. This method is essentially a pulse-echo method with a few variations in the velocity measuring technique. In this method, the pulse repetition frequency is divided by 100 or 1000, and the RF pulse generator is triggered at the divided frequency. However, the oscilloscope is triggered externally by the repetition rate generator so that a cycle-for-cycle match of all echoes is observed. Selective intensification of a pair of echoes is effected with a two-channel 'strobe' delay generator contained within the attenuation recorder (Matec model 2470) and with output to the Z-axis of the scope. These strobes simultaneously open two gates within the attenuation recorder so as to select the video forms of the same two echoes from the echo train. Following peak detection, the logarithmic difference of the two echoes is measured and displayed on the X-Y recorder. In practice, attenuation measurements have an accuracy of 1% and a resolution of 0.2 db. The method allows a continuous

Table 1. Chemical composition, density and annealing temperature of the alkali silicate glasses. Also included are data for fused silica (CGW 7940) [1, 3, 8]

Glass	Composition Mole % M_2O	Composition Mole % SiO_2	Density	Annealing Temp. °C
CGW 7940 (fused silica)	0	100	2.207	1020
			Li_2O-SiO_2 Glasses	
K-199	20	80	2.282	
K-154	25	75	2.306	
K-171	28	72	2.322	
K-163	30	70	2.331	
K-162	35	65	2.348	
K-197	35	65	2.349	
			Na_2O - SiO_2 Glasses	
K-110	10	90	2.288	575
K-111	15	85	2.336	540
K-112	20	80	2.383	520
K-113	25	75	2.431	510
K-114	30	70	2.474	495
K-115	35	65	2.495	475
K-116	40	60	2.520	450
			K_2O - SiO_2 Glasses	
K-196	15	85	2.337	
K-194	20	80	2.380	
K-192	25	75	2.422	

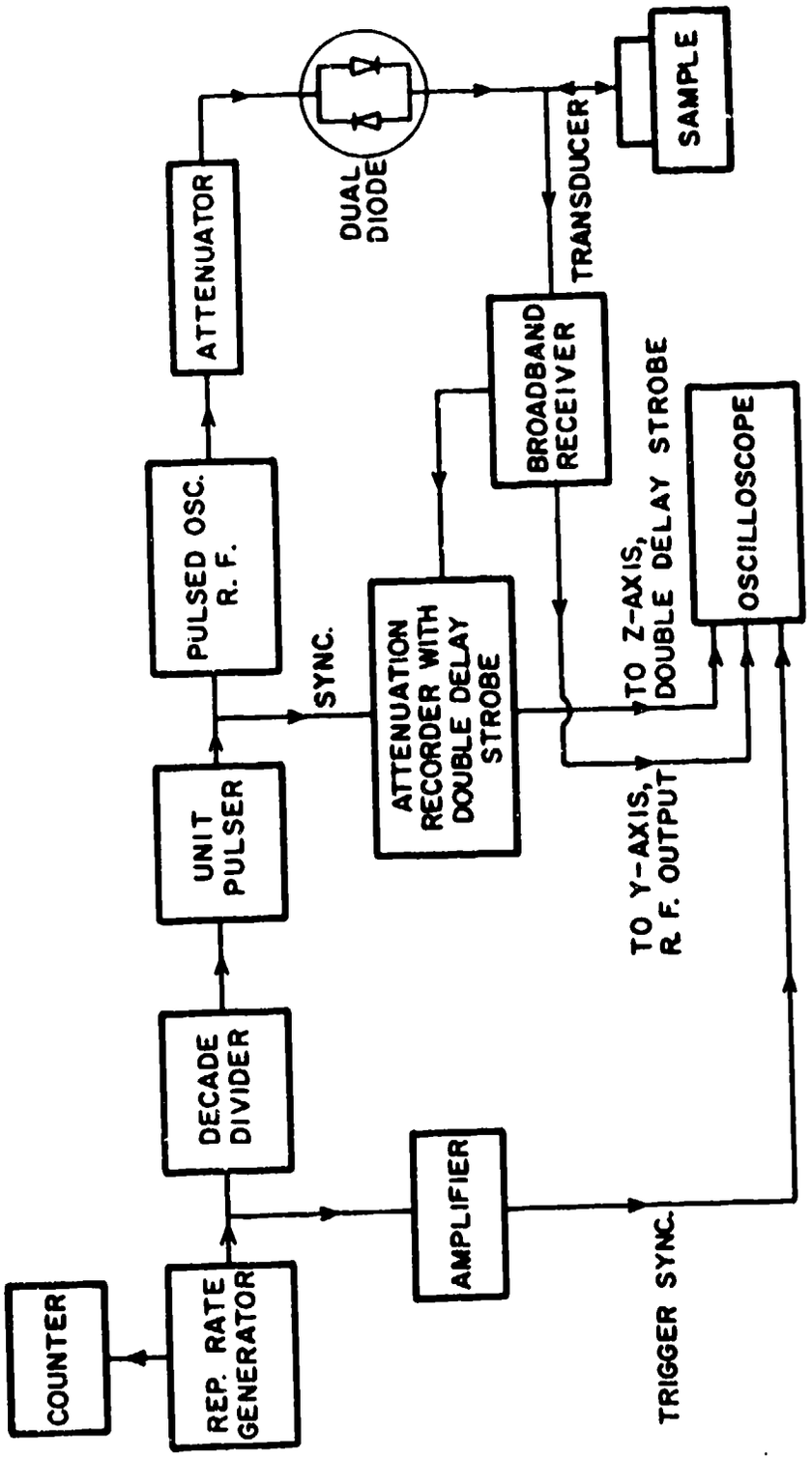

Fig. 1. Electronics setup used in ultrasonic velocity and attenuation measurements (from reference [14]).

monitoring of the attenuation as a function of temperature, and resolving any relaxational phenomena within the absorption spectra.

Twenty MHz, X- and Y-cut, 6-mm diameter, quartz transducers were bonded to the specimen with either Nonaq (Fisher Scientific Co.) or DC 200 silicon fluid (Dow Corning) having viscosity of 12,500 cs.

Results and Discussion

The composition dependence of 30 MHz longitudinal, α_p, and shear attenuation, α_s, was investigated in 17 alkali silicate glasses at room temperature. Of these, seven were Li_2O-SiO_2, seven Na_2O-SiO_2, and three K_2O-SiO_2 glasses. The results of attenuation versus the M_2O content, listed in Table 2 and plotted in Figure 2, show that both the α_p and α_s generally increase with the M_2O content. As compared with the nearly linear composition-dependence of α_p, the α_s varies curvilinearly with composition, the concavity of the curves being toward the composition-axis. Among the glasses studied, the Na_2O-SiO_2 glasses have highest α_p and α_s values. For given M_2O content, α_p value increases in the order of Na > K > Li glasses, whereas the α_s value increases in the order of Na > Li > K glasses (Fig. 2). The best-fit equations relating the linear dependence of α_p and quadratic dependence of α_s to the M_2O content, M, respectively, for the three types of alkali silicate glasses are listed in Table 3.

Table 2. Composition Dependence of 30 MHz Longitudinal and Shear Attenuation in Alkali Silicate Glasses

Glass No.	Composition, Mole %		Attenuation, db/cm		α_s/α_p
	M_2O	SiO_2	Longitudinal (α_p)	Shear (α_s)	
	Li_2O-SiO_2 glasses				
K-199	20	80	3.50	6.97	1.99
K-154	25	75	4.03	7.60	1.89
K-171A	28	72	4.82	8.95	1.86
K-163	30	70	5.11	9.12	1.78
K-170	32	68	5.06	10.18	2.01
K-162	35	65	5.37	11.01	2.05
K-197	35	65	5.36	10.90	2.03
	Na_2O-SiO_2 glasses				
K-110	10	90	2.60	5.40	2.08
K-111	15	85	3.70	7.61	2.06
K-112	20	80	4.31	9.22	2.14
K-113	25	75	5.12	11.95	2.33
K-114	30	70	6.12	14.89	2.43
K-115	35	65	7.05	17.75	2.52
K-116	40	60	7.90	20.21	2.56
	K_2O-SiO_2 glasses				
K-196	15	85	2.51	5.35	2.13
K-194	20	80	3.27	7.09	2.17
K-192	25	75	3.88	8.90	2.29

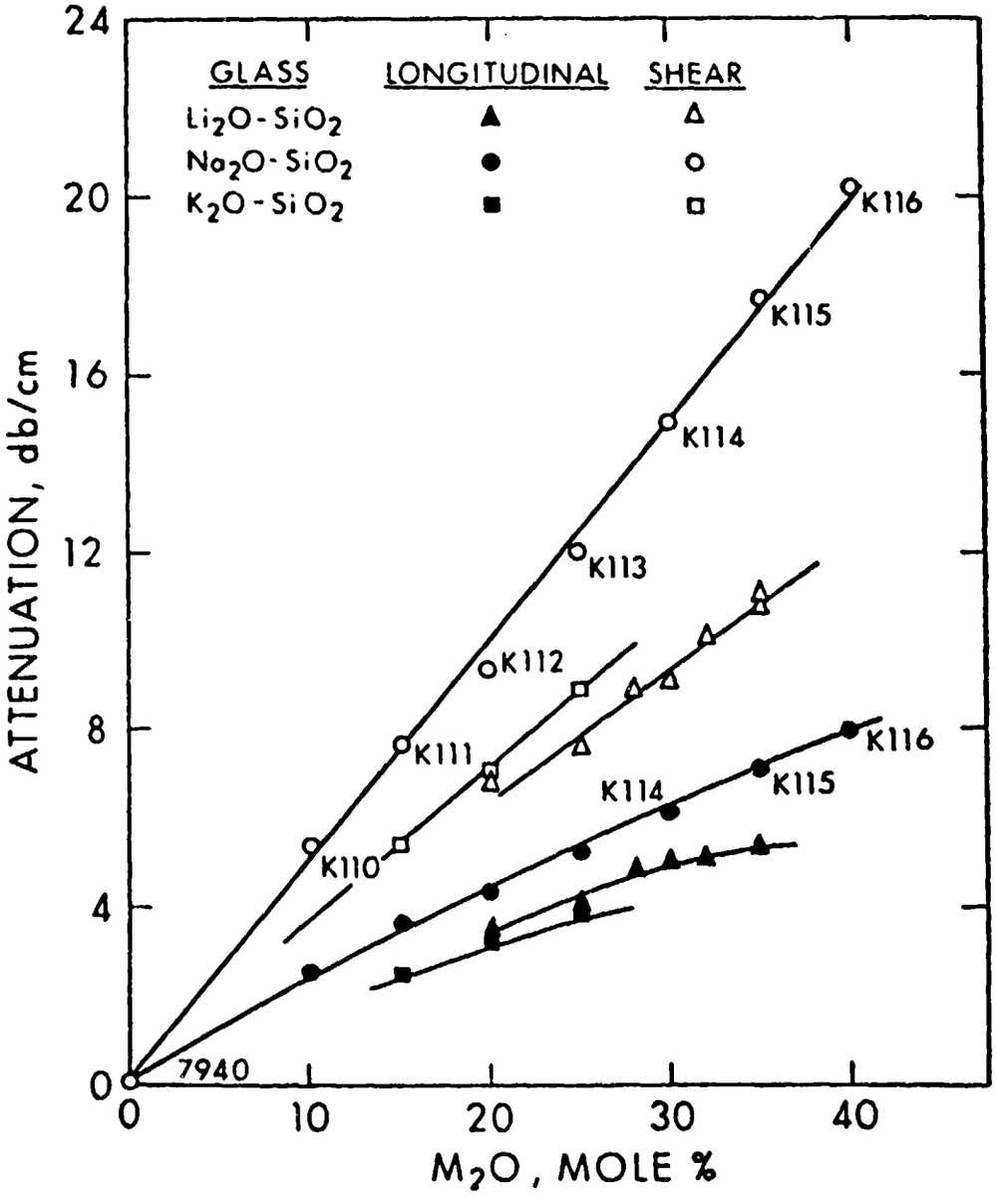

Fig. 2. Composition dependence of ultrasonic attenuation of longitudinal and shear waves in alkali silicate glasses at room temperature.

Table 3. Results of the analyses of data in Table 2, expressed as $\alpha_p = A + BM$ and $\alpha_s = C + DM + EM^2$, where M is mole % M_2O. Units of α_p and α_s coefficients A and C: db/cm; B and D: db/cm mole %; and E: db/cm (mole %)^2

	Best-Fit Values			Best-Fit Values			
Glass Type	A	B	Correlation Coefficient	C	D	E	Standard Deviation
Li_2O-SiO_2	1.040	0.127	0.969	6.350	-0.116	0.0071	0.26
Na_2O-SiO_2	0.898	0.174	0.998	1.845	0.314	0.0038	0.32
K_2O-SiO_2	0.480	0.137	0.998	0.550	0.299	0.0014	0

For the alkali silicate glasses investigated, the ratio α_s/α_p ranges between 2 and 2.6, being $\sim$ 2 for Li_2O-SiO_2 containing 10 mole % Li_2O, slightly decreasing and then increasing with increasing M; for the Na_2O-SiO_2 and K_2O-SiO_2 glasses, the ratio monotonically increases from $\sim$ 2.1 (for 15 mole % K_2O) to $\sim$ 2.6 (for 40 mole % K_2O).

The frequency (f) dependence of α_p was studied in the 10 to 90 MHz range for the 10 alkali silicate glasses in which M_2O content varies from 15 to 40 mole %. Results are given in Table 4. The relationship between α_p and f for the three alkali silicate glasses, containing 25 mole % M_2O, is shown in Figure 3A. Figure 3B is a similar α_p versus f plot for the three types of alkali silicate glasses for which the frequency dependence of α_p was studied in the maximum frequency range.

As can be seen in Figure 3, relationship between α_p and f is linear, within experimental errors, for all the glass compositions studied. By assuming an exponential relationship of α_p to f (as was commonly found), $\alpha_p = kf^{\chi}$, where k and χ are constants, we calculated χ to be $\sim$ 1 (1.00 $\pm$ 0.09) for all the glass compositions. This then excludes any possibility of Akhieser-type phonon-phonon interaction loss, which would have yielded values of $\chi >> 1$. The attenuation α_p was also found to be independent of the power of the ultrasonic generator (within receiver linearity), which shows that the attenuation is not hysteresis-type loss.

The temperature dependence of α_p and α_s at 30 MHz, investigated in the range of 80 to 300°K for seven lithium and three

Table 4. Frequency dependence of longitudinal attenuation (α_p) in alkali silicate glasses; k and x are the best-fit values for the assumed relation $\alpha_p = kf^x$

Glass No. and Composition*	α_p, db/cm at Frequency, MHz						k	x
	10	30	50	70	90	110	db. sec/cm	
Li_2O-SiO_2 glasses								
K-199 (20)	1.30	3.50	6.17	8.60	11.90	14.43	-0.917	1.011
K-154 (25)	1.79	4.03	6.80	10.31			-0.651	0.882
K-163 (30)	1.99	5.11	8.75	12.79			-0.662	0.948
K-162 (35)	2.05	5.37	9.11	12.71			-0.636	0.941
Na_2O-SiO_2 glasses								
K-113 (25)	1.75	5.12	9.07	13.23	16.35		-0.794	1.03
K-115 (35)	2.54	7.05	11.75				-0.546	0.948
K-116 (40)	3.0	7.90	13.2				-0.441	0.914
K_2O-SiO_2 glasses								
K-196 (15)	83	2.51	4.45	6.63	9.53	11.49	-1.207	1.105
K-194 (20)	1.01	3.27	5.72	8.46			-1.087	1.088
K-192 (25)	1.24	3.88	6.63				-0.948	1.041

*M_2O content of glass is given in parentheses.

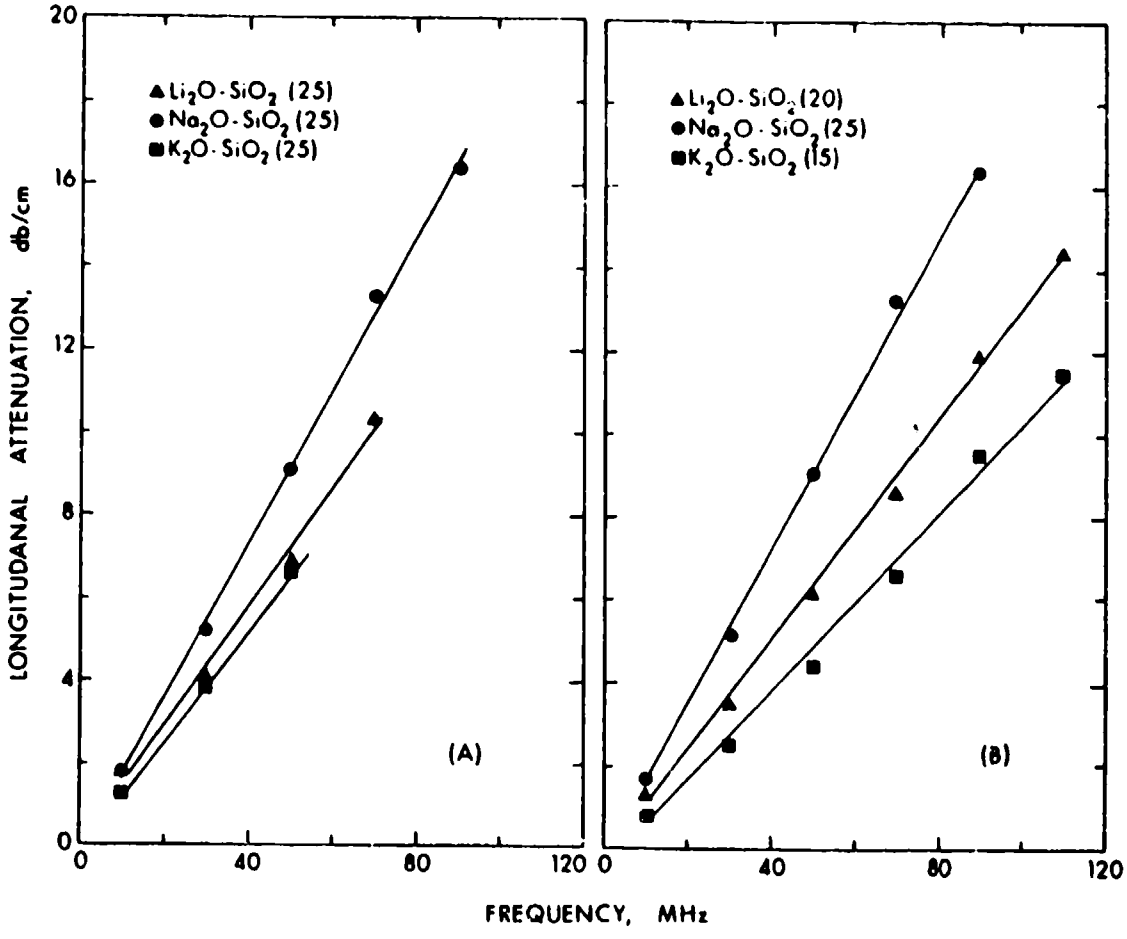

Fig. 3. Frequency dependence of longitudinal wave attenuation in alkali silicate glasses at room temperature.
(A): alkali silicate glasses containing 25 mole % M_2O;
(B): the three types of alkali silicate glasses for which frequency dependence of α_p has been examined in maximum frequency range.

potassium silicate glasses, are presented in Figures 4-7. Similar data for seven sodium silicate glasses were reported in an earlier paper [14] and are reproduced in Figure 8. One of the important findings of the previous study of Na_2O-SiO_2 glasses [14] was the broadening of the low-temperature attenuation peak (observed at $\sim$ 47°K in fused silica) with increasing Na_2O content, which was explained as being caused by either thermal broadening [1], or a wider distribution of activation energies, or superposition of the high-temperature alkali ion relaxation, the latter possibility existing at least for the low-silica glasses. The other important finding was the shift of peak attenuation temperature toward higher temperature with increasing Na_2O content (see Fig. 8). In view of this and the limited temperature range (80 to 300°K) of previous and present studies, the low-temperature attenuation peaks below 80°K could not be observed for the low-alkali glasses. In the study of Na_2O-SiO_2 glasses [14], the attenuation peak above 80°K was observed for only those which contained 20 or higher mole % Na_2O (Fig. 8). In the present study of the lithium silicate glasses, the corresponding low-temperature attenuation peak is not observed for any of the glasses (Fig. 4); the attenuation peaks presumably occur between 47 and 80°K, more so near 47°K, which is outside the temperature range of our study. In Figure 5, showing temperature dependence of α_p for the three potassium silicate glasses, we observe an attenuation peak at $\sim$ 103°K for the K 192 glass which contains 25 mole % K_2O. The temperature dependences of α_s for

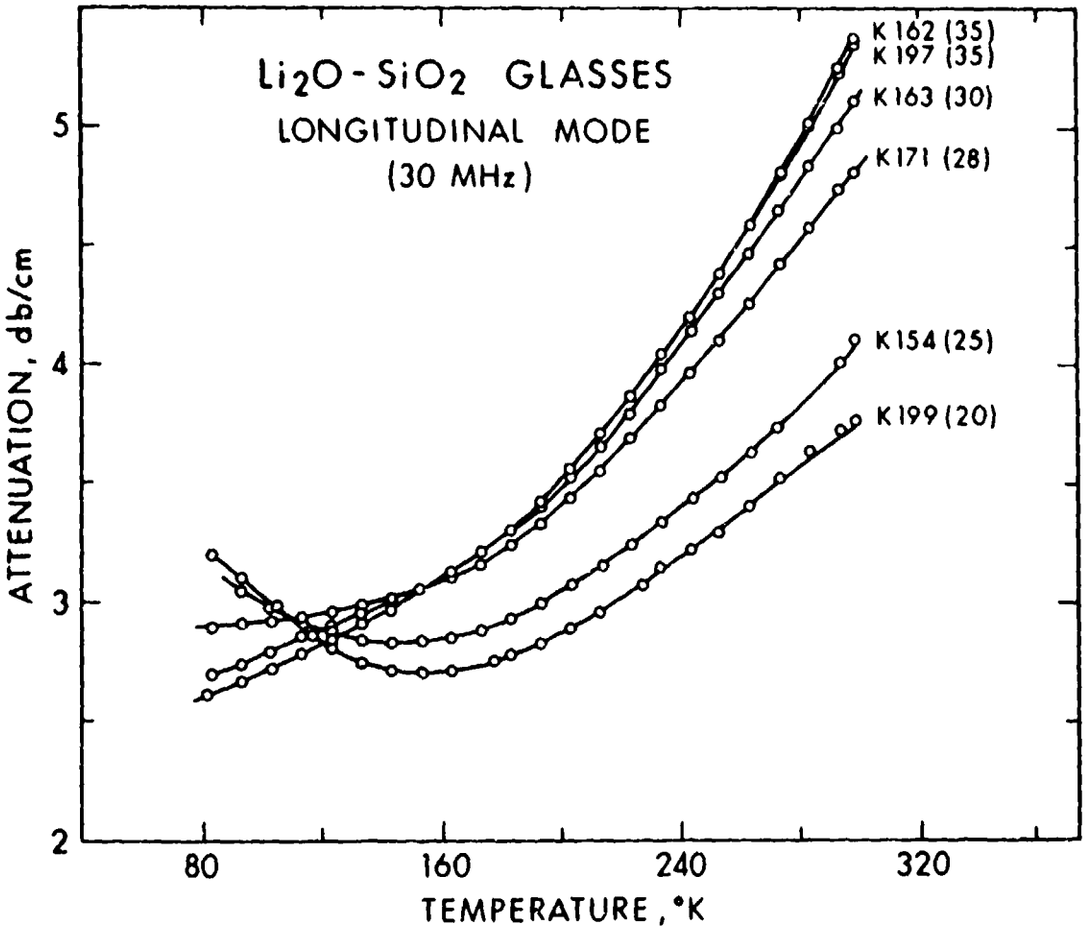

Fig. 4. Temperature dependence of longitudinal wave attenuation in Li_2O-SiO_2 glasses.

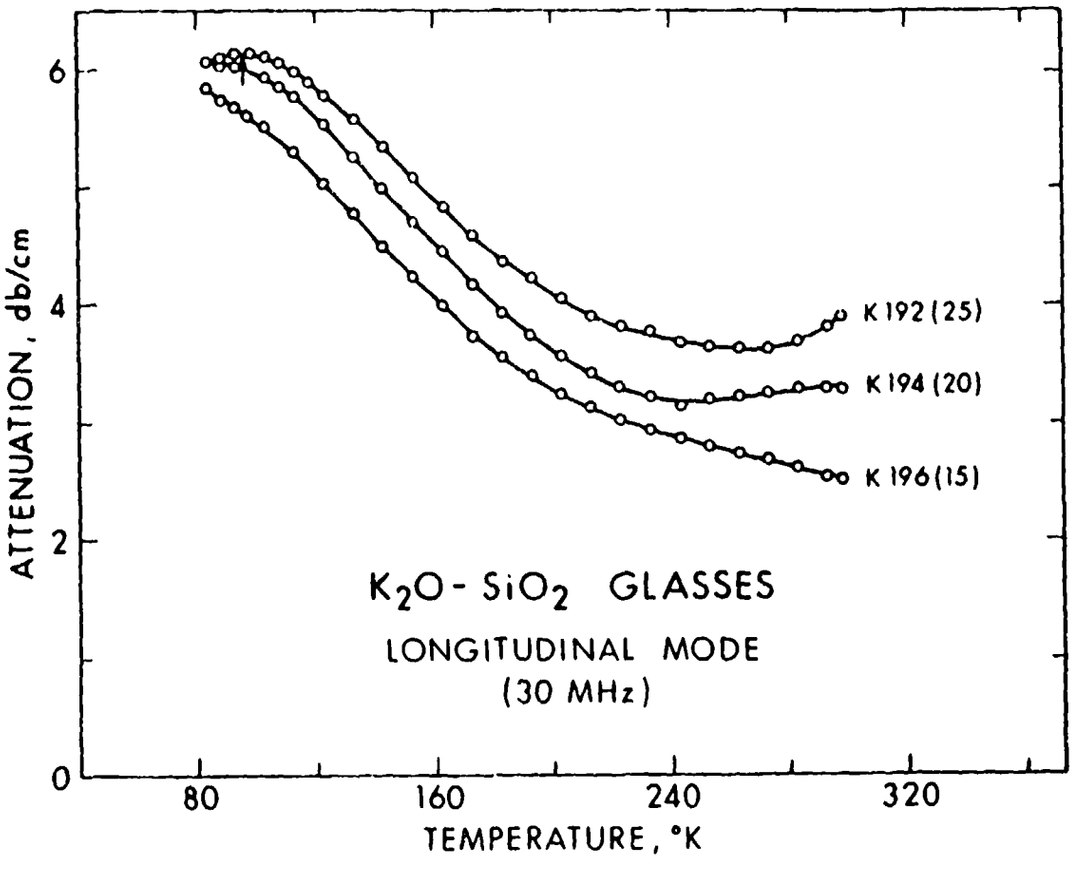

Fig. 5. Temperature dependence of longitudinal wave attenuation in K_2O-SiO_2 glasses.

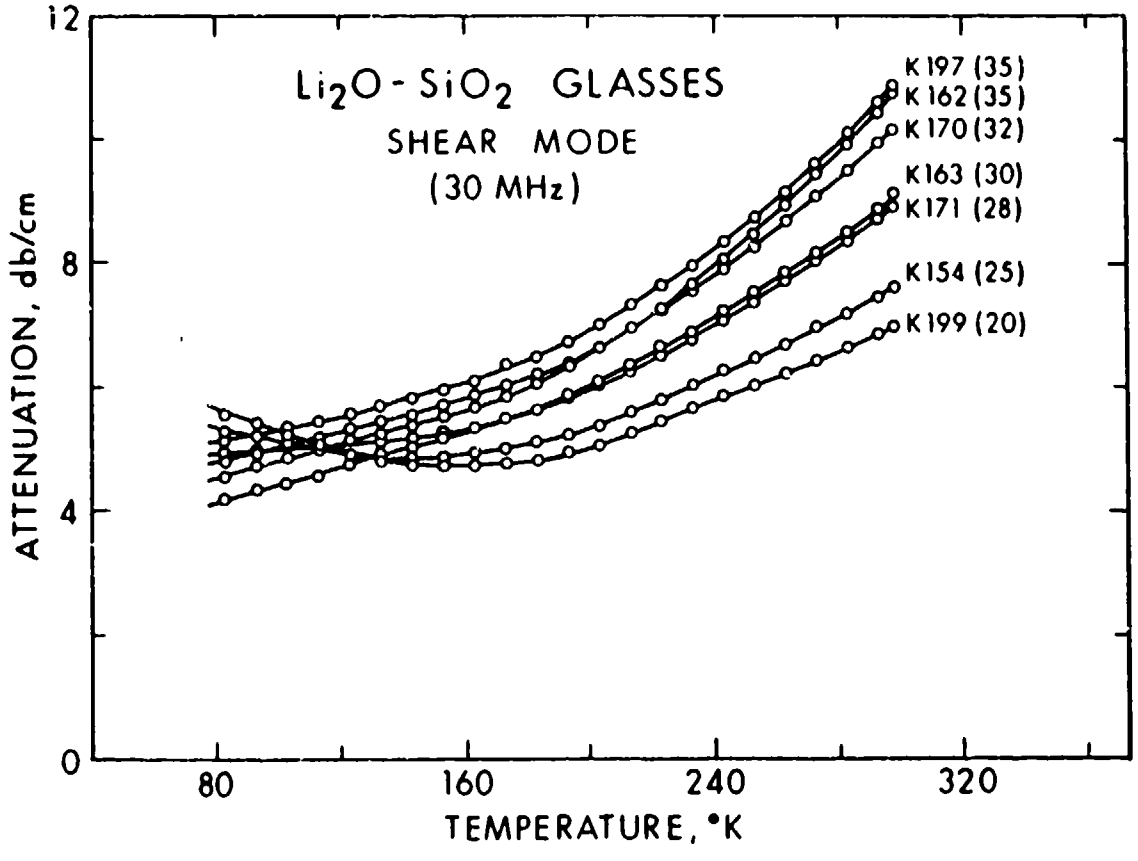

Fig. 6. Temperature dependence of shear wave attenuation in Li_2O-SiO_2 glasses.

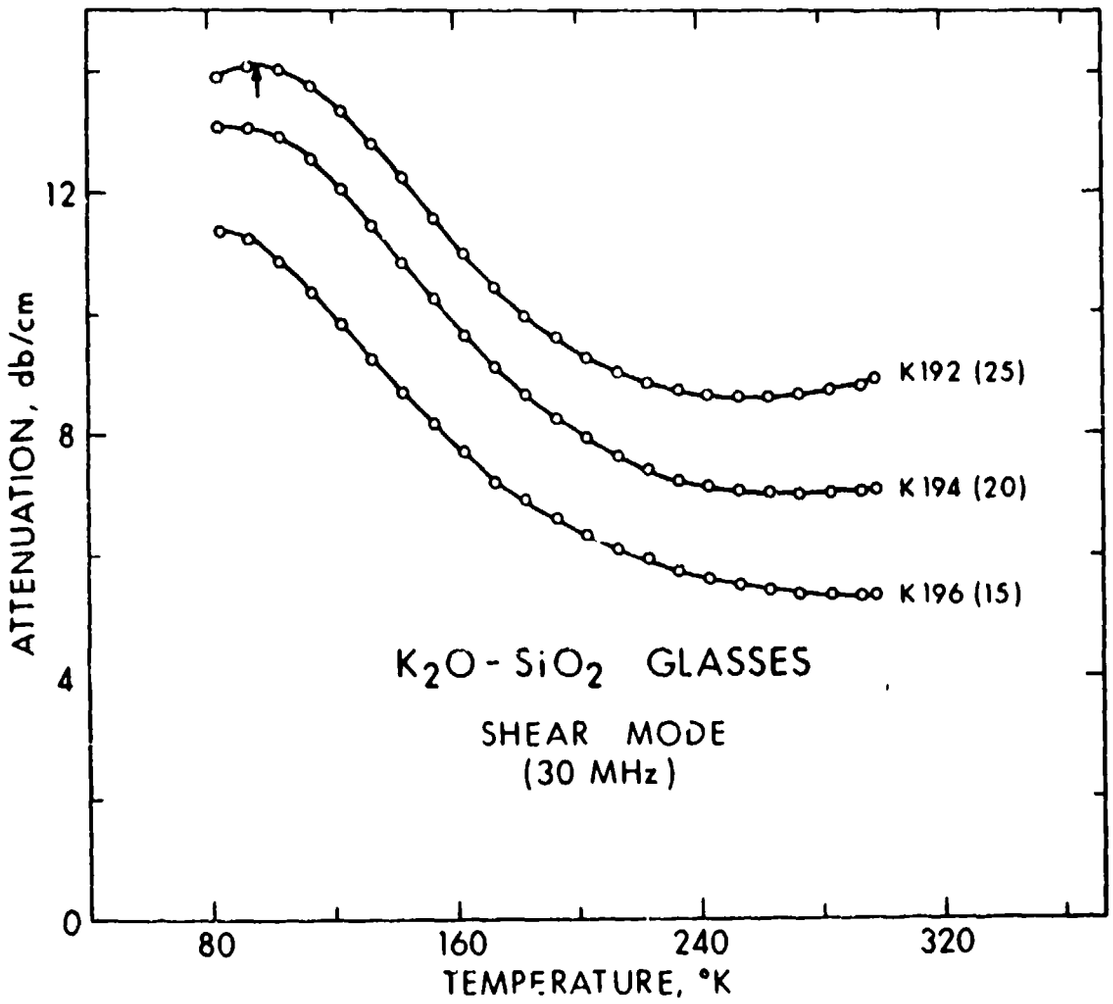

Fig. 7. Temperature dependence of shear wave attenuation in K_2O-SiO_2 glasses.

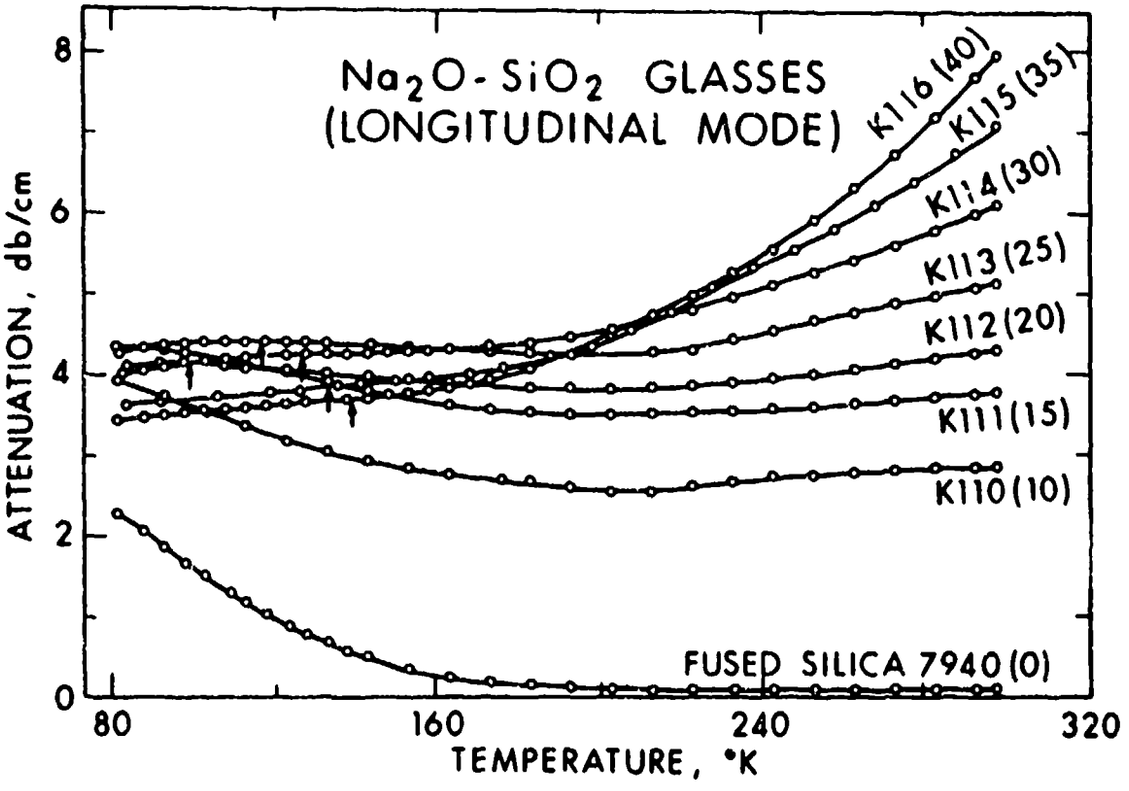

Fig. 8. Temperature dependence of longitudinal wave attenuation for Na_2O-SiO_2 glasses; the values in parentheses denote mole % Na_2O.

those glasses (Figs. 6 and 7) follow the same trends as their temperature dependence of α_p (Figs. 4 and 5). A comparison of the trends in the α_p versus temperature curves for the K_2O-SiO_2 glasses (Fig. 5) indicates that the attenuation peak for the K 194 (20 mole % K_2O) and K 196 (15 mole % K_2O) glasses would be observed at temperatures below 80°K.

In order to examine the low-temperature structural relaxation, it would be of interest to find if the attenuation peak in K_2O-SiO_2 glasses shifts in a trend similar to that in Na_2O-SiO_2 glasses, by extrapolating the attenuation versus temperature curves. Because of the broadening of the peak, there is significant uncertainty in predicting the peak attenuation temperatures in this manner, especially for the low alkali glasses, as was the case for the glasses K 110 and K 111 (Fig. 8) [14]. Nonetheless, an examination of Figures 4 and 6 indicates a strong support for our previous finding that the peak attenuation temperature does shift toward higher temperature with increasing alkali content. This point may be further tested by conducting experiments in the 50 to 80°K range.

In order to examine the low-temperature structural relaxation mechanism present in fused silica and also in alkali silicate glasses, it would be of interest to compute, from the frequency dependence of peak sound attenuation temperature, the most probable activation energies for different alkali concentrations. As attenuation data at different frequencies are not yet available, no attempt can be made to calculate the activation

energies. However, from the shift of the peaks to higher temperatures, it is suggested that in some systematic fashion the activation energy is increasing with increasing alkali content.

Although the high temperature alkali relaxation seems to obscure the low temperature side of the attenuation curve, at least for low-silica glasses, it is clearly indicated by the magnitude of the attenuation curves that the magnitude of the peak attenuation (see Figs. 4, 6 and 8), and thus the relaxation strength, decreases with increasing alkali concentration. However, this behavior is not observed in potassium silicate glasses (Figs. 5 and 7), which could be because of a relatively slower decrease of K ion relaxation strength with temperature. Phenomenologically, the attenuation process can be interpreted on the basis of a structural model in which the alkali molecule modifies the existing Si-O-Si bridge. This modification may result in the formation of a weaker Si-O-M bond or an unbridged Si-O bond. The former type of modification would impede the movement of the oxygen atoms, and since the movement of the oxygen atom is assumed to be the cause of attenuation, this would result in a decrease in attenuation accompanied by an increase in the activation energy. The latter structure would, however, make no contribution to the attenuation α. In other words, loosening of the structure occurs with the addition of alkali ions. This is compatible with the internal friction data at low frequencies [10].

Figure 9 shows the temperature dependence of longitudinal attenuation in the three types of alkali silicate glasses containing 25 mole % M_2O. It appears that the effect of alkali ions on the peak attenuation temperature is increasing in order of Li > K > Na. No comments can be made on the intensity of structural relaxation peak as it is hard to resolve from alkali ion relaxation contribution.

At 30 MHz, one would expect to observe alkali ion relaxation as temperature-dependence of longitudinal and shear attenuation increases with increasing alkali content. The effect of composition on the internal friction at much lower frequencies for Na_2O-SiO_2 system, studied by Forry [10], shows an increase in intensity and decrease in peak temperature as the Na_2O content increases. In light of this and our results (Figs. 4-5 and 9), it may be concluded that the high temperature attenuation peak would shift toward lower temperature, accompanied by a decrease in the activation energy, with increasing alkali content. A similar shift in the high temperature relaxation is also observed for the Na_2O-GeO_2 system [12]. However, because of the limited temperature data, no comparative study on the strength of alkali ion relaxation can be made. It is desirable to investigate further the composition dependence of alkali ion relaxation at high temperatures and low frequencies in the alkali silicate glasses.

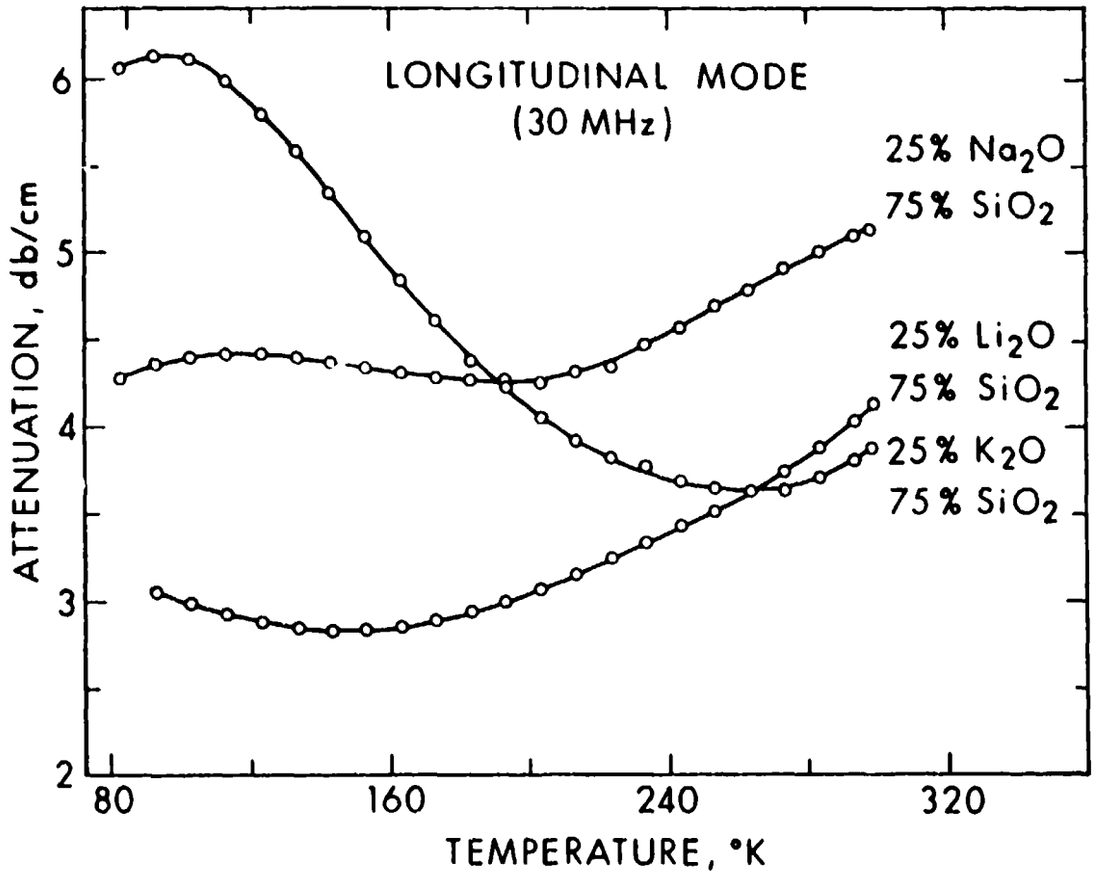

Fig. 9. Temperature dependence of longitudinal wave attenuation for the alkali silicate glasses containing 25 mole % M_2O.

References

[1] O.L. Anderson and H.E. Bommel, J. Amer. Ceram. Soc. 38, 125 (1955).

[2] R.E. Strakna, Phys. Rev. 121, 2020 (1961).

[3] R.E. Strakna and H.T. Savage, J. Appl. Phys. 35, 1445 (1964).

[4] J.W. Marx and J.M. Silversten, J. Appl. Phys. 24, 81 (1953).

[5] M.E. Fine, H. Van Duyne and N.T. Kenny, J. Appl. Phys. 25, 402 (1954).

[6] H.J. McSkimin, J. Appl. Phys. 24, 988 (1953).

[7] J.T. Krause and C.R. Kurkjian, J. Amer. Ceram. Soc. 51, 226 (1968).

[8] J.T. Krause, J. Appl. Phys. 42, 3035 (1971).

[9] M.R. Vukcevich, J. Noncryst. Solids 11, 25 (1972).

[10] K.E. Forry, J. Amer. Ceram. Soc. 40, 90 (1957).

[11] I.L. Hopkins and C.R. Kurkjian, in Physical Acoustics, 2B, edited by W.P. Mason, Academic Press, New York, 91-163 (1965).

[12] C.R. Kurkjian and J.T. Krause, J. Amer. Ceram. Soc. 49, 134 (1966).

[13] D.H. Chung, D.J. Silversmith, and B.B. Chick, Rev. Sci. Instr. 40, 718 (1969).

[14] M.H. Manghnani and B.K. Singh, in Proceed. of the Tenth International Congress on Glass, The Ceramic Society of Japan, Kyoto, 11-104--11-117 (in press).

[15] D.E. Day, Wiss. Ztschr. Friedrich-Schiller-Univ. Jena, Math. Nat. R. 23, 295 (1974).

SECTION II

ELASTICITY OF ALKALI SILICATE GLASSES

The elastic parameters of the 21 glasses in the systems Li_2O-SiO_2, Na_2O-SiO_2, and K_2O-SiO_2 with systematic compositional variation (M_2O content varying from 10 to 55 mole %) have been investigated both at ambient pressure and temperature as well as to 5 kbar and to 300°C. The results are given in Table 1. In a given M_2O-SiO_2 glass system, the elastic properties can be related to the M_2O content or SiO_2/M_2O ratio. The composition-dependence of the moduli is shown in Figures 1 through 3. The Li_2O-SiO_2 glasses behave differently from the Na_2O-SiO_2 and K_2O-SiO_2 glasses in that the addition of M_2O causes an increase in Young's and shear moduli in the former and a decrease in the latter. The bulk modulus, however, increases in all three cases. It appears that Li_2O does not weaken the silica structure, in contrast to the role of Na_2O and K_2O.

Figures 4 and 5 show the relationships between dK/dP, dμ/dT, dK/dT, and composition. The present results confirm the earlier findings that the anomalous behavior of silica-based glasses (decrease of moduli with pressure) can be quantitatively related to the SiO_2 content. Figure 6 shows a relationship between (d ℓn μ/dP) versus Poisson's for the alkali silicate glasses, which compares well with the other tetrahedrally coordinated glasses like SiO_2, GeO_2, and BeF_2 [1].

Table 1 Elastic parameters of the alkali silicate glasses at ambient conditions, and their pressure and temperature derivatives

Glass #	Composition (mole %) M_2O	SiO_2	ρ (gm/cm^3)	V_p (km/sec)	V_s (km/sec)	K (kb)	μ (kb)	E (kb)	σ	β (Mb^{-1})	$(\frac{dK}{dP})^{\dagger}$	$(\frac{d\mu}{dP})^{\dagger}$	$(\frac{dK}{dT})^{\dagger\dagger}$ (kb/deg)	$(\frac{d\mu}{dT})^{\dagger\dagger}$ (kb/deg)
						Li_2O-SiO_2 Glasses								
K199	20.0	80.0	2.282	6.033	3.724	408.8	316.4	754.5	.192	2.44	3.61	-1.20	.018 (0.015)	.034 (-0.038)
K154	25.0	75.0	2.306	6.105	3.727	432.2	320.3	770.6	.203	2.31	1.39	-0.640	-.051 (-0.055)	-.084 (-0.091)
K171A	28.0	72.0	2.322	6.149	3.722	449.2	321.6	778.9	.211	2.23	2.94	-0.194	.014 (0.005)	-.129 (-0.132)
K171B	28.0	72.0	2.322	6.149	3.720	449.6	321.3	778.5	.211	2.22	3.59	-0.143	- 052 (-0.065)	-.079 (-0.079)
K198	28.0	72.0	2.322	6.153	3.720	450.4	321.4	778.9	.212	2.22	3.42	-0.173	-.043 (-0.058)	-.084 (-0.083)
K163	30.0	70.0	2.331	6.176	3.715	460.2	321.8	782.9	.216	2.17	3.22	3.183	-.067 (-0.094	-.089 (-0.097)
K170	32.0	68.0	2.341	6.224	3.706	478.1	321.5	788.0	.225	2.09	3.96	3.384	- 113 (-0.120)	-.102 (-0.106
K162	35.0	65.0	2.348	6.302	3.708	497.6	326.4	803.4	231	2.01	4.82	3.523	-.076 (-0.101)	- 112 (-0.120)
K197	35.0	65.0	2.349	6.294	3.736	493.4	327.9	805.3	.228	2.03	5 84	3.551	- 136 (-0.149)	- 112 (-0.117)
						Na_2O-SiO_2 Glasses								
K110	10.0	90.0	2.288	5.565	3.478	339.5	276.8	652.9	.180	2.94	-2.16	-1 93	.063 (.063)	.004 (.004)
K111	15.0	85.0	2.336	5.457	3.355	345.1	262.9	629.0	.196	2.90	-0.22	-1.15	.030 (030)	- 021 -0.021
K112	20.0	80.0	2.383	5.382	3.251	354.6	251.8	610.8	.213	2.82	1.55	-0.46	-.017 (-0.017)	-.041 (-0.041)
K113	25.0	75.0	2.431	5.347	3.159	371.6	242.6	597.7	.232	2.69	3.18	3.06	-.060 (-0.060)	-.058 (-0.058)
K114	30.0	70.0	2.474	5.348	3.101	390.3	238.0	593.3	.247	2.56	4.11	3.39	- 097 (-0.098)	-.077 (-0.076)
K115	35.0	65.0	2.495	5.361	3.038	410.2	230.2	581.8	.264	2.43	4.91	3.67	-.122 (-0.133)	-.107 (-0.106)
K116	40.0	60.0	2.520	5.401	2.993	434.1	225.8	577.3	.278	2.30	5.83	3.84	-.182 (-0.182)	-.108 (-0.108)
						K_2O-SiO_2 Glasses								
K196	15.0	85.0	2.337	5.065	3.042	311.3	216.2	526.7	.218	3.22	1.41	-0.882	.041 (0.039)	-.005 (-0.004)
K194	20.0	80.0	2.380	4.935	2.881	316.2	197.5	490.4	.242	3.16	3.35	-0.247	.006 (0.006)	-.019 (-0.019)
K192	25.0	75.0	2.422	4.846	2.759	323.1	184.3	464.5	.260	3.10	4.13	-0.195	-.024 (-0.026)	-.034 (-0.034)

ρ = density; V_p = compressional wave velocity; V_s = shear wave velocity; K = bulk modulus; μ = shear modulus; E = Young's modulus; σ = Poisson's ratio; β = compressibility.

†: Values determined at 25°C.

††: Values shown were determined in the 25-100°C interval; values shown in parentheses were determined in the 25-200°C interval.

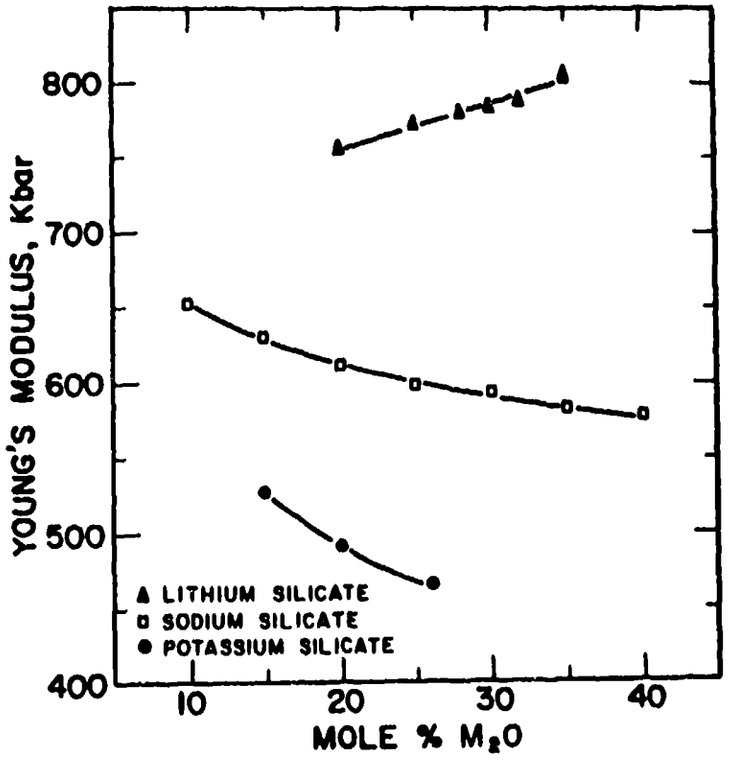

Fig. 1. Young's modulus versus mole % M_2O in alkali silicate glasses.

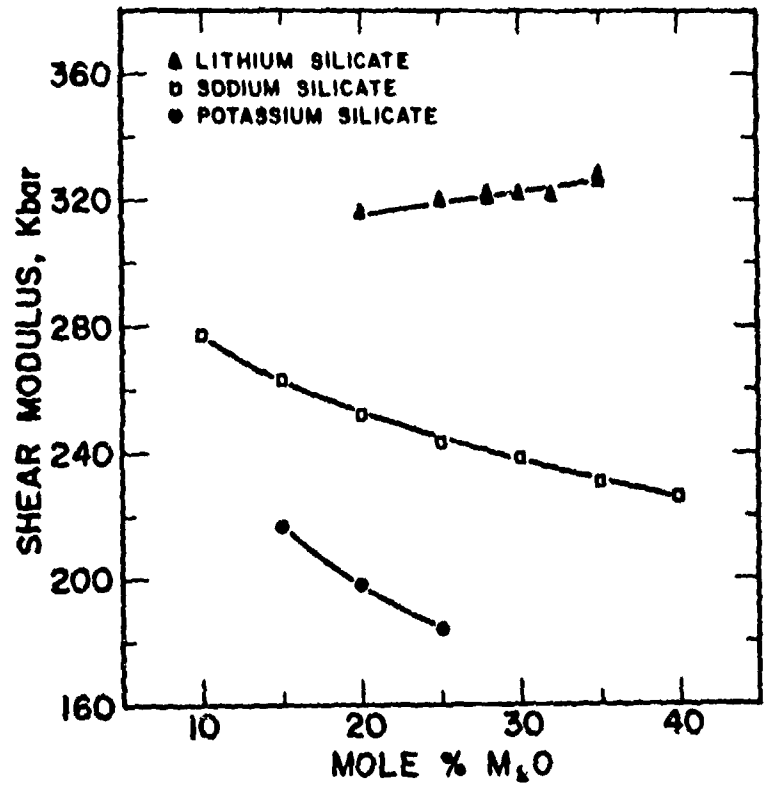

Fig. 2. Shear modulus versus mole % M_2O in alkali silicate glasses.

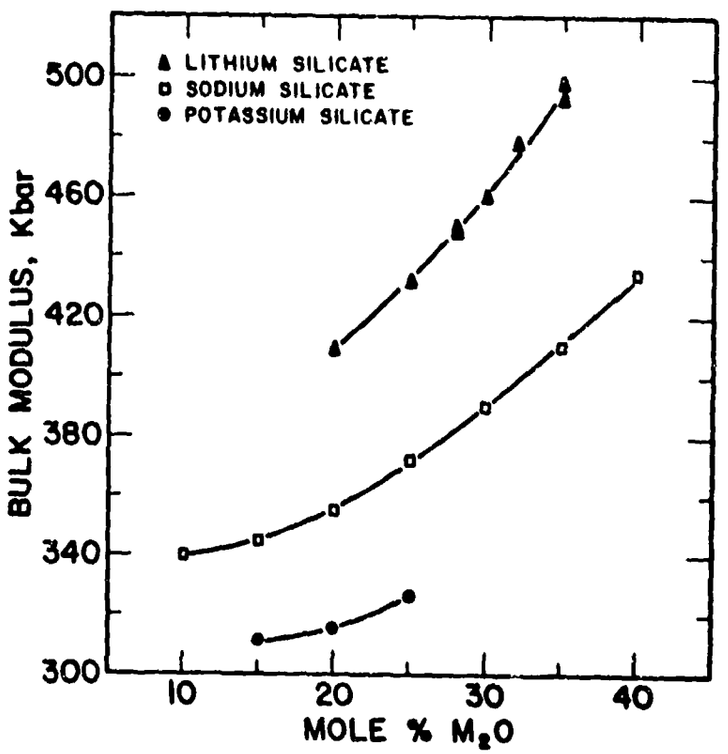

Fig. 3. Bulk modulus versus mole % M_2O in alkali silicate glasses.

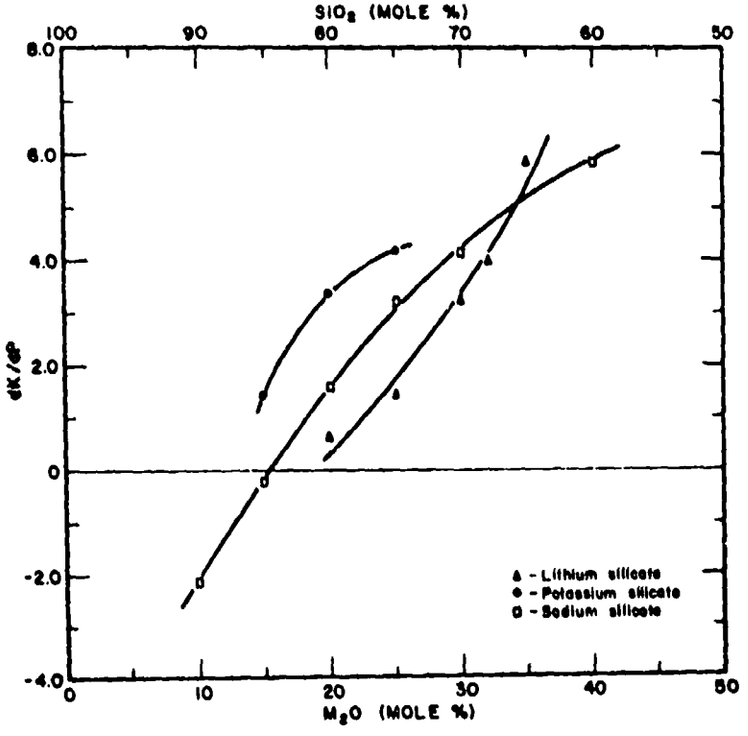

Fig. 4. dK/dP versus mole % M_2O in several M_2O-SiO_2 glasses.

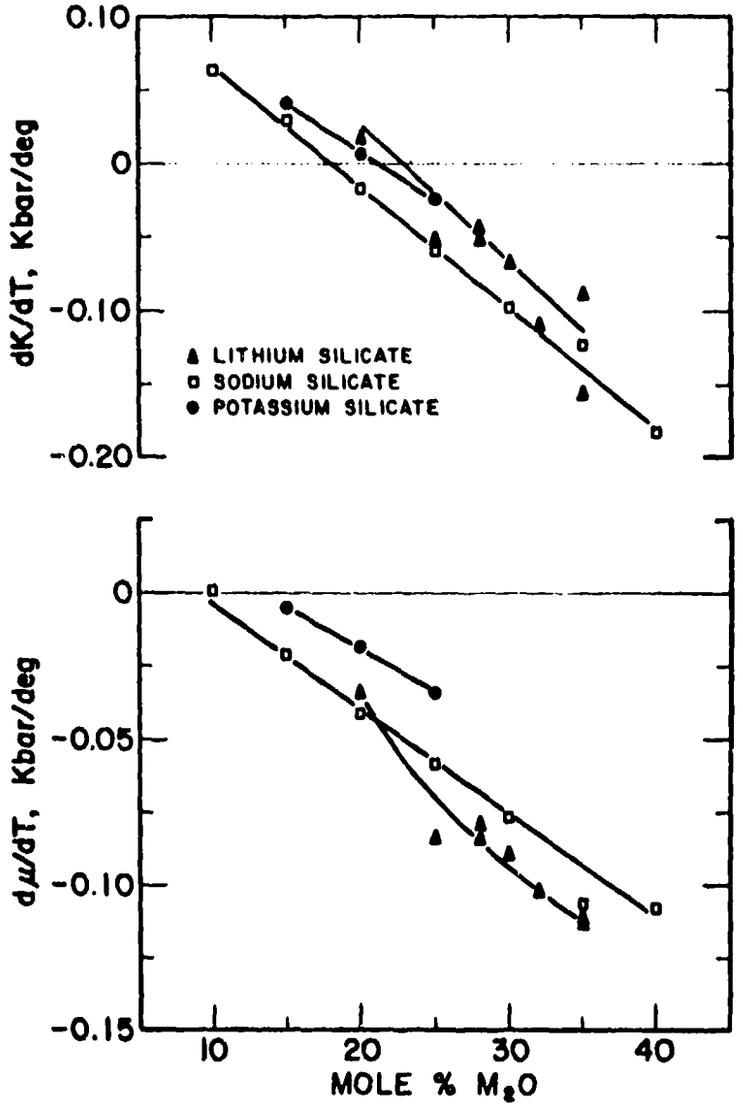

Fig. 5. dK/dT and dμ/dT versus mole % M_2O in several M_2O-SiO_2 glasses.

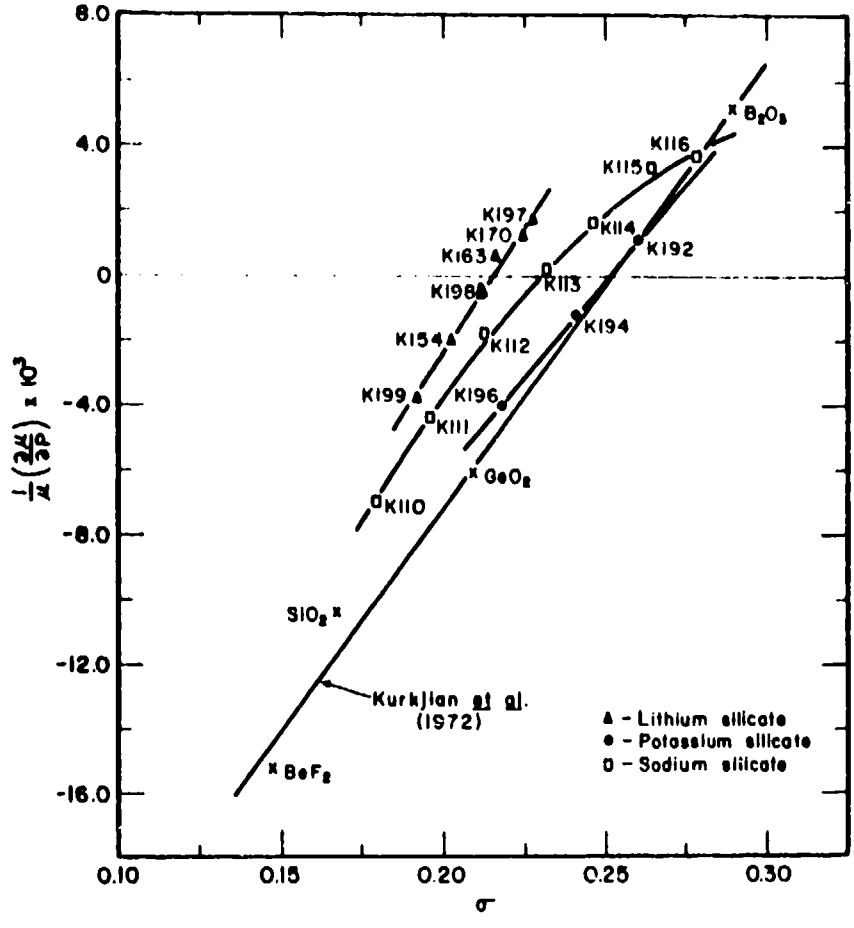

Fig. 6. $\frac{1}{\mu}\left(\frac{\partial \mu}{\partial P}\right)_T$ versus Poisson's ratio in several M_2O-SiO_2 glasses. The linear relationship for BeF_2, SiO_2, GeO_2, and B_2O_3, taken from Kurkjian et al. (1972), is shown here for comparison.

Reference

[1] C.R. Kurkjian, J.T. Krause, H.J. McSkimin, P. Andreatch, and T.B. Bateman, in Amorphous Materials, edited by R.W. Douglas and B. Ellis, John Wiley and Sons, 463 (1972).

SECTION III

THERMAL EXPANSIVITY OF ALKALI SILICATE GLASSES BETWEEN 25 AND 300°C

Introduction

A solid expands on heating because the atomic configuration corresponding to minimum free energy changes with temperature. Contributions to the free energy and hence to the thermal expansion of silicate glasses arise mostly from the kinetic energy of lattice vibrations and to a significantly lesser degree from potential energy of the atoms in the lattice.

It has been shown [1-3] that those vibrations in a network for which volume dependence of vibrational frequency ($d\omega/dV$) is negative make a negative contribution to thermal expansion. In silica structures such a negative contribution arises from the low frequency transverse of oxygen atoms between pairs of tetrahedrally coordinated atoms [4,5]; such vibrations are relatively more easily excited at low temperatures [6].

Smyth [5] has pointed out that ideally transverse vibration of oxygen atoms would be freest if the Si-O-Si angle were 180°. In fused silica this angle is around 148° but the transverse oxygen vibrations still contribute to the negative thermal expansion at low temperatures. At room temperature and above, fused silica has a small positive coefficient of thermal expansion, which indicates that these transverse modes are operative at room temperature and are, to some extent,

contributing negatively to the thermal expansion. Investigation of the thermal expansivity of alkali silicate glasses should provide a better understanding of the role of the transverse vibrational modes in the glass properties.

Additions of alkali oxide (M_2O) to silica results in network-filling, breaking of the Si-O-Si bonds and formation of weaker Si-O-M bonds, and modification of the Si-O-Si angles. The strength of the binding forces between M^+ and O^{2-} ions, and the polarizability of O^{2-} ions will also vary with M_2O content. Previous studies of the thermal expansion properties of alkali silicate glasses [7-10] show that the expansivity depends on the type and amount of M_2O present.

The purpose of this research is to systematically investigate the effects of composition as well as temperature on the thermal expansion properties of binary M_2O-SiO_2 glasses, where M is Li, Na, and K, and to interpret the results in terms of structural changes and the variations in restoring forces between metal and oxygen ions, and the polarizability of O^{2-} ions.

Experimental Methods

The Fizeau interferometer method [11,12] was used to measure linear thermal expansivity of 22 alkali silicate glasses (which included eight Li_2O-SiO_2, eight Na_2O-SiO_2, and six K_2O-SiO_2 glasses; see Table 1) as a function of temperature in the range of 25 to 300°C. The furnace assembly,

Table 1. Chemical composition, the temperature dependence of linear thermal expansion of alkali silicate glasses, expressed as $\alpha_\ell(T) = A_o + A_1 T + A_2 T^2$, and the calculated α_ℓ values at 25°C. Units: α_ℓ in 10^{-6}/°C; A_o in 10^{-4}/°C; A_1 in 10^{-6}/$(°C)^2$; A_2 in 10^{-8}/$(°C)^3$

Glass No.	Composition, Mole% SiO_2	Composition, Mole% M_2O	A_o	A_1	A_2	α_ℓ (25°C)
			Li_2O-SiO_2 Glasses			
K-199	80	20	-1.3293	5.202	0.46062	5.43
K-154	75	25	-1.6713	6.569	0.46248	6.80
K-171	72	28	-1.9034	7.458	0.62239	7.77
K-198	72	28	-1.8254	7.133	0.57322	7.47
K-163	70	30	-1.9721	7.720	0.67216	8.06
K-170	68	32	-2.1431	8.396	0.70609	8.75
K-162	65	35	-2.1546	8.432	0.74706	8.81
K-197	65	35	-2.2377	8.737	0.85621	9.17
			Na_2O-SiO_2 Glasses			
K-110	90	10	-1.0586	4.193	0.16548	4.12
K-111	85	15	-1.7975	7.149	0.16474	7.23
K-112	80	20	-2.3707	9.421	0.24623	9.67
K-113	75	25	-2.667	10.509	0.63500	10.83
K-114	70	30	-2.9657	11.666	0.78764	12.06
K-115	65	35	-3.4432	13.576	0.78685	13.97
K-116	60	40	-3.5612	14.193	0.89775	14.64
K-117	55	45	-3.9575	15.522	0.98450	16.01
			K_2O-SiO_2 Glasses			
K-196	85	15	-2.1892	8.727	0.12064	8.79
K-194	80	20	-2.7581	10.928	0.41740	11.14
K-192	75	25	-3.3162	13.150	0.48740	13.39
K-191	70	30	-3.9197	15.557	0.48657	15.80
K-189	65	35	-4.2321	16.766	0.64989	17.09
K-187-1	60	40	-4.6186	18.270	0.81867	18.68

interferometer, the photoelectric fringe detector, and viewing apparatus, manufactured by the Gaertner Scientific Company, were used in the experiments.

Test Specimens. The same alkali silicate glasses employed in the attenuation study (Section I of this report) were used. The test specimens were prepared by coring out three 6-mm-diameter, 10-mm-long cylinders from each glass; these were flat-ended at one end and coned at the other (at 45°). Both ends were then polished with 1-micron diamond compound optically flat to (1/4)λ of green mercury light. The difference in length of the three specimens was between 0.01 and 0.02 mm, which resulted in formation of 7 to 10 fringes.

Temperature Cycles. Temperature of test specimens during the heating cycle was continuously increased every 8 to 10 minutes at an approximate rate of 50°/hour. The fringe count and temperature were continuously monitored with a strip-chart recorder and a precision potentiometer. The initial temperature (T_o) was taken as 25°C.

During the cooling cycle, the temperature of the specimens decreased at a slower rate--30°C/hour. The initial temperature (T_o) in the cooling cycle was chosen as 300°C.

Theory of Interferometer Method. The method involves observing passage of Fizeau fringes, formed by interference of light beams reflected from two almost parallel glass surfaces separated by a distance. The condition for destructive

interference is $N\lambda_v = 2nd$, where N is an integer, λ_v is the wavelength of light in vacuum, n is the optical index of medium, and d is the optical distance between the two surfaces. For constructive interference the condition is $(N + 1)\lambda = 2nd$. The number of fringes crossing the field of view will depend upon optical path, that is, on the initial length and the expansivity of material under investigation. If the initial length of the test specimen and the optical index of the air at temperature T_o are L_o and n_o, respectively, we have

$$N_o = \frac{2n_o L_o}{\lambda_v} \quad . \tag{1}$$

In the present case we used the green mercury light, for which $\lambda_v = 5.461 \times 10^{-5}$ cm. Similarly, at a higher given temperature T_1, we have

$$N_1 = \frac{2}{\lambda_v} (n_o + \Delta n)\ (L_o + \Delta L) \tag{2}$$

where Δn and ΔL are the changes in n and L, respectively. In the Fizeau interferometer method used here, the fringe count $m = (N_1 - N_o)$ and is related to ΔL as:

$$m \approx \frac{2n_o \Delta L + 2L_o \Delta n}{\lambda_v} \quad . \tag{3}$$

Therefore, the coefficient of linear thermal expansion (α_ℓ) is:

$$\alpha_\ell = \frac{\Delta L}{L_o \Delta T} = \frac{m\lambda_v}{2L_o n_o \Delta T} - \frac{\Delta n}{n_o \Delta T} \qquad (4)$$

where $\Delta T = T_1 - T_o$.

Calculation of α_ℓ

The number of fringes varies as a function of temperature and can be expressed at reference temperature T_1 and initial temperature T_o as follows:

$$N_1 = a + a_1 T_1 + a_2 T_1^2 \qquad (5A)$$

and $$N_o = a + a_1 T_o + a_2 T_o^2 \qquad (5B)$$

where N_1 and N_o are number of fringes at T_1 and T_o, respectively; a, a_1 and a_2 are the coefficients. If $T_1 > T_o$ the number of fringes increases from T_o to T_1; the thermal expansion $(\Delta L/L_o)$ can then be derived from eqs. (4) and (5):

$$\left(\frac{\Delta L}{L_o}\right)_P = m\lambda_v/2L_o n_o - \Delta n/n_o = mK_o - K_1$$

$$= K_o \left[a_1(T_1 - T_o) + a_2(T_1^2 - T_o^2)\right] - K_1 \qquad (6)$$

where $K_o = \lambda_v/2L_o n_o$, $K_1 = \Delta n_o/n_o$, and P signifies a case of increasing temperature ($T_1 > T_o$). In the case of decreasing temperatures ($T_2 < T_o$), the number of fringes decreases with decreasing temperature (case Q). Assume in this case N_2 and

N_o' to be the number of fringes at T_2 and T_o, respectively. The corresponding equations are:

$$N_2 = b + b_1 T_1 + b_2 T_1^2 \tag{7A}$$

$$N_o' = b + b_1 T_o + b_2 T_o^2 . \tag{7B}$$

In this case, the thermal expansion is negative and the corresponding relationship to eq. (6) is given by

$$\left(\frac{\Delta L}{L_o}\right)_Q = - mK_o + K_1 = - K_o \left[b_1(T_2 - T_o) + b_2(T_1^2 - T_o^2)\right] K_1 \tag{8}$$

From eqs. (6) and (8), the mean value of thermal expansion is given by:

$$\left(\frac{\Delta L}{L_o}\right)_{mean} = \frac{\left(\frac{\Delta L}{L_o}\right)_P + \left(\frac{\Delta L}{L_o}\right)_Q}{2} = \frac{K_o}{2} \left[- T_o(a_1 - b_1) - T_o(a_2 - b_2) + T_1(a_1 - b_1) + T_1(a_2 - b_2)\right]$$

$$= K[A + BT_1 + CT_1^2] \tag{9}$$

where,

$$K = K_o/2 = \lambda_v/4L_o n_o ,$$

$$A = -T_o(a_1 - b_1) - T_o(a_2 - b_2) ,$$

$$B = (a_1 - b_1) \text{ , and}$$

$$C = (a_2 - b_2) \text{ .}$$

Therefore, the mean coefficient of linear thermal expansion (α_ℓ) is determined from eq. (10):

$$(\alpha_\ell)_{mean} = \frac{1}{\Delta T} \left(\frac{\Delta L}{L_o}\right)_{mean}$$

$$= \frac{K}{T} (A + BT_1 + CT_1^2) \text{ .} \qquad (10)$$

The general form of eq. (10) is:

$$\alpha_\ell(T) = \frac{K}{\Delta T} (A + BT + CT^2) \text{ .} \qquad (11)$$

The experimental procedure in the determination of function $\alpha_\ell(T)$ involves first, counting fringes as a function of temperature and evaluation of the coefficients A, B, and C by the least-squares method and second, calculation of thermal expansivity ($\Delta L/L_o$) as a function of temperature using eqs. (9) and (11).

Results and Discussion

Results of the measurements of the fractional length change ($\Delta L/L_o$), normalized to zero at 25°C, for the three types of alkali silicate glasses to 300°C are shown in Figures 1-3. The least-squares analysis of both increasing and decreasing temperature data was made to obtain the best-fit expansion versus temperature curves (Figs. 1-3). The ($\Delta L/L_o$) versus temperature data were analyzed to obtain best-fit equation expressing the temperature dependence of α_ℓ for each of the glasses: $\alpha_\ell(T) = A_o + A_1T + A_2T^2$, where A_o, A_1 and A_2 are the constant coefficients for a given glass (Table 1). These relations were then used to calculate α_ℓ at the various temperatues. Figures 4 and 5 show the composition dependence of α_ℓ for the three types of alkali silicate glasses calculated at 25°C and at the three higher temperatures (100 to 300°C), respectively. As can be seen from Figures 1-5, the expansivity of the three types of alkali silicate glasses varies systematically with composition and temperature.

Thermal Hysteresis. In the case of Li_2O-SiO_2 and K_2O-SiO_2 glasses the thermal expansion was investigated as a function of both increasing and decreasing temperatures (Figs. 1 and 3). The results show that the expansion values are lower for the cooling cycle than for the heating cycle. The thermal hysteresis effect, caused mostly by the difference in the heating and cooling rates, is relatively more conspicuous in the K_2O-SiO_2

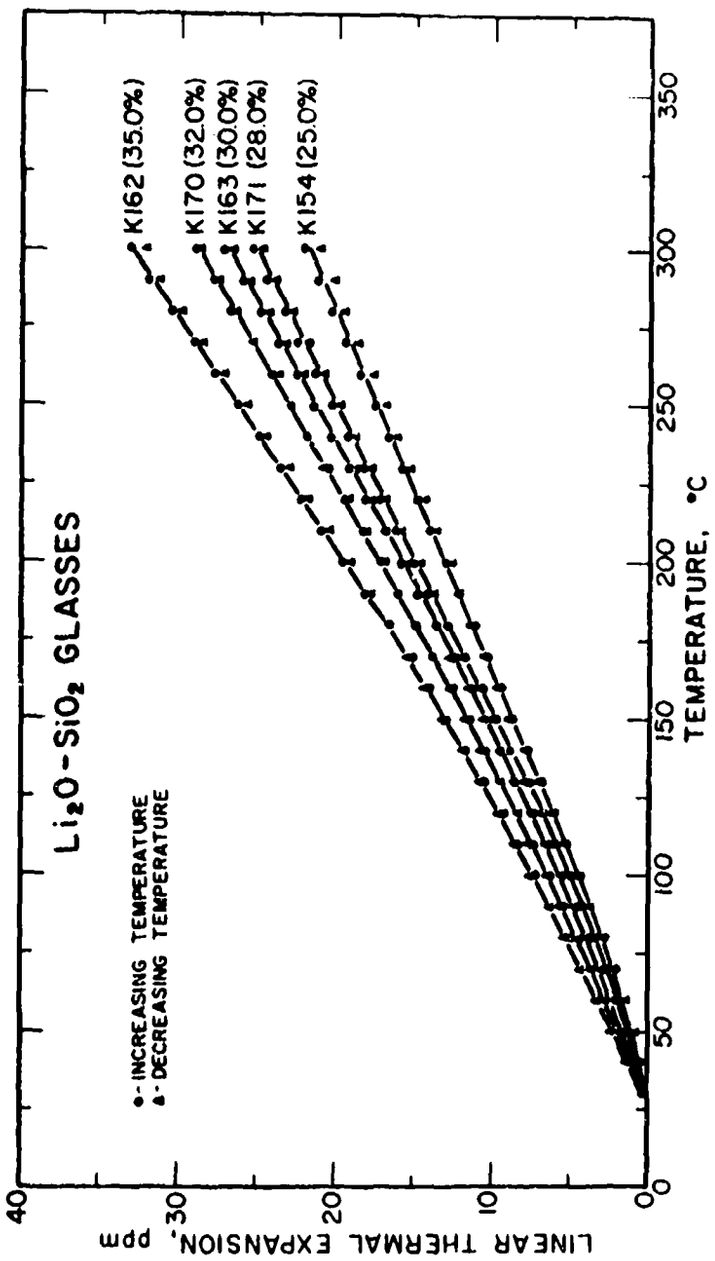

Fig. 1. Temperature dependence of the linear thermal expansion ($\Delta L/L_o$) of binary lithium silicate glasses.

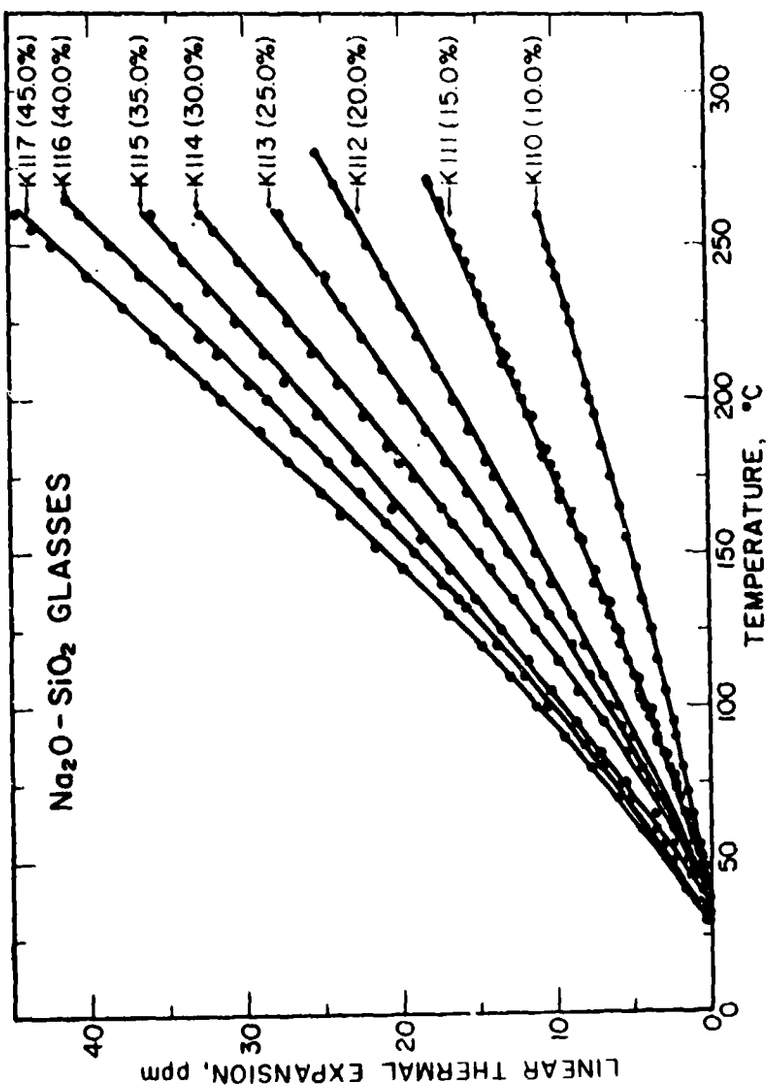

Fig. 2. Temperature dependence of the linear thermal expansion ($\Delta L/L_o$) of binary sodium silicate glasses.

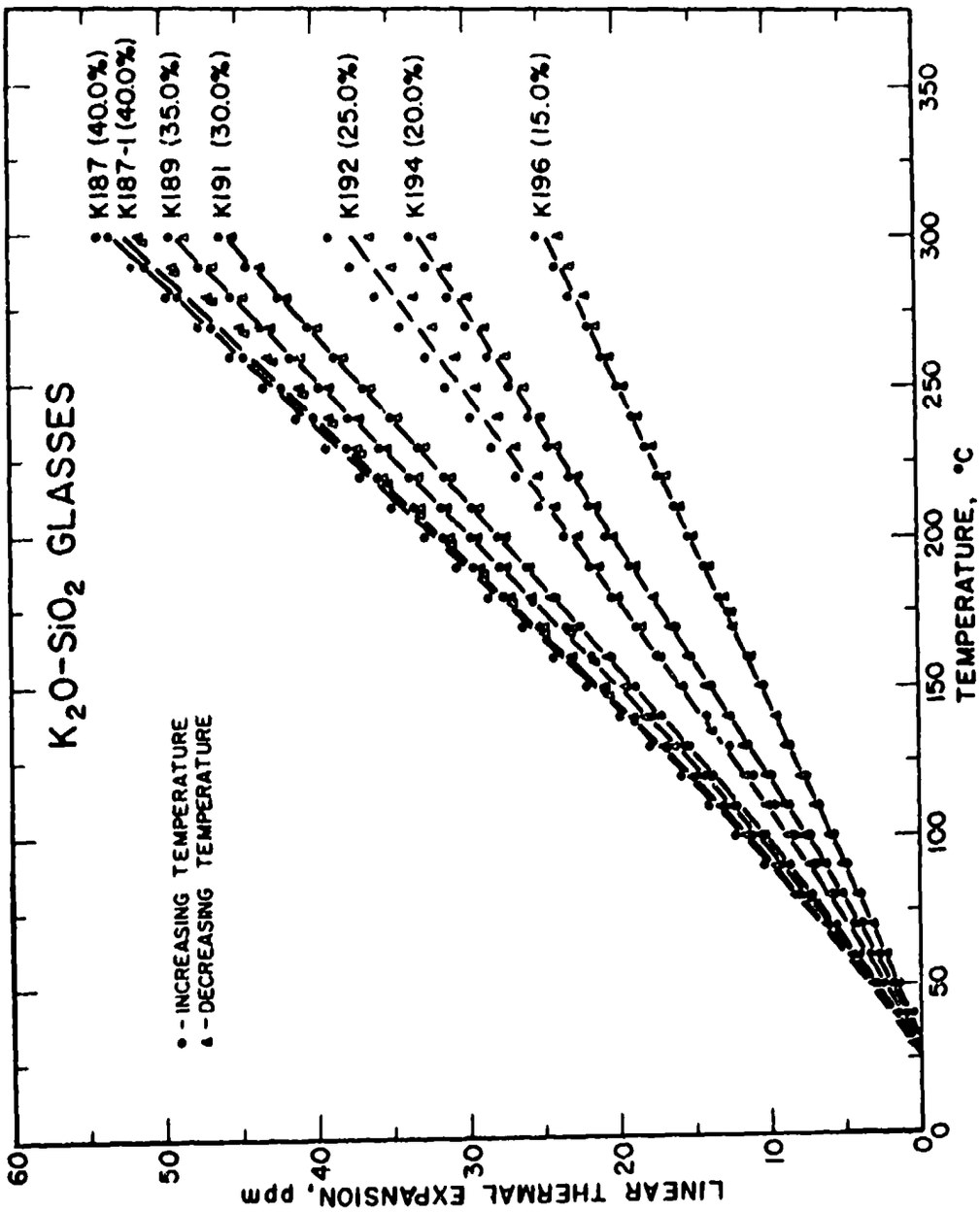

Fig. 3. Temperature dependence of the linear thermal expansion ($\Delta L/L_o$) of binary potassium silicate glasses.

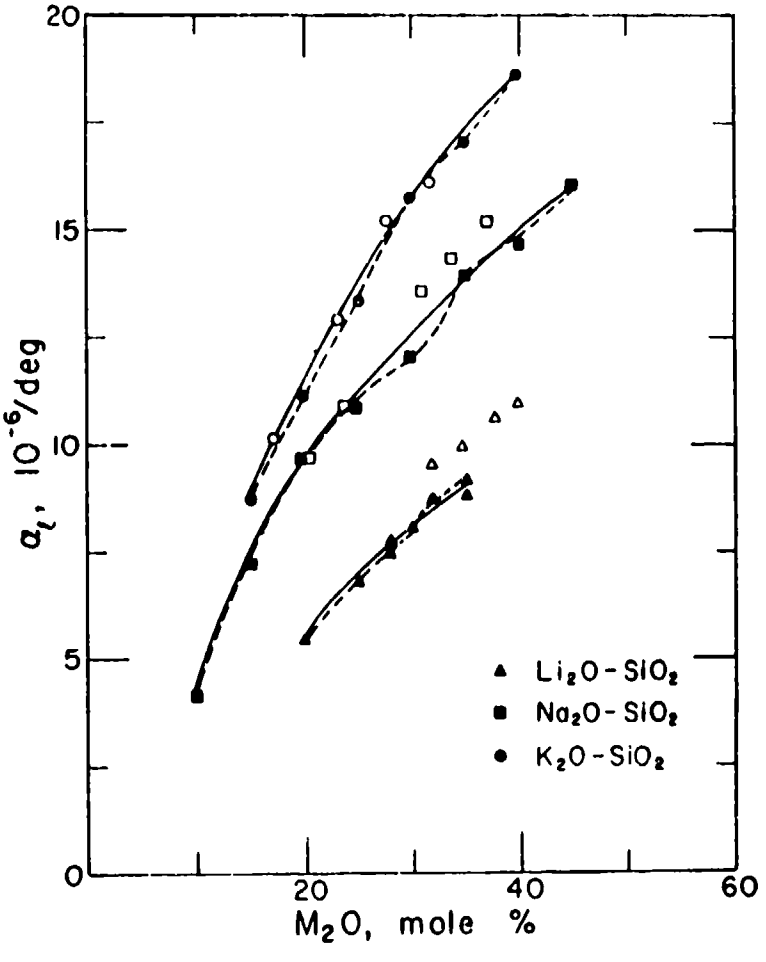

Fig. 4. Composition dependence of the linear thermal expansion coefficient (α_ℓ) for binary alkali silicate glasses at 25°C. The dashed lines indicate the breaks in the composition dependence of α_ℓ and the solid lines represent the mean curves based on the present study. The open symbols correspond to Shermer's data [10].

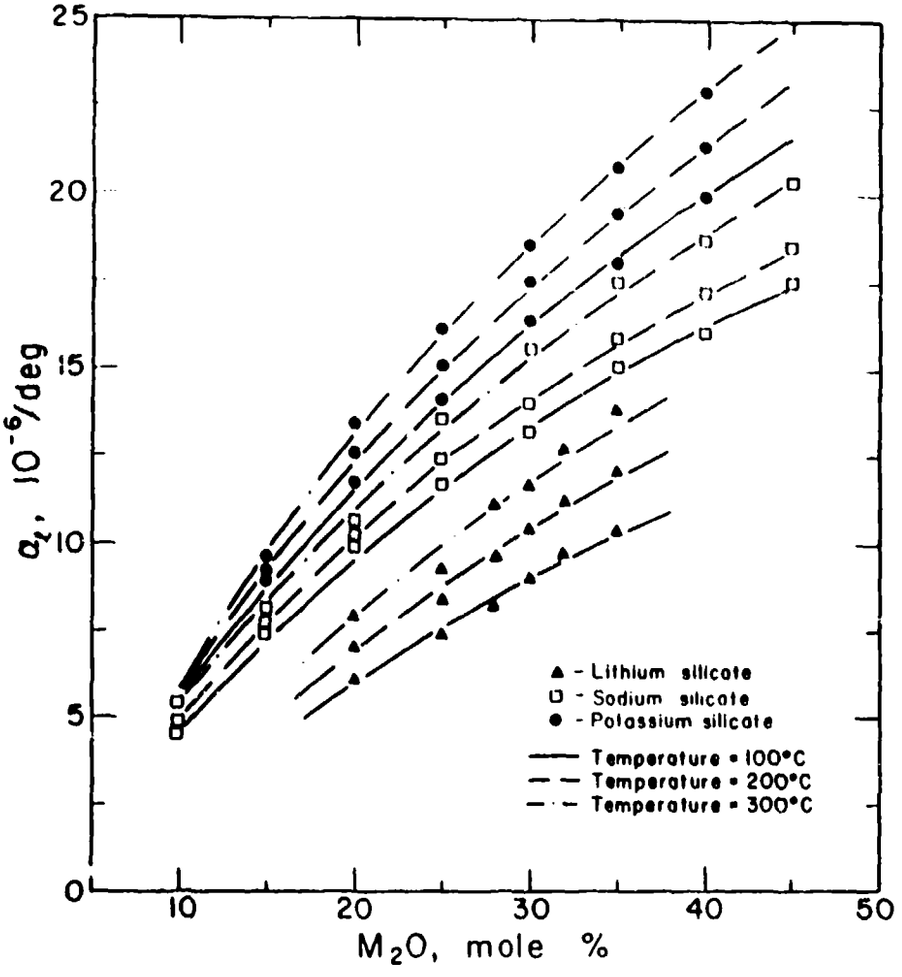

Fig. 5. Composition dependence of the mean linear thermal expansion coefficient (α_ℓ) for binary alkali silicate glasses at the various temperatures.

glasses than in the Li_2O-SiO_2 glasses, and may be explained by the larger thermal stresses present in the K_2O-SiO_2 glasses due to the larger size of the K^+ ions as compared to the Li^+ ions.

Temperature Dependence of Thermal Expansion. The thermal expansion of the alkali silicate glasses increases rapidly with increase in temperature (α_ℓ varies as quadratic in temperature). The temperature dependence of α_ℓ is quite similar for the three types of alkali silicate glasses (Figs. 1-3 and 5). The minor breaks in the α_ℓ-composition trends at room temperature (Fig. 4) can also be found to some extent at high temperatures (Fig. 5). For given M_2O content, the relative change in α_ℓ with increasing temperature has the trend: Li_2O-SiO_2 > Na_2O-SiO_2 > K_2O-SiO_2.

Composition Dependence of Thermal Expansion. The present room-temperature α_ℓ values for the alkali silicate glasses are in fairly good agreement with the previous data [10], except for slightly ($\sim$10%) lower values for the Li_2O-SiO_2 glasses determined in this study (Fig. 4). However, the present study confirms the earlier finding that, in general, the expansivity of the alkali silicate glasses increases with increasing M_2O content, the rate of increase being relatively higher for the low-M_2O glasses (Fig. 4); similar relation between α_ℓ and composition also holds true at higher temperatures (Fig. 5).

To interpret the composition dependence of thermal expansion we should understand the role of M_2O added to SiO_2 structure. Besides filling the interstitial space in the silica network

structure which results in the decrease of the openness of the silica structure, the addition of M_2O also causes destruction of the continuity of the silica structure (Si-O-Si bonds) and formation of the nonbridging oxygens and weaker Si-O-M bonds which result in the higher expansivity of glass [7,9,13]. The results plotted in Figs. 4 and 5 show increasing α_ℓ with increasing M_2O content. (By corollary, the elastic moduli decrease with increase in M_2O content, as mentioned in Section II of this report.)

The room temperature α_ℓ values of the Na_2O-SiO_2 and K_2O-SiO_2 glasses containing 15 mole % M_2O are, respectively, about 13 and 16 times that of silica for which $\alpha_\ell \approx 5.5 \times 10^{-7}$/deg [Table 1]. Such a rapid increase in the α_ℓ upon addition of small amounts of M_2O may be explained by appreciable changes in the asymmetry caused by the introduction of the nonbridging O^{2-} ions into the "flawless" Bernal liquid structure of silica [14]. (Si-O bond for a nonbridging O^{2-} ion is stronger than for a bridging O^{2-} ion). Subsequent additions of M_2O bring about relatively less drastic disproportionation of the stronger and weaker binding forces.

In a finer analysis of Figures 4 and 5, we can also see that α_ℓ does not vary smoothly with M_2O content, especially in the case of Na_2O-SiO_2 glasses; rather, there are breaks in the α_ℓ-composition trends (indicated by dashed lines in Fig. 4). The breaks occur approximately at 30, 28, and 26 M_2O mole %

composition of the Li_2O-SiO_2, Na_2O-SiO_2 and K_2O-SiO_2 glasses, respectively. In all three cases, the α_ℓ increases above these compositions. At higher M_2O contents, (~32 mole % K_2O and ~36 mole % Na_2O) the respective α_ℓ seem to decrease slightly from the normal trend. Such changes in α_ℓ are not unexpected in view of the fact that alkali silicate glasses do not have randomness of the silica-alkali structures [14-16] which would have otherwise produced smooth functions of α_ℓ versus M_2O composition. Most probably the formation of superlattice structure consisting of submicroscopic crystallites causes the α_ℓ to increase.

In the study of thermal expansivity of sodium silicate glasses, Blau [18] found breaks in the expansivity-composition curves at certain ratios of bridging and nonbridging oxygens, and he interpreted this as being some sort of a regularity in the distribution of the bridging and nonbridging O^{2-} ions. Parallel to this, we relate the breaks in the expansivity-composition trends to the varying degress of submicroscopic heterogeneity in the glasses [14].

The difference in the thermal expansion behavior of alkali silicate glasses having similar M_2O content is related to the different polarizability of nonbridging O^{2-} ions, which is mainly governed by the field strength and the size of M^+ ions [14]. The field strength of M^+ ions decreases in the order $Li^+(0.23) > Na^+(0.19) > K^+(0.13)$; their ionic size varies in

the opposite trend: $K^+(1.33) > Na^+(0.95) > Li^+(0.60)$. Large size and low field strength of K^+ ions introduce relatively high polarizability of nonbridging O^{2-} ions and weak Si-O-Si bonds, resulting in the high thermal expansion coefficients of K_2O-SiO_2 glasses as compared to the Na_2O-SiO_2 and Li_2O-SiO_2 glasses.

Contributions of the Various Oxides. The thermal expansion contributions of the oxides composing the glasses can be evaluated from the experimental values of the expansion coefficients of silicate glasses, assuming the additive property of these contributions [17,18]:

$$\alpha_\ell = \sum_i \alpha_i x_i \qquad (12)$$

where α_ℓ is the linear expansion coefficient of the glass, α_i are the empirical linear expansion coefficients of the oxides present, and x_i are the mole % of the oxides. The α_i thus calculated for Li_2O, Na_2O and K_2O in the alkali silicate glasses (Table 2) are found to be slightly lower than those determined from the other silicate and alumino-silicate glasses [18]. Using these α_i's, the α_ℓ values can be calculated and compared with the experimental α_ℓ values for the glasses (Table 3). Since the agreement between the experimental and calculated values is good (Table 3), the eq. (4) seems to hold well for the alkali silicate glasses. In other words, although the α_ℓ-composition relations for the alkali silicate glasses are

Table 2. Empirical coefficients of the thermal expansion contributions (α_i) of alkali oxides to the linear thermal expansion of alkali silicate glasses at 25°C

Glass type	Oxide	α_i, 10^{-8}/deg mole %	
		This study	Reference [17]
Li_2O-SiO_2	Li_2O	24.670	27.0
	SiO_2	0.843	0.63-3.8
Na_2O-SiO_2	Na_2O	34.268	39.50
	SiO_2	2.266	0.63-3.8
K_2O-SiO_2	K_2O	43.028	46.50
	SiO_2	3.194	0.63-3.8

Table 3. Comparison of experimental and predicted thermal expansion coefficients (α_ℓ in 10^{-6}/deg) for the alkali silicate glasses at 25°C. The SiO_2 content (in mole%) of the glass is given in parentheses

Glass No.	Experimental	Predicted
Li_2O-SiO_2 Glasses		
K-119 (80)	5.43	5.61
K-154 (75)	6.80	6.80
K-157 (72)	7.77	7.51
K-198 (72)	7.47	7.51
K-163 (70)	8.06	7.99
K-170 (68)	8.75	8.47
K-162 (65)	8.81	9.18
K-197 (65)	9.17	9.18
Na_2O-SiO_2 Glasses		
K-110 (90)	4.12	5.47
K-111 (85)	7.23	7.07
K-112 (80)	9.67	8.66
K-113 (75)	10.83	10.27
K-114 (70)	12.06	11.87
K-115 (65)	13.97	13.47
K-116 (60)	14.64	15.07
K-117 (55)	16.01	16.67
K_2O-SiO_2 Glasses		
K-196 (85)	8.79	9.16
K-194 (80)	11.14	11.16
K-192 (75)	13.39	13.15
K-191 (70)	15.80	15.14
K-189 (65)	17.09	17.13
K-187-1 (60)	18.68	19.12

not strictly monotonic, the mean relations (indicated by solid curves in Fig. 4) are useful in predicting α_ℓ from the composition of an alkali silicate glass.

One of the most interesting results from this study is that the α_1 for SiO_2 is not uniform in the three types of alkali silicate glasses; it varies from 0.843/deg mole % in the Li_2O-SiO_2 glasses to 3.194/deg mole % in the K_2O-SiO_2 glasses--a variation of the order of 4 (Table 2), which is comparable to that found in the other glasses $(0.5\text{-}3.8 \times 10^{-8}$/deg mole %) [17]. The large variation in the SiO_2 contribution may be explained by the large difference in the force constants of the Si-O bonds involving the nonbridging O^{2-} ions in the three types of alkali silicate glasses.

References

[1] A.J. Ledbetter, Phys. Chem Glasses 9, 1, (1968).

[2] J.T. Krause and C.R. Kurkjian, J. Am. Ceram. Soc. 51, 226 (1968).

[3] C.R. Kurkjian, J.T. Krause, H.J. McSkimin, P. Andreatch and T.B. Bateman, in Amorphous Materials, edited by R.W. Douglas and B. Ellis, Wiley-Interscience, 463 (1972).

[4] H.T. Smyth, J. Am. Ceram. Soc. 36, 140 (1955).

[5] H.T. Smyth, The structure of glass, in Introduction to Glass Science, edited by L.D. Pye, H.J. Stevens, and W.C. La Course, Plenum Press, New York, 61 (1972).

[6] G.K. White, Cryogenics 4, 2, (1964).

[7] A. Dietzel and H.A. Sheybany, Verres et Refractaires 2, 63 (1948); Ceramic Abstracts, 221g (1948).

[8] M.D. Karkhanavala, Glass Industry 33, 403 (1952).

[9] L. Shartsis, S. Spinner, and W. Capps, J. Am. Ceram. Soc. 35, 155 (1952).

[10] H.F. Shermer, J. Res. Nat. Bur. Stand. 57, 19 (1956).

[11] ASTM Designation 289-65T, ASTM Standards, Part 31, 905 (1968).

[12] W.A. Plummer and H.E. Hagy, Appl. Optics 7, 825 (1968).

[13] A. Dietzel, Naturwissenschaften 31, 110 (1943).

[14] W.A. Weyl and E.C. Marboe, The Constitution of Glasses, Vol. II (part one), 892 pp., John Wiley and Sons, New York, (1964).

[15] B.E. Warren and J. Biscoe, J. Am. Ceram. Soc. 21, 259 (1938).

[16] J. Biscoe, M.A.A. Bruesne and B.E. Warren, J. Am. Ceram. Soc. 24, 100 (1941).

[17] A.A. Appen, Silikattachnik 5, 113 (1954).

[18] H.H. Blau, J. Soc. Glass Technol. 35, 304 (1951).

SECTION IV

EFFECTS OF PHASE SEPARATION ON ELASTIC PROPERTIES AND THERMAL EXPANSIVITY

The phase studies were conducted by Mr. John Kay, R.P.I. The following method was used by him:

Fracture surfaces of the glasses were obtained, and etched as follows:

K_2O-SiO_2 glasses	-	10 seconds 2% HCl
some Li_2O-SiO_2 glasses	-	10 seconds 2% HCl
other Li_2O-SiO_2 glasses	-	10 seconds 2% HF
Na_2O-SiO_2 glasses	-	10 seconds 2% HF

Replica samples were made by shadowing a collodion replica of the sample surface with chromium and then coating it with carbon. Replicated surfaces were then viewed in a Hitachi HU-LLB electron microscope operated at 100 KV.

Results and Discussion

Phase separation is everywhere present in alkali silicate glasses. The volumetric percentage of relatively silica-rich phase varies from 11 to 15% in high-M_2O glasses to as high as 65 to 70% in glasses with 25 to 30% M_2O, and the particle size varies from 200 Å or less to 1/2 micron (Table 1).

In spite of large variations in phase separation (amount and size), the trends of elastic property-composition are quite systematic (see figures in section II).

We chose three Li_2O-SiO_2 glass samples (198, 171B, and K171A) with the same composition (28 mole % Li_2O) and varying degress of phase separation to study the effects of phase separation. K198 has an evenly dispersed phase separation with particle size averaging about 1000 Å in diameter (Plate I). 171B has an unevenly dispersed phase separation, the particle size being 500 to 100 Å (Plate II). This glass showed square-shaped crystals of about 0.75μ edge-length. Glass 171A has an evenly dispersed phase separation, the average particle size being ∿1000 Å .

Thus, in terms of particle size and composition, these specimens are quite similar. Inspection of Table 2 shows that there is no systematic variation in properties with the variation in the degree of phase separation, except in the pressure and temperature derivatives of the moduli and thermal expansion. The α_ℓ and dM/dT values seem to increase when phase separation increases.

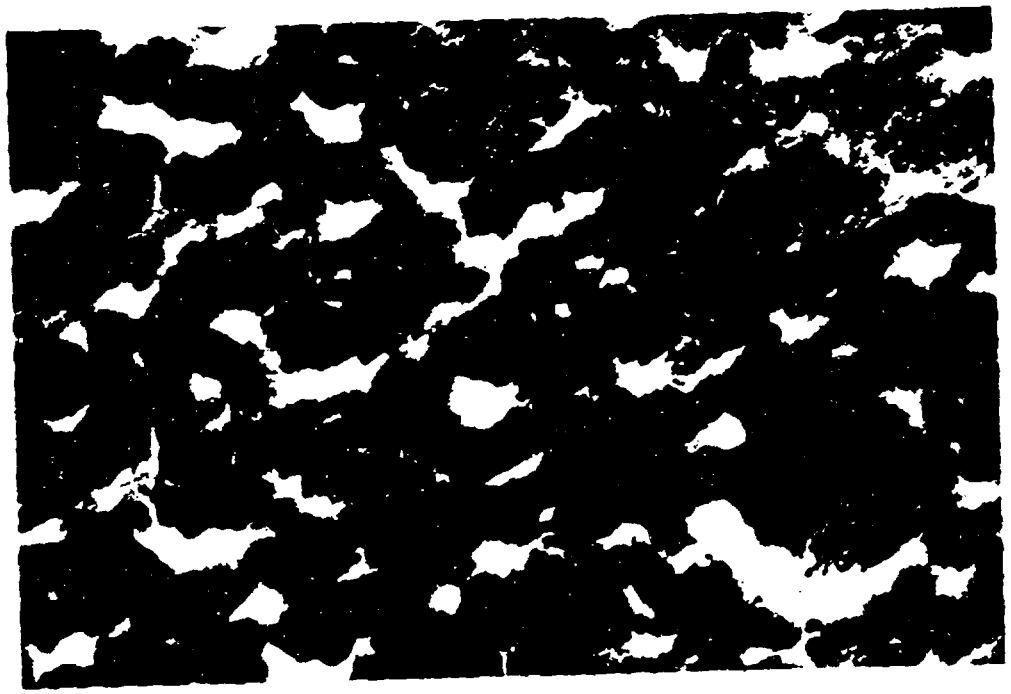

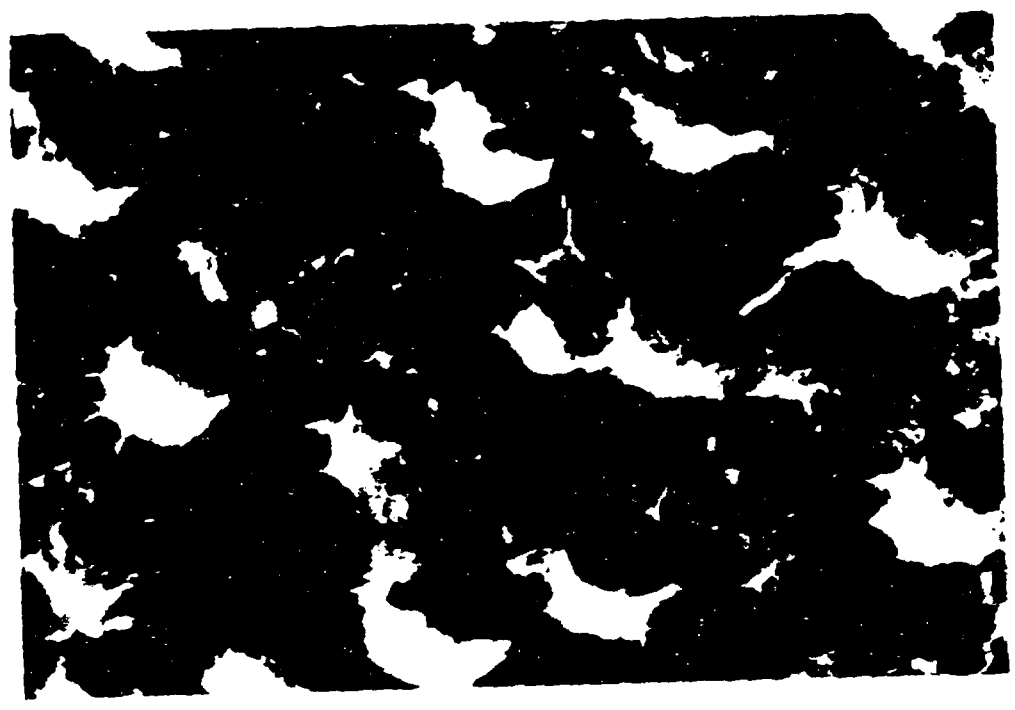

(above) Plate I. Electron micrograph of K-198 glass (X360,000).

(upper right) Plate II. Electron micrograph of K171B glass (X360,000).

(lower right) Plate III. Electron micrograph of K171A glass (X360,000).

Table 1. Volumetric percentage and particle size of phase separation in alkali silicate glasses

Glass No.	Composition (mole %) M_2O	SiO_2	Volume %	Average Particle Size
		Li_2O-SiO_2 Glasses		
K199	20.0	80.0	64	1/2 μ
K154	25.0	75.0	25	300-1500 Å
K171A	28.0	72.0	37	1000 Å
K171B	28.0	72.0	22	500-1000 Å
K198	28.0	72.0	17	1000 Å
K163	30.0	70.0	65-70	0.25-1 μ
K170	32.0	68.0	62	3200 Å
K162	35.0	65.0	70,11	1/2 μ
K197	35.0	65.0	11	3500 Å
		Na_2O-SiO_2 Glasses		
K110	10.0	90.0	60	500 Å
K112	20.0	80.0	45	500 Å
K114	30.0	70.0	26	1200 Å
K115	35.0	65.0	47	650 Å
K116	40.0	60.0	15	1000 Å
		K_2O-SiO_2 Glasses		
K196	15.0	85.0	15	400 Å
K194	20.0	80.0	75	700 Å
K192	25.0	75.0	50	200 Å

Table 2. Properties of three Li_2O-SiO_2 glasses (containing 28 mole % Li_2O) with varying degrees of phase separation of silica-rich phase

	K 198	K 171B	K 171A
SiO_2-rich phase, volume %	17	22	37
ρ, g/cm^3	2.322	2.322	2.322
V_p, km/sec	6.153	6.149	6.149
V_s, km/sec	3.720	3.720	3.722
K, kbar	450.4	449.6	449.2
μ, kbar	321.4	321.3	321.6
σ	.212	.211	.211
(dK/dP)	3.42	3.59	2.94
(dμ/dP)	-.17	-.14	-.19
(dK/dT), kbar/deg	-.043	-.052	-.014
(dμ/dT), kbar/deg	-.083	-.079	-.132
α_L, 10^{-6}/deg	7.47		7.7

SECTION V

EFFECTS OF COMPOSITION, PRESSURE, AND TEMPERATURE ON THE ELASTIC PROPERTIES OF SiO_2-TiO_2 GLASSES

Introduction

SiO_2-TiO_2 glasses containing low concentrations of TiO_2 (up to 11 wt %) form in homogeneous phase [1-3]; TiO_2 plays the role of network former just as SiO_2 does. Interest in the SiO_2-TiO_2 glass system has recently developed because of its low thermal expansion properties. The SiO_2-TiO_2 glass (Corning Code 7971) containing 7.4 wt % TiO_2 has nearly zero thermal expansion [4, 5] in the temperature range of 0 to 300°C. In a recent systematic study [6], it has been shown that small amounts of TiO_2 (up to 10 wt %) added to fused silica cause a linear decrease in the coefficients of thermal expansion of silica glass. More recently, Schultz [7,8] has discovered unique annealing methods for developing the low-expansion SiO_2-TiO_2 glass containing 12-20 wt % TiO_2.

Variations in the thermal expansion and other vibrational properties of the SiO_2-TiO_2 glasses, caused by the compositional variations, are directly related to the variations in the structure and lattice vibrations of the glass network. A number of workers have studied the effect of TiO_2 content on the various properties of the SiO_2-TiO_2 and related silicate glasses [6-19] and have interpreted the results in terms of

the changes in structure and coordination of the silicon and titanium ions. However, the elastic properties of the SiO_2-TiO_2 glasses have so far not been systematically investigated.

The purpose of this section is to report on the elastic properties of the SiO_2-TiO_2 glasses as a function of composition, pressure, and temperature, and to correlate the results with the variations in thermal expansion and other related anharmonic parameters.

Experimental Methods

Glass Specimens. The seven SiO_2-TiO_2 glasses used in this study were kindly supplied to us by Dr. P.C. Schultz of the Corning Glass Works. These were prepared by flame hydrolysis [6]. The TiO_2 content of the glasses ranges from 1.3 to 9.4 wt % (Table 1). Also included in this study is fused silica (Corning Code 7940), purchased from the Corning Glass Works.

Elastic measurements were made on the glasses in as-produced, unannealed state as well as after annealing. The annealing process involved heating the glasses to 1020°C for about 1-1/2 hours, and then cooling them slowly from 1020 to 700°C at a rate of 5°C/hour, and then allowing them to cool inside the furnace from 700°C to room temperature.

Density of the glass specimen was measured by the Archimedes method. The pulse superposition method [20] of measuring ultrasonic velocities was used. The details of the electronics

Table 1. Chemical composition, and the elastic parameters of SiO_2-TiO_2 glasses at 1 bar and 25°C. All the glass specimens were annealed before the measurements

Glass No.	Composition, wt % SiO_2	Composition, wt % TiO_2	ρ, g/cm^3	V_p, km/sec	V_s, km/sec	K, kbar	μ, kbar	E, kbar	σ
7940A (fused silica)	100	0	2.2007	5.947	3.769	361.6	312.6	728.0	.1645
T4A	98.7	1.3	2.2005	5.911	3.746	357.1	308.8	719.1	.1643
T1A	97.2	2.8	2.2001	5.872	3.717	353.2	304.0	708.8	.1656
T5A	95.4	4.6	2.1995	5.833	3.692	348.7	299.8	697.0	.1659
T6A	94.0	6.0	2.1992	5.803	3.672	345.3	296.5	691.6	.1662
T2A	92.7	7.3	2.1986	5.758	3.635	341.5	290.51	679.0	.1686
ULE 7971A	92.5	7.5	2.1993	5.783	3.653	344.2	293.5	625.6	.1680
T3A	90.6	9.4	2.1985	5.719	3.607	337.7	286.0	669.1	.1698

and high pressure and temperature equipment used, and the procedure to reduce the basic data are described elsewhere [19].

Results and Discussion

Effect of Annealing. The relations between composition and the elastic parameters, especially K and σ, are not so well defined for the unannealed glasses (Figs. 1-3). Following annealing, the relationships become systematic and more or less linear. It is interesting to note that annealing brings about an increase in V_s and ρ, but decrease in V_p. Similarly, μ and E increase and K decreases (that is, compressibility increases) after annealing. Annealing causes the removal of strains and rearrangement of the glass network such that the structure becomes more compact. We have also found compaction effect of annealing in a SiO_2-TiO_2 glass containing 14.7 wt % TiO_2. According to Schultz [personal communication, 1974], this compaction is related to a coordination change of titanium in the glass from 4 to 6. Based on Schultz's work [7-8], the effect of coordination change seems to occur in only high-TiO_2 (> 10 wt %) glasses.

Elastic Parameters at 1 bar and 25°C. The results of the elastic parameters as a function of composition are shown in Table 1 and Figures 1-3. McSkimin's (unpublished) data on V_p, V_s, E, and μ for fused silica and the Corning Code 7971 glass are in agreement with the present results. The elastic parameters (longitudinal velocity; V_p, shear velocity, V_s; bulk

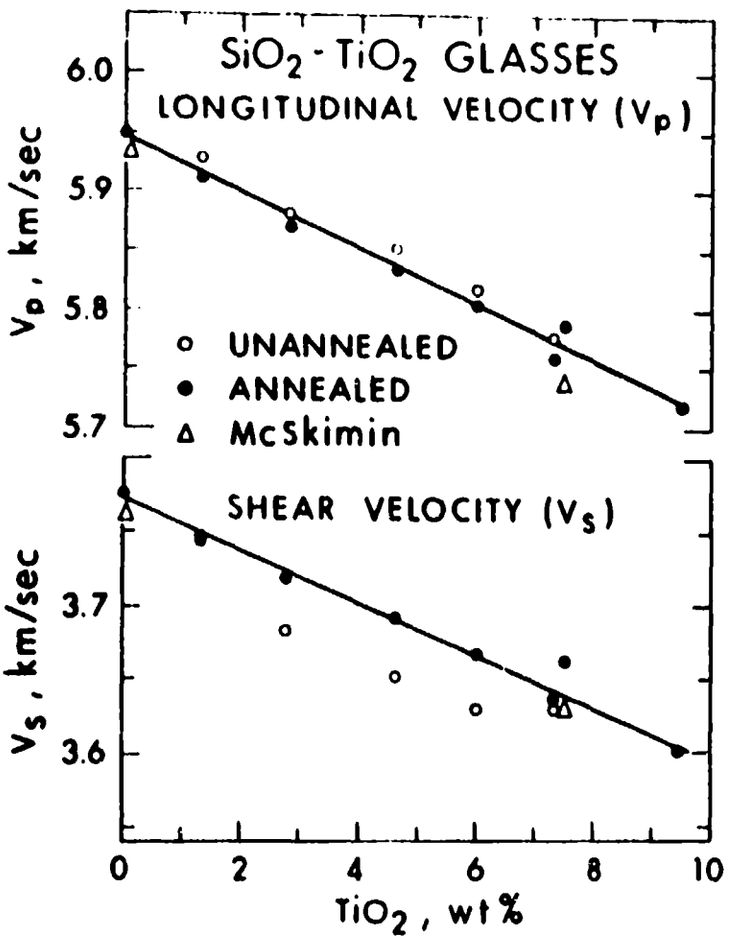

Fig. 1. Longitudinal (V_p) and shear wave (V_s) velocities versus TiO_2 content. Annealing causes a decrease in V_p and an increase in V_s. Triangles are McSkimin's (unpublished) 1972 data.

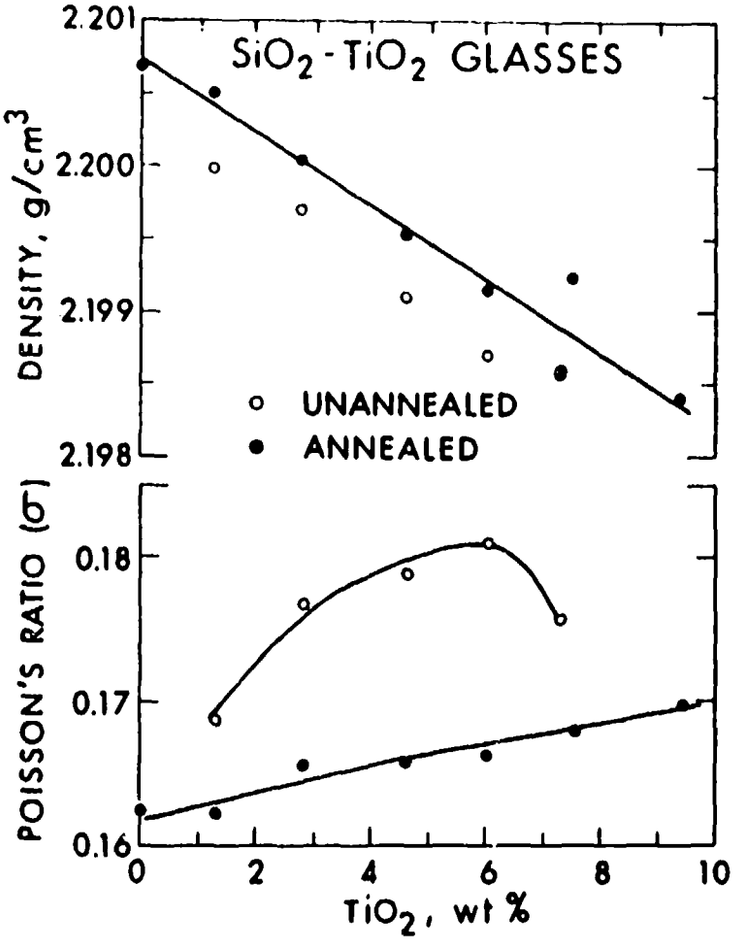

Fig. 2. Density (ρ) and Poisson's ratio (σ) vesus TiO_2 content. Annealing causes an increase in ρ and a decrease in σ.

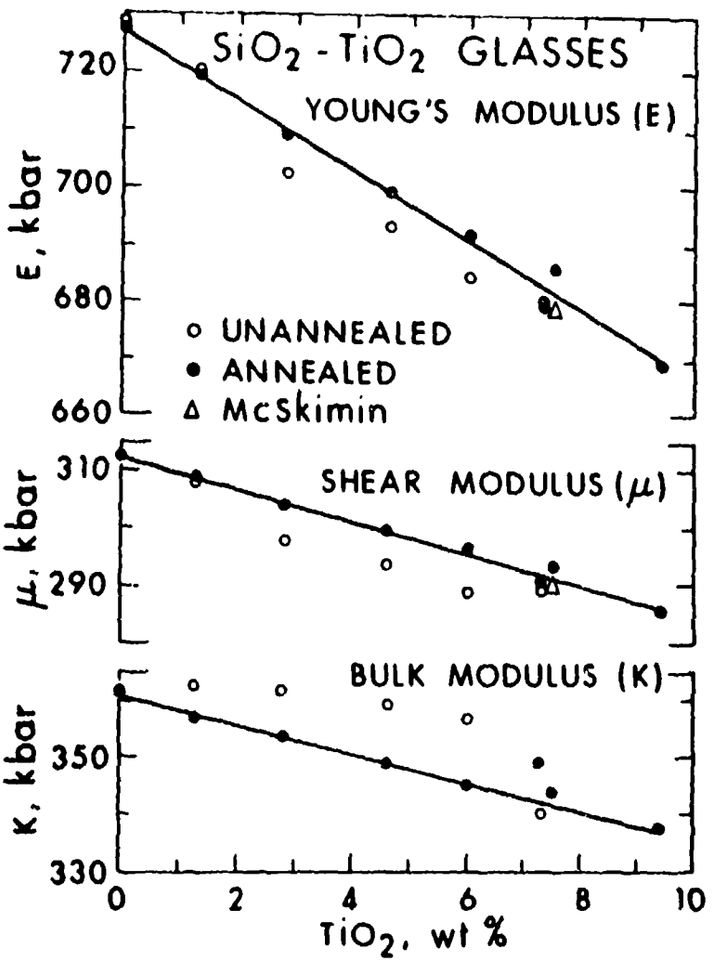

Fig. 3. Bulk (k), shear (μ) and Young's (E) moduli versus TiO_2 content. Annealing causes a decrease in K, and an increase in μ and E. Triangles are McSkimin's (unpublished) 1972 data.

modulus, K; shear modulus, μ; Young's modulus, E) and density (ρ) of the annealed SiO_2-TiO_2 glasses decrease more or less linearly with increase in the TiO_2 content. However, Poisson's ratio for these glasses increases linearly with TiO_2 content.

The decreases in the moduli are interpreted to be caused by weakening of the silica network. The Ti^{4+} ions have lower field strength than the Si^{4+} ions, and the average length of Ti-O bond is considered to be larger than that of the Si-O bond; hence the Ti-O and Si-O-Ti bonds in SiO_2-TiO_2 glasses are weaker than the correspondong Si-O and Si-O-Si bonds in silica glass. This view has been well supported by infrared absorption studies [9].

At low TiO_2 concentrations, Si-equivalent fourfold Ti ions exist in the coordination [1-3]. Hence a decrease in ρ with increasing TiO_2 content (Fig. 2) seems, at first, surprising in view of the fact that substituted Ti^{4+} ions are heavier than the Si^{4+} ions. Evans [1] has clearly demonstrated that the additions of small amounts of TiO_2 to the SiO_2-TiO_2 solid solution (cristobalite phase) cause the tetragonal a_o and c_o d-spacings of this phase to increase. Such an effect would explain the variations in density of the SiO_2-TiO_2 glasses. A decrease in density can thus be interpreted as being due to the increasing openness of the structure as TiO_2 is added. It appears that Si-O-Si and Si-O-Ti angles change such that the openness of the structure increases. That is, the Ti^{4+} ions would repel the O^{2-} ions farther than the Si^{4+} ions do.

Pressure Dependence of the Elastic Moduli

The pressure derivatives of the compressional and shear velocities, (dV_p/dP) and dV_s/dP), decrease with increase in TiO_2 content (Table 2; Fig. 4); the variation of (dV_s/dP) with composition is more systematic. There is a good agreement between McSkimin's and the present values of ($d\mu/dP$) and (dE/dP) for fused silica and the Corning Code 7971 glass (Fig. 5). As in fused silica, the values of (dK/dP), ($d\mu/dP$), and (dE/dP) in SiO_2-TiO_2 glasses are negative (anomalous) and become increasingly negative (more anomalous than fused silica) with increasing TiO_2 content (Table 2; Fig 5). Values of $d\mu/dP$ for all the glasses are negative (anomalous). This parameter becomes more negative with increase in TiO_2 content up to $\sim$5 wt % TiO_2, above which it becomes less negative (Fig. 6). The anomalous elastic behavior under pressure in fused silica has been explained in terms of its low (near-zero) thermal expansion. The presence of the low-frequency vibrational modes for which $d\omega/dV$ (where ω is frequency) is positive [6]. The presence of such modes also leads to an explanation for the negative thermal expansion of the SiO_2-TiO_2 glasses [6]. The negative thermal expansion in SiO_2-TiO_2 glasses has been attributed to the presence of the vibrational modes for which $d\omega/dV$ is positive [6], and this condition, characteristic of open structures, leads to negative values of (dM/dP), where M is any modulus [21]. It then appears that the addition of TiO_2 causes changes in the vibrational

Table 2. Pressure and temperature derivatives of the elastic parameters of SiO_2-TiO_2 glasses at 25°C and 1 bar, respectively. All the glass specimens were annealed before the measurements.

Glass No.	Composition, wt % SiO_2	Composition, wt % TiO_2	dK/dP	dρ/dP, g/cm^3 · Mbar	dμ/dP	dE/dP	dσ/dP, Mbar	dK/dT, kbar/deg	dμ/dT, kbar/deg	dE/dT, kbar/deg	dσ/dT, deg^{-1} x 10^4
7970A (fused silica)	100	0	-5.37	6.68	-3.53	-8.82	-1.01	.124	.051	.148	.45
T4A	98.7	1.3	-5.68	6.78	-3.56	-9.00	-1.24	.121	.052	.149	.43
T1A	97.2	2.8	-5.42	6.80	-3.56	-8.87	-1.00	.121	.050	.145	.43
T5A	95.4	4.6	-5.97	7.01	-3.55	-9.13	-1.52	.119	.050	.143	.44
T6A	94.0	6.0	-5.85	7.06	-3.54	-9.05	-1.42	.119	.048	.141	.44
T2A	92.7	7.3	-5.96	7.20	-3.60	-9.20	-1.47	.120	.048	.140	.45
ULE 7971A	92.5	7.5	-5.88	7.10	-3.60	-9.16	-1.36	.119	.047	.138	.46
T3A	90.6	9.4	-5.77	7.26	-3.59	-9.09	-1.30	.117	.047	.137	.46

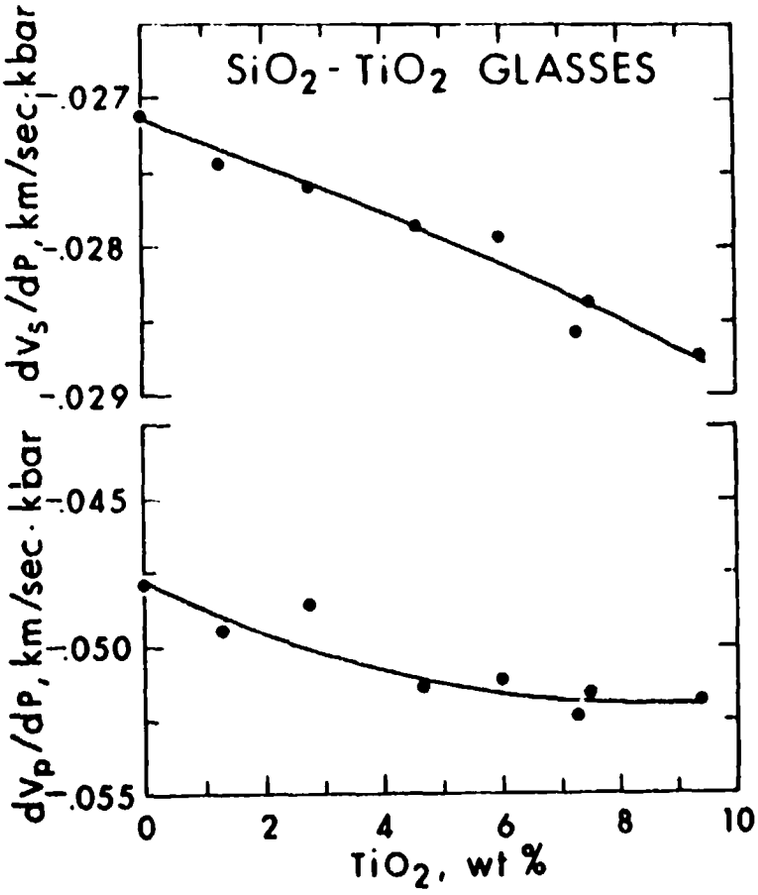

Fig. 4. Composition dependence of (dV_p/dP) and (dV_s/dP) glasses in SiO_2-TiO_2.

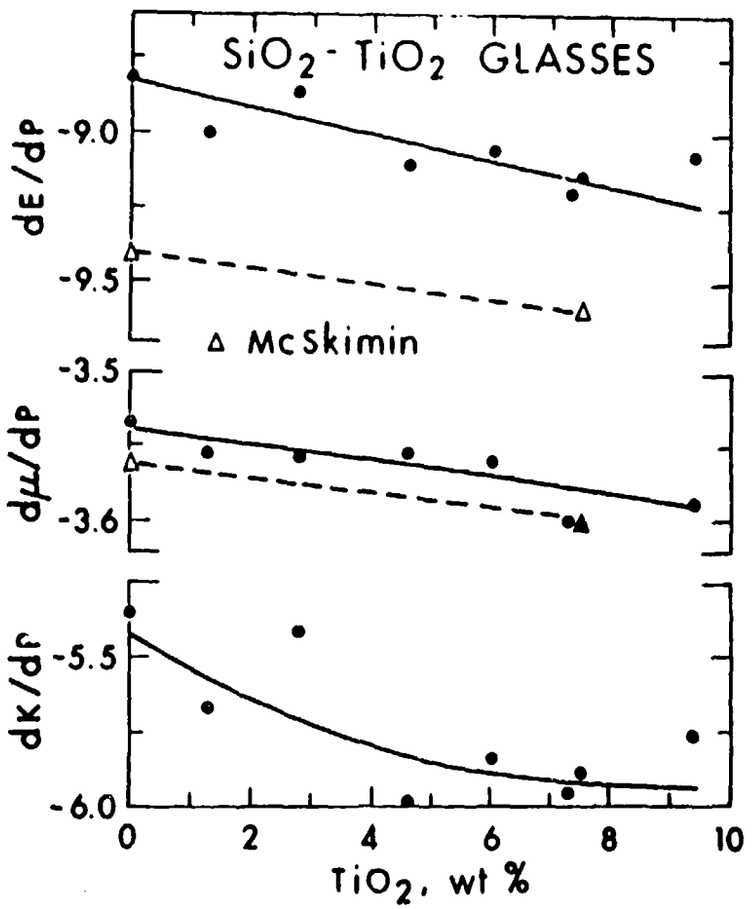

Fig. 5. Composition dependence of dE/dP, dμ/dP, and dK/dP in SiO_2-TiO_2 glasses. Open triangles are McSkimin's (unpublished) 1972 data; solid triangle is superimposition of the present and McSkimin's data for dμ/dP.

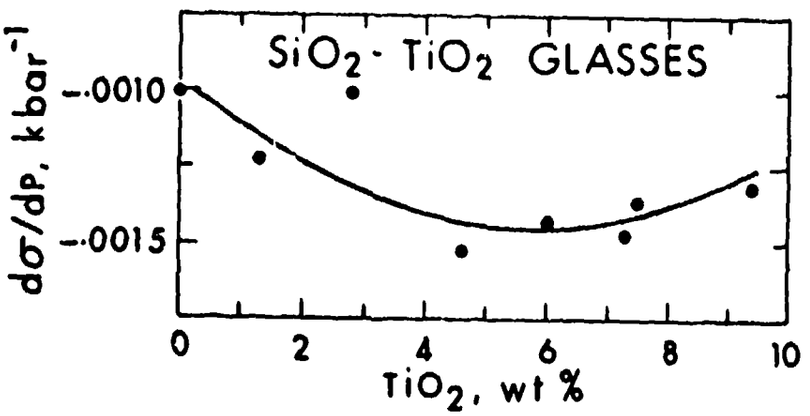

Fig. 6. $d\sigma/dP$ versus TiO_2 content.

properties of such modes so that $d\omega/dV$ becomes more positive, leading to more negative thermal expansion and more anomalous elastic behavior under pressure. Thus, the more negative values of dM/dP with increasing TiO_2 content are compatible with the thermal expansion data.

Densification

The pressure-density data for a solid can be used for calculating its bulk modulus, K_o, and initial pressure derivative $K_o' = (\partial K/\partial P)_{P=o}$ through the Birch-Murnaghan equation of state [24]:

$$P = (3/2\ K_o \{(\rho_o/\rho)^{7/3} - (\rho_o/\rho)^{5/3}\}\{1 - \xi\ [(\rho_o/\rho)^{2/3} - 1]\} \quad (1)$$

where $\xi = 3(4 - K_o')/4$. Inversely, if K_o and K_o' are known, (ρ/ρ_o) can be evaluated as a function of pressure.

Using eq. (1) and the data for fused silica and the SiO_2-TiO_2 glasses containing 7.3 wt % TiO_2 (Table 2), (ρ/ρ_o) was calculated to 60 kbar (Fig. 7). As seen, the glass containing TiO_2 shows higher densification (ρ/ρ_o). At 20 kbar the difference between (ρ/ρ_o) ratios would be ~7%.

Mode Grüneisen Parameters

The mode Grüneisen parameters γ_i are evaluated from the pressure dependence of acoustic mode velocity V_i:

$$\gamma_i = \frac{1}{V_i \beta} \left(\frac{dV_i}{dP}\right),$$

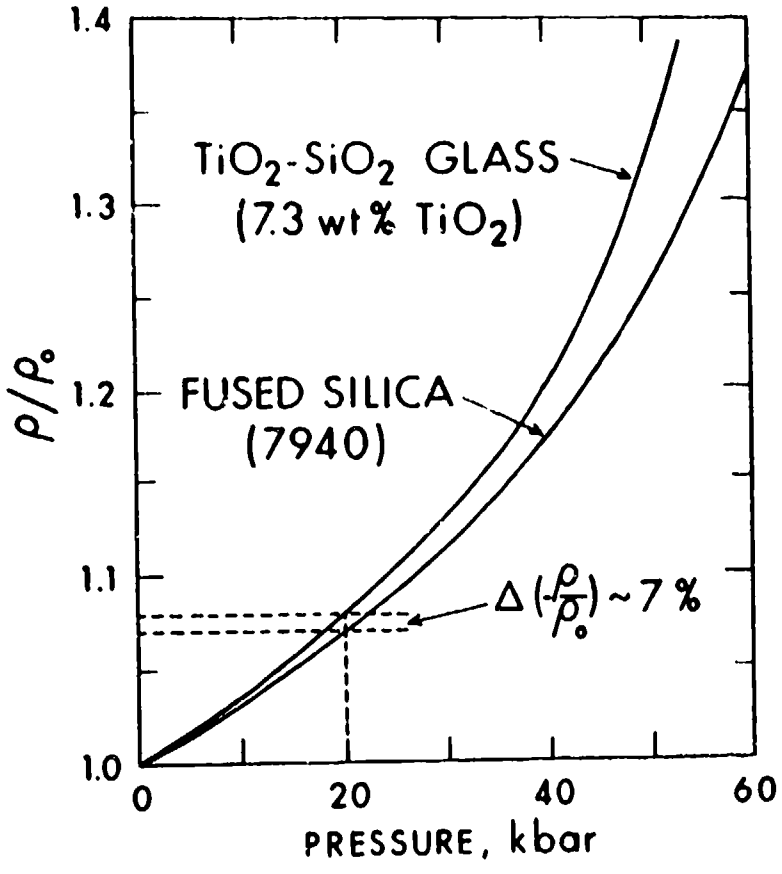

Fig. 7. Densification of fused silica and SiO_2-TiO_2 glass containing 7.3 wt % TiO_2.

where β is the isothermal compressibility. Assuming only the contributions from acoustic mode, the high- and low-temperature limiting values of the Gruneisen parameter, γ_{HT} and γ_{LT}, can be evaluated from (dV_s/dP) and (dV_p/dP) using the known relations [22,23]. As in fused silica, the γ_{HT} values for all the SiO_2-TiO_2 glasses are negative (Fig. 8). As seen, γ_{HT} becomes more negative with TiO_2 content.

Temperature Dependence of Elastic Moduli

The temperature and composition dependence of K, μ and E measured to 300°C are shown in Figure 9. The temperature derivatives of the moduli (dM/dT) are positive (anomalous) and remain the same in the temperature range of the investigation. The values of (dM/dT) decrease with increase in TiO_2 content (Fig. 10). That is, the glasses become less anomalous in the thermal behavior, in contrast to the more anomalous behavior under pressure.

The contributions to total change in modulus M due to temperature effect can be considered as intrinsic and extrinsic parts:

$$dM = \left(\frac{\partial M}{\partial T}\right)_V dT + \left(\frac{\partial M}{\partial V}\right)_T dV \quad . \qquad (2)$$

(total) (intrinsic) (extrinsic)

It can be shown that the measured total (dM/dT) is related to the measures $(\partial M/\partial P)_T$:

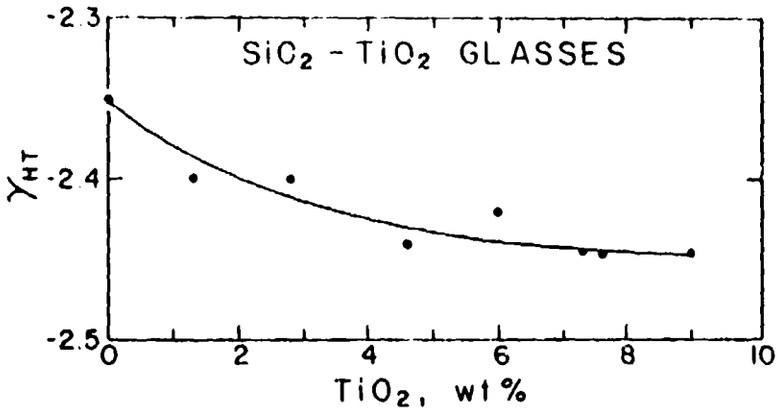

Fig. 8. Variation of Grüneisen parameter γ_{HT} in SiO_2-TiO_2 glasses.

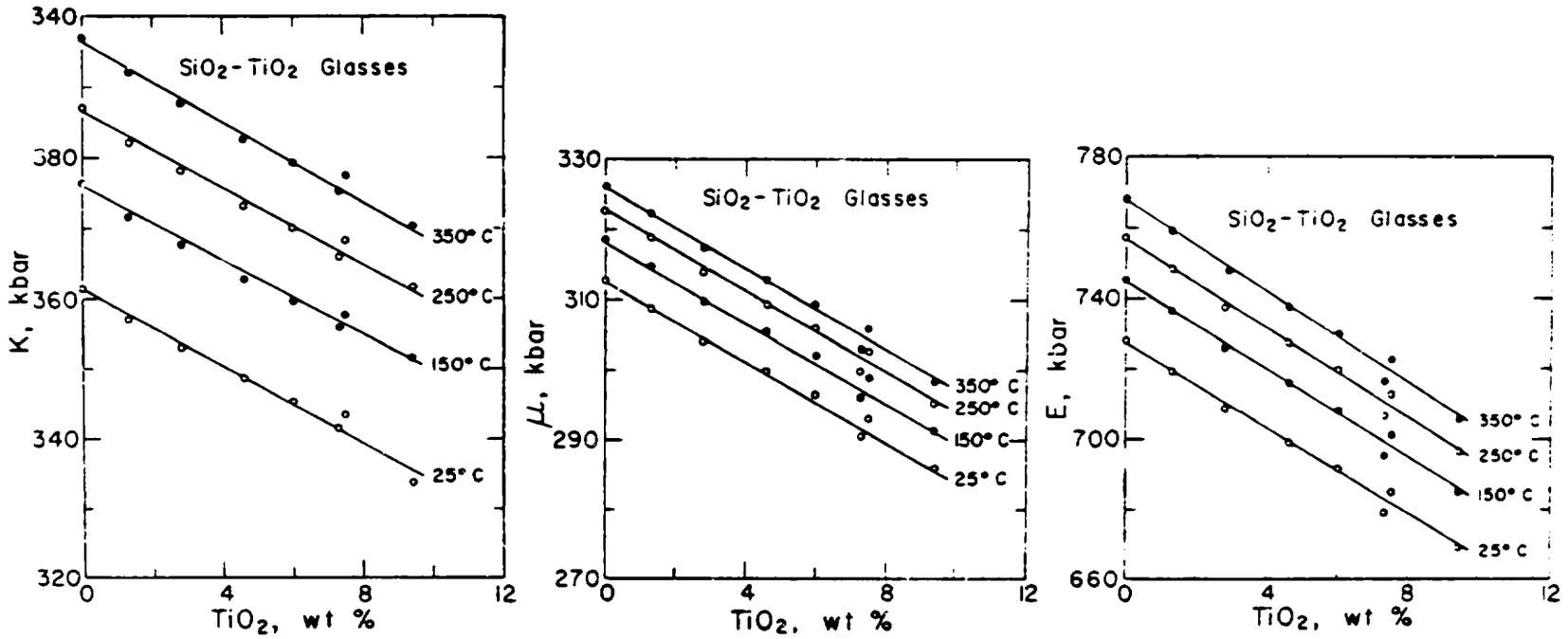

Fig. 9. Bulk (K), shear (μ), and Young's (E) moduli versus TiO_2 content for SiO_2-TiO_2 glasses at different temperatures.

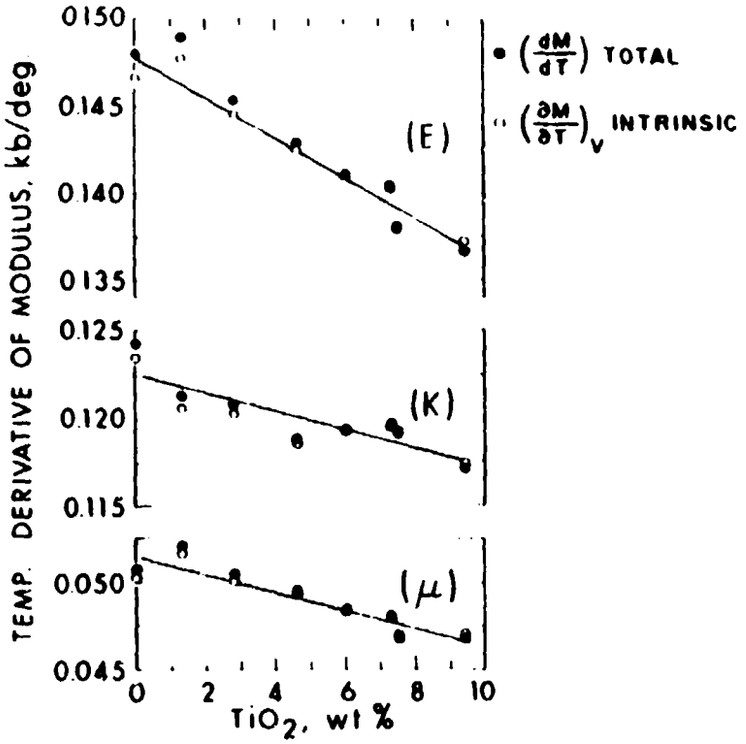

Fig. 10. Composition dependence of the total and intrinsic temperature derivatives of bulk (K), shear (μ), and Young's (E) moduli of SiO_2-TiO_2 glasses.

$$\left(\frac{dM}{dT}\right)_P = \left(\frac{\partial M}{\partial T}\right)_V - \alpha K \left(\frac{\partial M}{\partial P}\right)_T .$$

(total) (intrinsic) (extrinsic)

Using the data of Tables 1 and 2, and the thermal expansion coefficients [6], the two contributions were calculated (Table 3). As seen, the main contributions to total (dM/dT) are from the intrinsic effect (see also Fig. 10).

Summary and Conclusions

The density and elastic parameters of the SiO_2-TiO_2 glasses studied show more or less systematic variation with composition.

V_p, V_s, ρ, E, K, and μ decrease more or less linearly with increase in TiO_2 content. Poisson's ratio for the unannealed glasses first increases and then decreases with increase in TiO_2 content, whereas the annealed glasses show increasing values of σ in a systematic manner. The systematic variations of elastic properties indicate that the coordination number of Ti^{4+} ions remains the same [4] in this range of composition; this is in agreement with earlier studies.

Annealing causes density and V_s to increase, and V_p to decrease. The temperature-dependence of moduli is mainly due to intrinsic effect for these glasses. The temperature derivatives of moduli are positive and anomalous, and become less anomalous with increase in TiO_2 content.

Table 3. Intrinsic and extrinsic contributions to the total temperature derivatives of bulk (k) and shear (μ) moduli in SiO_2-TiO_2 glasses

Glass	TiO_2 wt.%	$\frac{dK}{dT}$ (total)	= $\left(\frac{\partial K}{\partial T}\right)_V$ (intrinsic)	$-\alpha K\left(\frac{\partial K}{\partial P}\right)_T$ (extrinsic)	$\frac{d\mu}{dT}$ (total)	= $\left(\frac{\partial \mu}{\partial T}\right)_V$ (intrinsic)	$-\alpha K\left(\frac{\partial \mu}{\partial P}\right)_T$ (extrinsic)
Fused silica Corning Code 7940	0	.1243	.1235	$+7.89 \times 10^{-4}$	5.08×10^{-2}	5.02×10^{-2}	$+1.67 \times 10^{-6}$
T4A	1.3	.1213	.1206	+7.36	5.21	5.02	+1.50
T1A	2.8	.1208	.1203	+4.99	5.05	5.02	+1.08
T5A	4.6	.1188	.1185	+2.90	4.95	4.93	+0.58
T6A	6.0	.1193	.1193	+0.81	4.84	4.84	+0.16
T2A	7.3	.1196	.1200	-1.01	4.80	4.81	-0.21
ULE7971A	7.5	.1191	.1192	-1.30	4.68	4.69	-0.27
T3A	9.4	.1171	.1174	-3.77	4.68	4.70	-0.82

Adding of TiO_2 to SiO_2 structure causes pressure derivatives of the velocities and moduli to become more negative (i.e., more anomalous). That is, the anomalous behavior of fused silica is enhanced by addition of TiO_2. In contrast, the temperature dependence of moduli is less anomalous as TiO_2 is added.

The acoustic mode gammas, γ_{HT}, become negative when TiO_2 content of glass increases. This is in agreement with the thermal expansion studies. Decrease in thermal expansion with addition of TiO_2 is related to the influence of TiO_2 on acoustic lattice vibration frequencies.

References

[1] D.L. Evans, J. Amer. Ceram. Soc. 53, 63 (1970).

[2] M.E. Nordberg, U.S. Pat. 2,326,059 (1943).

[3] Corning Glass Works, Low Expansion Materials Bulletin (1969).

[4] R.W. Ricker and F.A. Hummel, J. Amer. Ceram. Soc. 34, 271 (1951).

[5] R.C. DeVries, R. Roy, and E.F. Osborn, Trans. Brit. Ceram. Soc. 53, 525 (1954).

[6] P. Schultz and H.T. Smyth, in Amorphous Materials, edited by R.W. Douglas and B. Ellis, Wiley-Interscience, New York, 453 (1972).

[7] P.C. Schultz, U.S. Pat. 3,690,855 (1972).

[8] P.C. Schultz, abstract of paper presented at the 6th All-Union Conference on the Structure of Glass, Leningrad, March 1975.

[9] J. Arndt, Proceed. 4th International Conference on High Pressure, Kyoto, 1974, The Physico-Chemical Society of Japan, 317 (1975).

[10] A. Dietzel, Naturwissenschaften 31, 22 (1943).

[11] M.A. Bezborodov and I.I. Kisel, Diklady Akad. Nauk S.S.S.R. 103, 1073 (1955).

[12] D.S. Carson and R.D. Maurer, J. Non-cryst. Solids 11, 368 (1973).

[13] G.J. Copley, A.D. Redmond and B. Yates, Phys. Chem. Glasses 14, 73 (1973).

[14] W.A. Plummer and H.E. Hagy, Appl. Optics 7, 825 (1968).

[15] C.R. Kurkjian and G.E. Peterson, Phys. Chem. Glasses 15, 12 (1974).

[16] R.C. Turnbull and W.G. Lawrence, J. Amer. Ceram. Soc. 35, 48 (1952).

[17] H.J.L. Trap and J.M. Sterels, Phys. Chem. Glasses 1, 107 (1960).

[18] C. Hirayama and D. Berg, Phys. Chem. Glasses 2, 145 (1961).

[19] M.H. Manghnani, J. Amer. Ceram. Soc. 55, 360 (1972).

[20] J.H. McSkimin, J. Acoust. Soc. Amer. 33, 12 (1961).

[21] O.L. Anderson and G.J. Dienes, Chap. 18 in Non-Crystalline Solids, edited by V.D. Fretchette, John Wiley & Sons, Inc. New York (1960).

[22] T.H.K. Barron, Phil. Mag. 46, 720 (1955).

[23] D.E. Schuele and C.S. Smith, J. Phys. Chem. 25, 801 (1964).

[24] F. Birch, J. Geophys. Res. 57, 227 (1952).

PUBLISHED PAPERS

PRESSURE AND TEMPERATURE DEPENDENCE OF THE ELASTIC MODULI OF Na_2O-TiO_2-SiO_2 GLASSES

By

Murli H. Manghnani

(HIG Contribution No. 453)

Reprinted from the Journal of The American Ceramic Society, Vo. 55, No 7 July, 1972

Pressure and Temperature Dependence of the Elastic Moduli of Na_2O-TiO_2-SiO_2 Glasses

MURLI H. MANGHNANI*

Hawaii Institute of Geophysics, University of Hawaii, Honolulu, Hawaii 96822

Ultrasonic interferometry was used to measure elastic-wave velocities and moduli in six Na_2O-TiO_2-SiO_2 glasses; three glasses contained 20 mol% TiO_2 and three 25 mol% TiO_2. The elastic moduli and their pressure derivatives varied systematically with the SiO_2/Na_2O molar ratio of the glasses. In the group of glasses which contained 20 mol% TiO_2, dK/dP (K = bulk modulus) decreased linearly from 4.85 to 2.58 as the SiO_2/Na_2O ratio increased; in the other group, dK/dP decreased from 4.00 to 3.05. Similarly, $d\mu/dP$ (μ = shear modulus) decreased with the SiO_2/Na_2O ratio, but somewhat nonlinearly. The extrinsic and intrinsic contributions to the temperature dependencies of the elastic moduli are evaluated in light of the measured pressure dependencies of these moduli.

I. Introduction

THE glass-forming areas of the ternary system Na_2O-TiO_2-SiO_2 have been surveyed by Hamilton and Cleek[1] and by Bayer and Hoffmann.[2] Hamilton and Cleek[1] and Turnbull and Lawrence,[3] who investigated the effect of compositional variation on the physical and optical properties of the Na_2O-TiO_2-SiO_2 glasses, found that their densities and refractive indices increased with increasing TiO_2 content. Various investigations of the effect of TiO_2 content on the thermal expansion, viscosity, and electrical properties of Na_2O-TiO_2-SiO_2 glasses have been summarized[4]; however, no study of their elastic properties has been reported. It was the purpose of the present work to report the elastic properties of these glasses and to investigate the effects of glass composition, pressure, and temperature on their elastic behavior.

Physical properties of silicate glasses, e.g. mechanical strength and elastic moduli, are, in general, related to the density of the Si–O–Si bridges in the random network structure of glass.[5,6] Addition of network-modifying oxides such as Na_2O causes a breakdown of some of the bridges and formation of the relatively weaker Si–O–Na bridges in proportion to the amount of Na_2O added. For example, it has been pointed out[6] that the Young's moduli of glasses in a simple binary Na_2O-SiO_2 system decrease systematically with increasing Na_2O content. The role of network-modifying ions of high field strength, e.g. Ti, in increasing the moduli of silicate glasses has also been emphasized.[7] The effects of the SiO_2/Na_2O molar ratio and TiO_2 content on the elastic properties of the glasses in the Na_2O-TiO_2-SiO_2 system are therefore of interest.

II. Experimental Methods

Pulse-superposition ultrasonic interferometry was used to measure the compressional and shear velocities and thus the elastic moduli of six glasses to 7 kbars and 300°C. The velocity-measuring technique[8] was used previously in studies of the elasticity of glasses under pressure.[9,10] An rf pulse is applied to the transducer which is bonded with resin[†] to the specimen, and the pulse repetition frequency (f) of the rf pulse oscillator is adjusted to cause an echo within a particular pulse-echo train to coincide with an earlier echo in the next train, resulting in maximum intensity of the echo pulses.

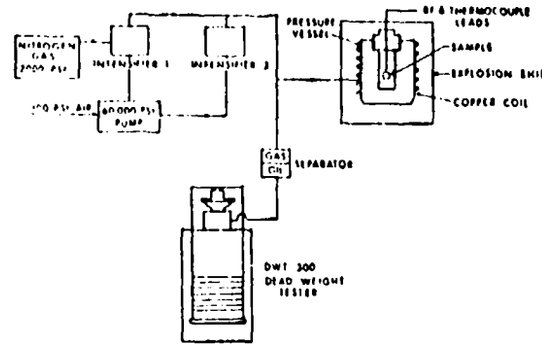

Fig. 1. Pressure-generating system.

Under resonant conditions, f is equal to the reciprocal of the round-trip transit time of the pulse in a specimen of length l, and the velocity is calculated from $v = 2lf$.

The precision of the basic frequency measurement[8] is ≈ 1 part in 10^6. The correction for the phase angle, γ, which is associated with the bond between the transducer and the specimen and the reflections of the waves at the transducer, is given[8] by $\gamma/360f$; γ does not usually exceed 1° to 2° for a well-prepared thin bond. The error in the velocity values resulting from ignoring this correction at ambient and high pressures, as was done in the present study, is believed to be $<0.1\%$ in the range investigated. The moduli reported are estimated to be accurate to within $\pm 0.3\%$ when all the other overall errors, i.e. those in the length and density measurements, are taken into consideration.

X- and Y-cut quartz transducers of 30 MHz natural resonant frequency were used to generate the compressional and shear waves in the specimen. A two-stage pressure-generating system[‡] (Fig. 1) was used in which the initial gas pressure of ≈ 2000 psi was intensified to 40,000 psi in the first stage and 200,000 psi in the second stage. Nitrogen was the pressure medium. Measurements were made following increasing and decreasing pressure cycles to 100,000 psi (≈ 6.9 kbars). An interval of 15 to 20 min was usually allowed between the pressure change and a pulse repetition frequency (prf) measurement. The pressure on the specimen was monitored using

Presented at the 72nd Annual Meeting, The American Ceramic Society, Philadelphia, Pa., May 6, 1970 (Glass Division, No. 28-G-70). Received December 6, 1971; revised copy received March 4, 1972. Contribution No. 453 from the Hawaii Institute of Geophysics.

Supported by the Office of Naval Research under Contracts No. N00014-67-A-0387-0005, NR 032-515, and N00014-67-A-0387-0012, NR 032-527 with the University of Hawaii.

*Part of this work was done at the Air Force Cambridge Research Laboratories, Terrestrial Science Laboratory, Bedford, Mass.

†Resin 276-V9, Dow Chemical Co., Midland, Mich.

‡Harwood Engineering Co., Inc., Walpole, Mass.

Table I. Chemical Compositions of the Na_2O-TiO_2-SiO_2 Glasses

Glass No.	Code No. (Ref. 1)	Constituents (mol%) Na_2O	TiO_2	SiO_2
1	E1986	30.0	20.0	50.0
2	E1909	25.0	20.0	55.0
3	E1990	17.5	20.0	62.5
4	E2011	27.5	25.0	47.5
5	E2010	22.5	25.0	52.5
6	E1991	17.5	25.0	57.5

a 120-Ω Manganin coil placed inside the vessel and a resistance bridge*; the coil was calibrated for pressure with a dead-weight tester† to 60,000 psi. Uncertainties in the absolute pressures measured with the dead-weight tester are estimated[11] to be <0.1% at 60,000 psi. Thus the reported pressure derivatives of the elastic moduli are <±1% in error. During a prf measurement, the test specimen in the pressure vessel was maintained at 25°±0.1°C by constant-temperature water circulating in coils wound around the vessel.

The temperature dependence of the elastic moduli of these glasses was investigated to 300°C by using a thermally insulated furnace powered by a solid-state temperature-control device. A special high-temperature rubber seal was used to bond the transducer to the specimen, which was heated at a rate of ≈2°C/min. Specimen temperature was increased in intervals of ≈10°C and maintained to ±0.1°C during prf measurements.

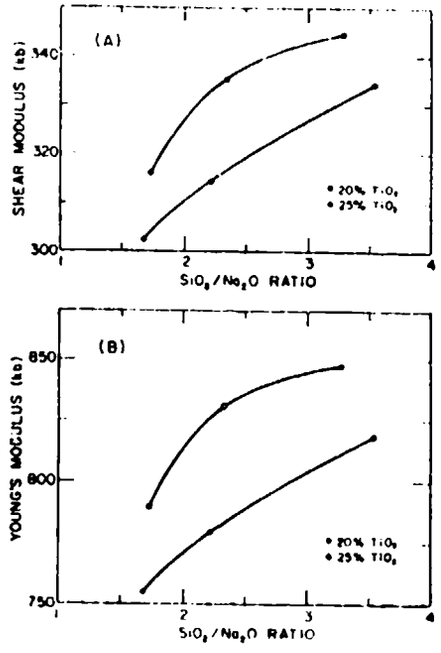

Fig. 2. Plots of *(A)* shear modulus and *(B)* Young's modulus vs SiO_2/Na_2O ratio in Na_2O-TiO_2-SiO_2 glasses.

III. Specimens

The physical properties of glass specimens from the same batch as those used in the present study† were reported by Hamilton and Cleek†; their compositions are given in Table I. All the specimens were heated for 4 to 6 h at a temperature ≈40°C below the sag point and cooled at 2.5°C/h to 350°C (see Ref. 1).

Investigation[1,3] of the crystallization behavior of glasses in the system Na_2O-TiO_2-SiO_2 has shown that those with compositions similar to those in Table I form in homogeneous phases. Phase separation occurs only when the TiO_2 content is higher (>30 mol%) and/or the SiO_2 content lower (<10 mol%). Variations in the elastic moduli, measured under atmospheric conditions in three mutually perpendicular directions in each of the six specimens, were within experimental error, thus characterizing the isotropic behavior of the specimens.

IV. Discussion of Results

(1) Measurements at 1 Bar and 25°C

The elastic properties of the glasses measured at 1 bar and 25°C are given in Table II. The relations between these properties and chemical composition can be interpreted in terms of the SiO_2/Na_2O ratio or in terms of the structural parameter Y, as introduced by Trap and Stevels[10] in discussing SiO_2-based glasses. The parameter Y, which represents the number of bridging oxygen ions/SiO_4 tetrahedron, is computed as $Y=6-200/p$, where p is the SiO_2 content (in mol%). Thus, for pure SiO_2 glass $Y=4$; it decreases as network-modifying oxides are introduced. In the present case, the SiO_2/Na_2O ratio and Y parameter (Table II) have the same significance in that both represent a measure of the number of Si–O–Si bridges and the openness of the structure. For glasses with similar TiO_2 contents, the compressional and shear wave velocities (v_p and v_s) and the shear and Young's moduli (μ and E) increase and the density (ρ) and Poisson's ratio (σ) decrease with increasing SiO_2/Na_2O ratio (and Y). These increases in μ and E are not linear (Fig. 2); the rate of increase is greater for the lower SiO_2/Na_2O ratios. Figure 2 also shows that increasing the TiO_2 content increases the moduli; further, for the glasses with the higher TiO_2 content the effect of the SiO_2/Na_2O ratio in increasing the moduli is less. The relations shown in Fig. 2 can be used to estimate the moduli of glasses of intermediate composition.

The bulk modulus, K, varies neither as appreciably nor as uniformly as the other moduli with the SiO_2/Na_2O ratio. Comparison of the data for glasses 1 and 3 and for glasses 4 and 6 shows that the lower the SiO_2/Na_2O ratio, the higher the bulk modulus (and the lower the compressibility). Similar findings

*Carey-Foster bridge, Harwood Engineering Co., Inc.
†DWT 300, Harwood Engineering Co., Inc.
†Obtained through the courtesy of G. W. Cleek, National Bureau of Standards, Washington, D. C.

Table II. Elastic Properties of the Na_2O-TiO_2-SiO_2 Glasses at 1 Bar and 25°C

Glass No.	SiO_2/Na_2O molar ratio	Y	ρ (g/cm³)	v_p (km/s)	v_s (km/s)	K (kbars)	μ (kbars)	E (kbars)	σ
1	1.67	2.00	2.749	5.731	3.315	500.0	302.1	754.4	0.249
2	2.22	2.36	2.740	5.794	3.386	501.1	314.1	779.5	.241
3	3.54	2.80	2.703	5.895	3.516	493.9	334.2	818.0	.224
4	1.73	1.79	2.811	5.806	3.353	526.4	315.9	789.8	.250
5	2.33	2.19	2.800	5.906	3.461	529.5	334.5	830.7	.239
6	3.28	2.52	2.771	5.955	3.526	523.4	344.5	847.5	.230

NOTE: Y=structural parameter, ρ=density, v_p=compressional wave velocity, v_s=shear wave velocity, K=bulk modulus, μ=shear modulus, E=Young's modulus, and σ=Poisson's ratio.

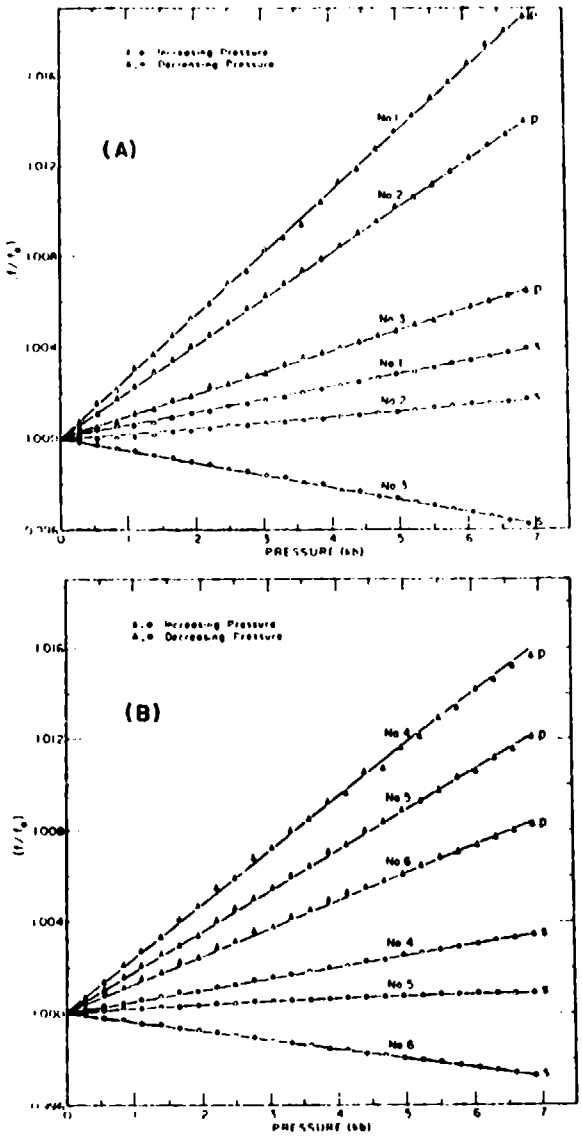

Fig. 3. Plots of frequency ratio, f/f_o, vs pressure for *(A)* glasses containing 20% TiO_2 and *(B)* glasses containing 25% TiO_2 (*p* indicates longitudinal wave; *s*, shear wave).

were reported by Weir and Shartsis[17] in their study of alkali silicate glasses. The explanation for the decrease in compressibility with decreasing SiO_2/Na_2O ratio is that the degree of atomistic void-space in the glass structure diminishes with the introduction of Na_2O.

(2) Measurements Under Pressure

Plots of the prf ratio, f/f_o, where f and f_o are the frequencies at a given pressure and at 1 bar, respectively, vs pressure for the longitudinal and shear modes of wave propagation are shown in Fig. 3. These relations exhibit no hysteresis, indicating that the glasses are completely elastic in this pressure range and do not undergo the permanent densification that may occur at much higher pressures.

(A) Densification Densification of silica and silicate glasses under pressure has been the subject of several studies.[15-18] Bridgman and Simon[15] reported that vitreous SiO_2 undergoes a permanent densification of 7% at 200 kbars and that no observable densification occurs below 100 kbars, whereas Cohen and Roy[16] achieved a 7% densification of SiO_2 glass at only 55 kbars. The threshold pressure and the rate of increase of density are functions of glass composition and temperature and the degree of the nonhydrostatic nature of the applied pressure. It has also been pointed out[18] that the shearing effect under nonhydrostatic conditions is important in densification. The densification of a silicate glass is regarded as the "folding up" of its disordered vitreous structure, such that the Si–O bond angles are altered without apparent changes in the tetrahedral Si–O distances. Most studies of the densification of glasses have been conducted at very high pressures.[15,16]

In situ densification at pressures much lower than the threshold pressures, in the pressure range in which the behavior of the glasses is completely elastic, can be studied precisely using ultrasonic measurements. The specimen length and density ratios (l/l_o and ρ/ρ_o) at pressure P are given by[19]:

$$(l/l_o) = (\rho_o/\rho)^{1/3} = \left[1 + \frac{1+\alpha\gamma T}{\rho_o}\int_0^P \frac{dP}{3A-4B}\right]^{1/3} \qquad (1)$$

where α is the coefficient of volumetric thermal expansion, γ is the Gruneisen parameter, T is the temperature (°K), $A = \nu_{po}(f/f_o)^2$, and $B = \nu_{so}(f/f_o)^2$; the zero subscripts indicate values under ambient conditions (1 bar and 25°C). Using Eq. (1), ρ/ρ_o at pressures to ≈7 kbars was calculated for all the glasses; in all cases, the relation between ρ/ρ_o and P was linear. The ρ/ρ_o values at 6.9 kbars are listed in Table III. The glasses with the higher SiO_2/Na_2O ratios show the greater compression (i.e. have higher ρ/ρ_o values), and those with the lower TiO_2 content (glasses 1–3) exhibit a more pronounced effect of increasing SiO_2/Na_2O ratios in increasing compression.

(B) Pressure Derivatives of Elastic Properties: The velocities (ν_p and ν_s) and the elastic moduli at a given pressure were calculated from the measured prf's for the compressional and shear modes (f_p and f_s):

Compressional velocity, $\nu_p = 2lf_p$.
Shear velocity, $\nu_s = 2lf_s$.
Bulk modulus, $K = \rho(\nu_p^2 - {}^4/_3\nu_s^2)$.
Shear modulus, $\mu = \rho\nu_s^2$.
Young's modulus, $E = (9K\mu)/(3K+\mu)$.
Poisson's ratio, $\sigma = 1 - (E/2\mu)$.

The pressure derivatives thus determined (Table III) are systematically related to composition, i.e. to the SiO_2/Na_2O ratio. The relation between the elastic-wave velocities (ν_p and ν_s) and pressure is shown in Fig. 4; ν_p increases with pressure in all cases. The value of $(d\nu_s/dP)$ is positive and decreases with increasing SiO_2/Na_2O ratio, whereas $(d\nu_s/dP)$

Table III. Pressure Derivatives of the Elastic Properties of the Na_2O-TiO_2-SiO_2 Glasses

Glass No.	$d\nu_p/dP$ (km/s-Mbars)	$d\nu_s/dP$ (km/s-Mbars)	dK/dP	$d\mu/dP$	dE/dP	$d\sigma/dP$ (Mbars^{-1})	ρ/ρ_o (at 6.9 kbars)
1	12.0	−0.20	4.85	0.53	2.29	1.57	1.0130
2	8.03	−1.24	3.68	0.37	1.76	1.34	1.0132
3	1.69	−4.19	2.69	−0.15	0.47	1.24	1.0136
4	9.69	−0.35	4.00	0.51	2.03	1.19	1.0125
5	6.70	−1.64	3.64	0.29	1.56	1.25	1.0126
6	3.43	−3.55	3.05	−0.06	0.73	1.29	1.0128

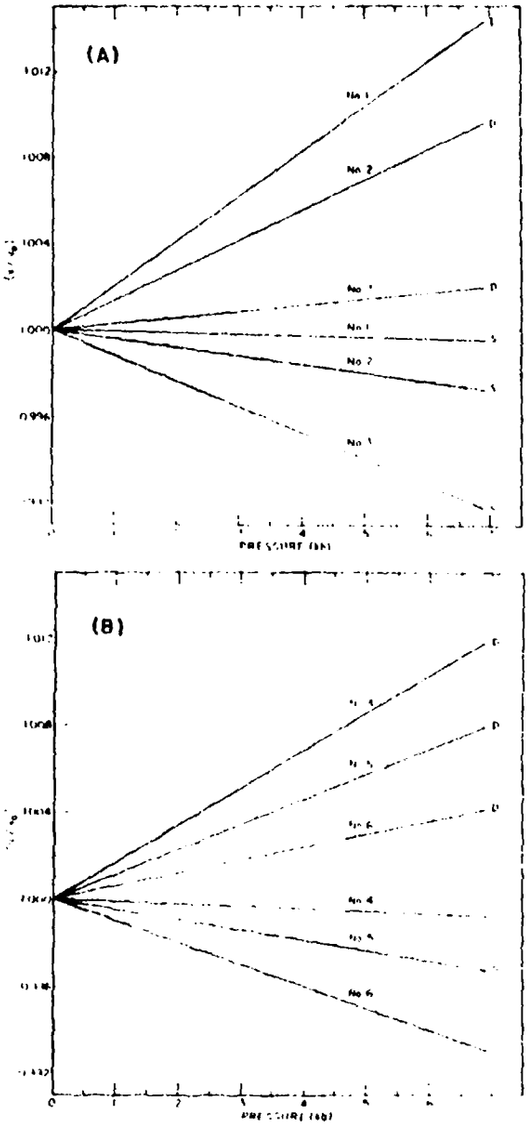

Fig. 4. Plots of velocity ratio, v/v_0, vs pressure for (*A*) glasses Nos. 1–3 and (*B*) glasses Nos. 4–6 (*p* indicates longitudinal wave; *s*, shear wave; v_0, velocity at 1 bar).

is negative and becomes increasingly negative with increasing SiO_2/Na_2O ratio.

For all the glasses, the bulk modulus increases with pressure (Fig. 5(A)); this behavior is normal. For most crystalline oxide solids, dK/dP varies from 4 to 6 at pressures near zero; for the glasses investigated, dK/dP varied from 2.59 to 4.85. In general, dK/dP decreases linearly with increasing SiO_2/Na_2O ratio (Fig. 6(*A*)). However, the relations clearly differ with TiO_2 content. It is predicted that dK/dP will be zero for the glass with 20 mol% TiO_2 and an SiO_2/Na_2O ratio of 22.9. The shear modulus decreases with pressure for glasses 3 and 6 (which have the maximum SiO_2/Na_2O ratio) and increases with pressure for the other glasses (Fig. 5(B)). Further, in contrast to the relation between dK/dP and the SiO_2/Na_2O ratio, which is linear, that between $d\mu/dP$ and the SiO_2/Na_2O ratio is not (Fig. 6(B)).

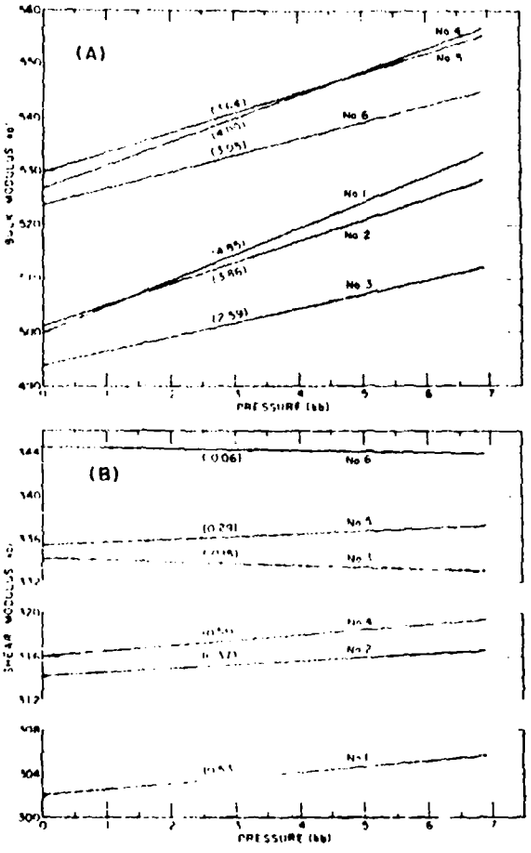

Fig. 5. Pressure dependence of (*A*) bulk modulus and (*B*) shear modulus for the glasses; pressure derivatives are given in parentheses.

For all the glasses studied, dE/dP ranges from 2.29 to 0.47 and decreases with increasing SiO_2/Na_2O ratio. The values of $d\sigma/dP$ are positive and range from 1.19 to 1.57/Mbar (Fig. 7).

(3) *Measurements to 300°C at 1 Bar*

The temperature dependence of elastic moduli is a measure of changes in the intrinsic structure of a material and involves both the odd- and even-powered terms of the anharmonic expansion. The effects of temperature on the elastic properties were investigated to 300°C. The variation with temperature, T, of any modulus, M, is given by:

$$\frac{M_T}{M_0} = \frac{\rho_T}{\rho_0}\left(\frac{f_T}{f_0}\right)^2\left(\frac{l_T}{l_0}\right)^2 = \left(\frac{f_T}{f_0}\right)^2\frac{l_0}{l_T} \qquad (2)$$

The length ratio (l_0/l_T) was estimated from thermal expansion data[14] and used to compute the elastic moduli. Figure 8 and Table IV show the temperature dependencies of the bulk and shear moduli. The dK/dT and $d\mu/dT$ values become increasingly negative with increasing temperature and, for a given temperature, become systematically less negative with increasing SiO_2/Na_2O ratio. This result is obviously related to the anomalous temperature behavior of vitreous SiO_2, which is known to exhibit positive dM/dT values[15,16] ($dK/dT = 0.111$ kbars/°C; $d\mu/dT = 0.045$ kbars/°C). Thus, as the amount of SiO_2 in the composition of Na_2O-TiO_2-SiO_2 glasses increases, dM/dT becomes less negative (more positive). The relations between dK/dT and $d\mu/dT$ and the SiO_2/Na_2O ratio, although

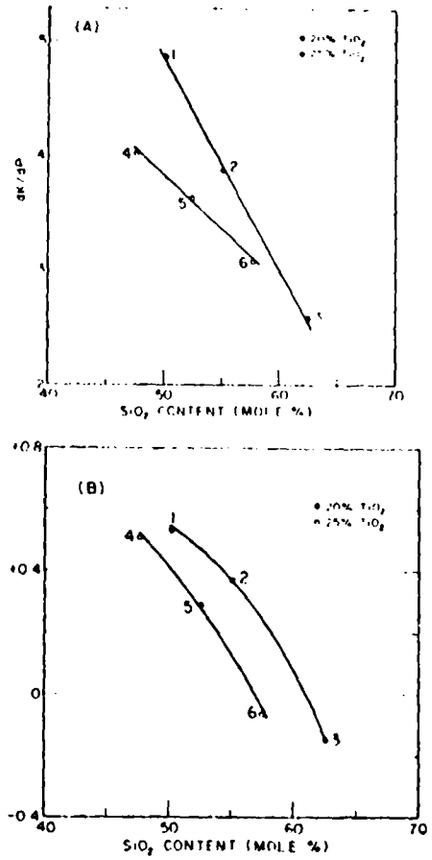

Fig. 6. Relation between *(A) dK/dP* and *(B) dμ/dP* and SiO_2 content for Na_2O-TiO_2-SiO_2 glasses.

nonlinear, can be used to predict the elastic behavior of Na_2O-TiO_2-SiO_2 glasses under various temperature conditions.

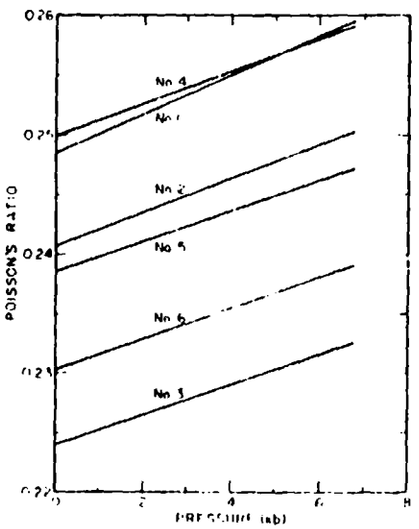

Fig. 7. Poisson's ratio as a function of pressure for the glasses.

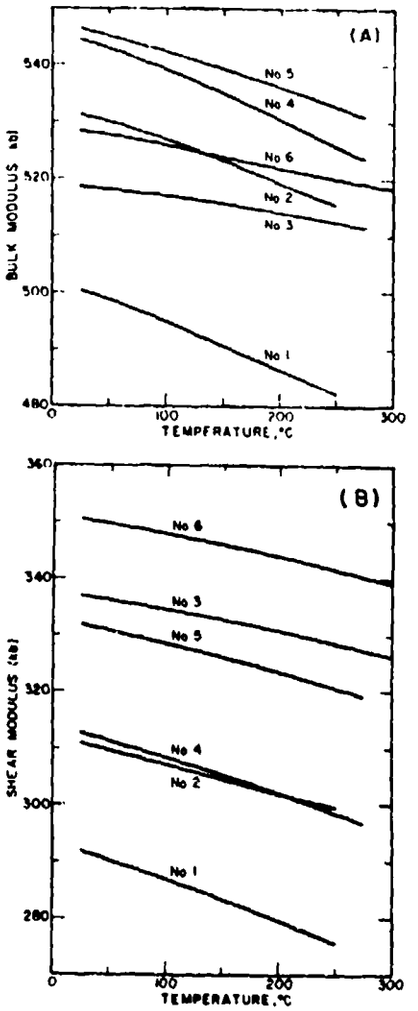

Fig. 8. Temperature dependence of *(A)* bulk modulus and *(B)* shear modulus of Na_2O-TiO_2-SiO_2 glasses.

The total temperature derivative of an elastic modulus, M, given by $(dM/dT)_P$, is related to the intrinsic (temperature) and extrinsic (volume) effects by

$$\left(\frac{dM}{dT}\right)_P = \left(\frac{\partial M}{\partial T}\right)_V - \alpha K \left(\frac{\partial M}{\partial P}\right)_T \qquad (3)$$

where α is the coefficient of volumetric thermal expansion. Using the data given in Tables II through IV, the intrinsic and extrinsic coefficients in Eq. (3) were calculated (Table V). In all cases, $(dK/dT)_P$ is negative and $(\partial K/\partial T)_V$ is positive, implying that the sign of $(dK/dT)_P$ is governed by the sign of $(\partial K/\partial P)_T$, i.e. that the observed temperature dependence of K results primarily from volume change (thermal expansion). The contribution to $(dK/dT)_P$ of the intrinsic (temperature) effect, with opposite sign, varies from 1 to ≈44%, of the observed $(dK/dT)_P$. In the case of the temperature dependence of μ, the main contribution to $(d\mu/dT)_P$ is the intrinsic (temperature) effect; very small contributions result from volume change. In the case of glasses 3 and 6, which have higher SiO_2/Na_2O ratios than the other two specimens in a series of glasses with similar TiO_2 contents, the sign of the contribution from the extrinsic effect (volume change) is opposite to that

Table IV. Temperature Dependence of the Elastic Properties of Na_2O-TiO_2-SiO_2 Glasses

Glass No.	Linear thermal expansion coeff. ($\times 10^7$)	SiO_2/Na_2O molar ratio	K (kbars)	μ (kbars)	σ	dK/dT (kbars/°C)	$d\mu/dT$ (kbars/°C)	$d\sigma/dT$ (°C$^{-1}\times 10^5$)
1	134	1.67	500.3	291.8	0.256	−0.081	−0.071	1.7
2	116	2.22	531.1	310.9	.255	−0.070	−0.051	0.7
3	89	3.54	518.6	336.9	.233	−0.025	−0.036	1.3
4	124	1.73	544.2	312.6	.259	−0.080	−0.063	1.0
5	107	2.33	546.4	331.9	.247	−0.057	−0.048	0.9
6	89	3.28	528.3	350.3	.228	−0.035	−0.038	1.0

Table V. Intrinsic and Extrinsic Coefficients for Eq. (3)*

Glass No.	Measured $\left(\frac{dM}{dT}\right)_P$ (kbars/°C)	Calculated $\left(\frac{\partial M}{\partial T}\right)_V$ (kbars/°C)	Measured $\alpha K\left(\frac{\partial M}{\partial P}\right)_T$ (kbars/°C)
		M=bulk modulus, K	
1	−0.081	+0.0165 (20.4)†	−0.0975 (120.4)
2	−0.070	+0.0013 (1.9)†	−0.0713 (101.9)
3	−0.025	+0.0109 (43.6)†	−0.0359 (143.6)
4	−0.080	+0.0010 (1.3)†	−0.0810 (101.3)
5	−0.057	+0.0068 (11.9)†	−0.0638 (111.9)
6	−0.035	+0.0080 (22.9)†	−0.0430 (122.9)
		M=shear modulus, μ	
1	−0.071	−0.0603 (84.9)	−0.0107 (15.1)
2	−0.051	−0.0442 (86.7)	−0.0068 (13.3)
3	−0.036	−0.0381 (105.8)	+0.0021 (5.8)†
4	−0.063	−0.0527 (83.7)	−0.0103 (16.3)
5	−0.048	−0.0429 (89.4)	−0.0051 (10.6)
6	−0.038	−0.0388 (102.1)	+0.0008 (2.1)†

*Contributions to total effect (in %) are shown in parentheses.
†Sign is opposite that of dM/dT.

of $(d\mu/dT)_P$ because $(d\mu/dP)_T$ in these cases is negative. When the temperature variations of both K and μ are considered (Table V), a tendency of the extrinsic effect (volume change) to decrease with decreasing SiO_2/Na_2O ratio is noted.

V. Summary

(1) The elastic moduli of the Na_2O-TiO_2-SiO_2 glasses vary systematically with composition; the SiO_2/Na_2O ratio is the most important factor. A network-modifying oxide such as TiO_2 increases the moduli and their pressure derivatives.

(2) The Na_2O-TiO_2-SiO_2 glasses studied behave as normal crystalline solids under pressure and temperature except for Nos. 3 and 6, which exhibit negative $d\mu/dP$ values. This anomaly is related to the vitreous SiO_2 content. The pressure and temperature derivatives of the moduli vary systematically but not always linearly with the SiO_2/Na_2O ratio. These relations can be used to predict the elastic behavior of glass at moderately high pressures and temperatures.

(3) The observed effect of temperature on the bulk moduli of the glasses investigated results primarily from volume changes associated with thermal expansion. The temperature dependence of shear moduli of these glasses, however, is related principally to the intrinsic (temperature) effect.

Acknowledgments

The writer wishes to express his gratitude to Given Cleek, National Bureau of Standards, Washington, D. C., for making the glass specimens available for this study. Part of the work was conducted during a National Research Council–National Academy of Sciences senior postdoctoral research associateship tenable at the Air Force Cambridge Research Laboratories, Bedford, Mass. Thanks are due Ethel McAfee for invaluable editorial help.

References

[1] E. H. Hamilton and G. W. Cleek, "Properties of Sodium Titanium Silicate Glasses," *J. Res. Nat. Bur. Stand.*, **61** [2] 89–94 (1958).
[2] G. Bayer and W. Hoffmann, "Primary Crystallization of Glasses in the System Na_2O-TiO_2-SiO_2 and Its Relation to Immiscibility," *Glass Technol.*, **7** [3] 94–97 (1966).
[3] R. C. Turnbull and W. G. Lawrence, "Role of Titania in Silica Glasses," *J. Amer. Ceram. Soc.*, **35** [2] 48–53 (1952).
[4] M. D. Beals and J. H. Strimple, "Effects of Titanium Dioxide in Glass: IV," *Glass Ind.*, **44** [12] 679–83, 94 (1963).
[5] R. J. Charles; pp. 1–38 in Progress in Ceramic Science, Vol. 1. Edited by J. E. Burke. Pergamon Press Inc., Elmsford, N. Y., 1961.
[6] H. T. Smyth, "Elastic Properties of Glasses," *J. Amer. Ceram. Soc.*, **42** [6] 276–79 (1959).
[7] K. L. Lowenstein, "Studies in the Composition and Structure of Glasses Possessing High Young's Moduli: I," *Phys. Chem. Glasses*, **2** [3] 69–82 (1961).
[8] H. J. McSkimin, "Pulse Superposition Method for Measuring the Ultrasonic Wave Velocities in Solids," *J. Acoust. Soc. Amer.*, **33** [1] 12–16 (1961).
[9] M. H. Manghnani and W. M. Benzing, "Pressure Derivatives of Elastic Moduli of Vycor Glass to 8 Kilobars," *J. Phys. Chem. Solids*, **30** [9] 2241–45 (1969).
[10] T. J. Sokolowski and M. H. Manghnani, "Adiabatic Elastic Moduli of Vitreous Calcium Aluminates to 3.5 Kilobars," *J. Amer. Ceram. Soc.*, **52** [10] 539–42 (1969).
[11] D. P. Johnson and D. H. Newhall, "Piston Gage as a Precise Pressure-Measuring Instrument," *Trans. ASME*, **75**, 301–10 (1953).
[12] H. J. L. Trap and J. M. Stevels, "Conventional and Invert Glasses Containing Titania: I," *Phys. Chem. Glasses*, **1** [4] 107–18 (1960).
[13] C. E. Weir and L. Shartsis, "Compressibility of Binary Alkali Borate and Silicate Glasses at High Pressures," *J. Amer. Ceram. Soc.*, **38** [9] 299–306 (1955).
[14] P. W. Bridgman and I. Simon, "Effect of Very High Pressures on Glass," *J. Appl. Phys.*, **24** [4] 405–13 (1953).
[15] H. M. Cohen and R. Roy, "Densification of Glass at Very High Pressure," *Phys. Chem. Glasses*, **6** [5] 149–61 (1965).
[16] E. B. Christiansen, S. S. Kistler, and W. B. Gogarty, "Irreversible Compressibility of Silica Glass as a Means of Determining Distribution of Force in High-Pressure Cells," *J. Amer. Ceram. Soc.*, **45** [4] 172–77 (1962).
[17] R. K. Cook, "Variation of Elastic Constants and Static Strains with Hydrostatic Pressure: Method for Calculation from Ultrasonic Measurements," *J. Acoust. Soc. Amer.*, **29** [4] 445–49 (1957).
[18] J. H. Strimple and E. A. Giess, "Glass Formation and Properties of Glasses in the System Na_2O-B_2O_3-SiO_2-TiO_2," *J. Amer. Ceram. Soc.*, **41** [7] 231–37 (1958).
[19] G. J. Dienes, "Temperature-Dependence of the Elastic Moduli of Vitreous Silica," *J. Phys. Chem. Solids*, **7** [4] 290–94 (1958).
[20] O. L. Anderson and G. J. Dienes; Chapter 18 in Non-Crystalline Solids. Edited by V. D. Frechette. John Wiley & Sons, Inc., New York, 1960.

INFRARED SPECTRA OF SEVERAL GLASSES AT HIGH PRESSURES

By

J. R. Ferraro, M. H. Manghnani, and A. Quattrochi

(HIG Contribution No. 414)

Infrared spectra of several glasses at high pressures*

J. R. Ferraro, M. H. Manghnani,† & A. Quattrochi‡

Chemistry Division, Argonne National Laboratory, Argonne, Illinois

The infrared absorption spectra of crystalline α-quartz, fused silica, and Pyrex and Vycor (Corning Glass Works) glasses were studied at pressures up to 58·8 kb. The spectra of the fused silica and glasses are more simple than those of α-quartz, and their three main absorption bands appear at higher frequencies than in the case of α-quartz. The intertetrahedral Si stretching mode at ~800 cm⁻¹ is found to be comparatively more sensitive to pressure, whereas the intratetrahedral Si-O stretching mode at ~1100 cm⁻¹ is less affected by pressure. The Grüneisen gammas γ_i, calculated from the pressure dependence of the infrared vibration mode frequencies, are compared with the γ_{th} values and those deduced from the pressure dependences of the elastic parameters. The negative γ values are discussed in terms of the anomalous thermal expansion and elastic behaviour of glasses.

Glass is a possible material for the hulls of undersea vehicles and, therefore, there has been considerable interest in the study of its structure and the behaviour under pressure. Various physical tools have been used to characterise the glassy state and to elucidate the structure; one of these is vibrational spectroscopy. Much effort has already been devoted to the infrared study of glasses at ambient temperatures and pressures. Infrared absorption studies have been made on the crystalline polymorphs and the vitreous forms of SiO_2 [1-13] and several Raman studies [14-17] have also been conducted on quartz at high temperatures. More recently the Raman spectrum of α-quartz was studied under pressure.[18] However, the infrared absorption spectra of glasses at high pressures have not been investigated to any great extent.[19]

The basic structure of various polymorphs of silica and silicate glasses consists of SiO_4 groups in which silicon atoms are tetrahedrally bound to four oxygen atoms, each being common to two tetrahedra. Thus, each oxygen atom is coordinated to two silicon atoms and six oxygen atoms. In silica based glasses the arrangement of the individual SiO_4 tetrahedra is repeated in a random fashion. The infrared spectra of the silicate glasses correspond to the vibrations of the SiO_4 groups are and characterised by at least three main absorption bands at ~1100, ~800, and ~460 cm⁻¹. Lippincott *et al.*[7] assigned the various absorptions based on a T_d symmetry: the high-frequency absorption, ~1100 cm⁻¹, to the Si–O stretching mode corresponding to the motion of silicon and oxygen atoms in opposite directions within tetrahedra, ←SiO→ ←Si; the intermediate frequency absorption, ~800 cm⁻¹, to the Si stretching mode in which the Si stretches between tetrahedra, ←SiOSi→; and the low frequency absorption, ~460 cm⁻¹, to the bending modes which involve a combination of the O–Si–O bending mode within the tetrahedra, and the Si–O–Si bending mode between the tetrahedra. Normally, this latter absorption appears as a broad band in the infrared; its position has been evaluated in terms of the changes which occur in the Si–O–Si angle between tetrahedral units in the glass structure.[20, 21] Anderson & Dienes[22] have pointed out that the low frequency Si–O–Si bending vibration is responsible for the anomalous behaviour of vitreous silica under pressure (that is the increase in compressibility with pressure). One of the aims of this study was to investigate the pressure dependences of the infrared vibrational frequencies for α-quartz and the silicate glasses, and to correlate the results in terms of their anomalous thermal expansion and elastic behaviour.

Experimental

Corning Glass Works glasses of commercial grade were employed in this study. The specimens were crushed in a ball mill, and finally powdered by extensive grinding in an agate mortar.

The infrared absorption spectra at ambient conditions were obtained by use of a Beckman IR-12 spectrophotometer and the KBr pellet method was used.

An opposed diamond anvil cell linked with a Perkin–Elmer No. 301 spectrophotometer equipped with a 6× beam condenser was used to obtain the low frequency infrared absorption spectra (<650 cm⁻¹) at high pressure. Studies >650 cm⁻¹ at high pressures were made with a Beckman IR-12 equipped with a 6× beam condenser. The powdered sample was loaded in the cell, and the pressure alternately increased and

* Based on work performed under the auspices of the U.S. Atomic Energy Commission. Supported by the Office of Naval Research, contract numbers N00014-67-A-0387-005, NR 032-515, and N00014-67-A-0387-0012, also NR 032-527 with University of Hawaii.

† Resident Associate under the Faculty Research Participation Program. Permanent Address: Hawaii Institute of Geophysics, University of Hawaii, Honolulu. Hawaii Institute of Geophysics, Contribution No. 414.

‡ Present address: U.S. Tobacco Co., Chicago, Illinois

(Reproduced from Physics and Chemistry of Glasses, v. 13, no. 4, p. 116-121 (1972).)

HIG Contribution No. 414

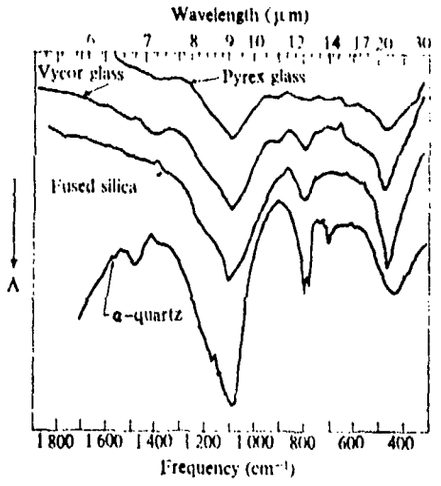

Figure 1. *Infrared spectra of α-quartz and several glasses*

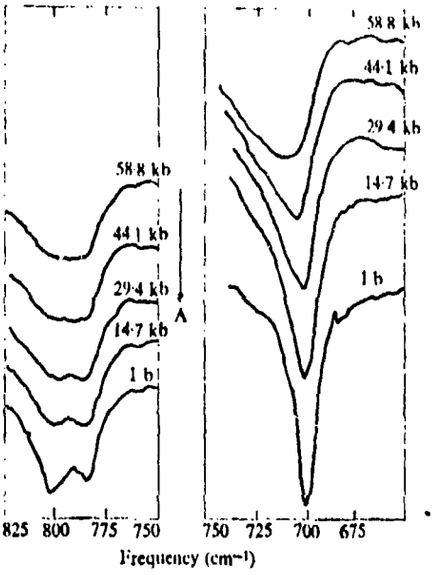

Figure 2. *Pressure dependences of the Si stretching vibrations in α-quartz*

decreased to distribute the material evenly between the anvils. During the pressure cycling the sample was observed under a microscope. A description of the pressure cell and the method used in pressure calibration has been previously reported.[23, 24]

Results

Infrared spectra of α-quartz and silicate glasses

The material α-quartz, belongs to the trigonal system and has a D_3 symmetry with 3 SiO_2 units per primitive unit cell.[25] Thus a total of 24 optical modes of A_1, A_2, and E species are predicted

$$\Gamma = 4A_1(R) + 4A_2(IR) + 8E(IR, R)$$

where R and IR represent the Raman and infrared activity, respectively. The infrared spectrum is observed to be simpler than that predicted by the selection rules using the D_3 symmetry; however, some question has arisen concerning the suitability of assigning the spectrum of α-quartz in terms of a D_3 symmetry as five A_1 polarised Raman active bands are observed instead of the four predicted by the selection rules.

Figure 1 compares the infrared spectra of the three glasses with that of α-quartz. As can be seen, the spectra of the glasses are simpler and have only three main absorption bands, whereas α-quartz shows additional absorptions at ~700 (*w*) and ~1480 cm^{-1} (*m* to *w*), and a doublet is observed near 800 cm^{-1}. The observed frequencies of the major bands at atmospheric pressure are given in Table 1. The three main characteristic absorptions of fused silica and of Vycor and Pyrex glasses are at higher frequencies than those of α-quartz, indicating larger force constants for these vibrations.

Table 1. *Assignments of the principal vibrational frequencies of α-quartz, fused silica, and Vycor and Pyrex glasses*

Vibrational mode	*Frequency (cm^{-1}) in α-quartz*	*Fused silica*	*Vycor*	*Pyrex*
$\delta_{SiOSi} + \delta_{OSiO}$	459	475	469	471
$\nu_{\leftarrow SiOSi\rightarrow}$	783 and 800 (doublet)	815	814	812
$\nu_{\leftarrow SiO\rightarrow \leftarrow Si}$	1082	1087	1100	1095
$\nu_{\leftarrow SiO\leftarrow Si}$	1168	—	—	—
ν_{HO}	—	—	1384	1390

Pressure dependences of the infrared vibrations

α-quartz. Table 2 and Figure 2 present the pressure dependences of the vibrational frequencies of α-quartz. As shown, the frequency of the broad Si–O stretching band at ~1080 cm^{-1} decreases slightly and the shoulder at 1168 cm^{-1} shows negligible change with

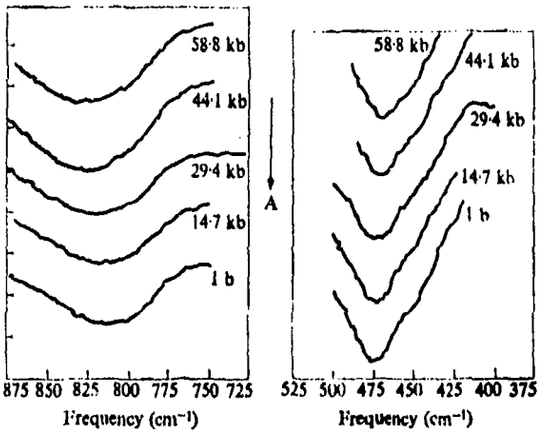

Figure 3. *Pressure dependence in fused silica*
(a) The Si stretching vibration
(b) The SiOSi and OSiO bending vibrations

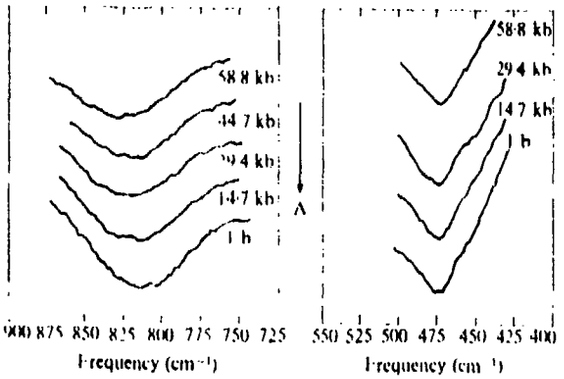

Figure 4. *Pressure dependence in Vycor glass*
(a) The Si stretching vibration
(b) The SiOSi and OSiO bending vibrations

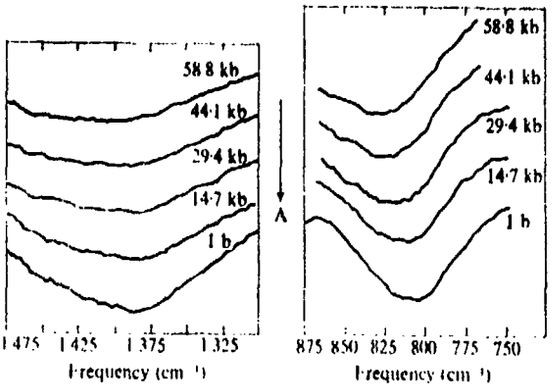

Figure 5. *Pressure dependence in Pyrex glass*
(a) The B–O stretching vibration
(b) The Si stretching vibration

increasing pressure. The Si stretching frequencies at ~700–800 cm⁻¹ and the mixed bending mode at ~460 cm⁻¹ are relatively more sensitive to pressure and have positive dependence. The frequency of the doublet at 783 and 798 cm⁻¹ increases up to ~30 kb, at which pressure it disappears, and a single broad band appears. The latter shows little pressure dependence at higher pressures.

Fused silica. Figure 3 and Table 2 show the effects of pressure on the infrared vibrations of fused silica. The frequency of the mixed bending mode in fused silica near 475 cm⁻¹ decreases with increasing pressure, but that of the Si stretching near 815 cm⁻¹ increases and that of the Si–O stretching mode near 1090 cm⁻¹ shows no change, within experimental error, with increasing pressure.

Vycor and Pyrex glasses. Figures 4 and 5 and Table 2 show the effects of pressure on the vibrational frequencies of Vycor and Pyrex glasses. The frequency of the mixed bending mode for both of these glasses near 469 cm⁻¹ is observed to be independent of pressure. For both glasses, which contain B_2O_3 (3% in Vycor and 13% in Pyrex) the B–O stretching mode at ~1385 cm⁻¹ shifts towards higher frequency. The mode at ~1100 cm⁻¹ decreases in frequency with pressure for Vycor, and is independent of pressure for Pyrex. For both glasses the Si stretching vibration increases in frequency with pressure.

Table 2. *Effect of pressure on the principal vibrational frequencies of crystalline α-quartz, fused silica, and Vycor and Pyrex glasses**

Pressure (kb)	*Frequency (cm⁻¹) Si–O–Si O–Si–O bending*	*Si stretching*	*Si stretching*	*Si–O stretching*	*B–O stretching*
α-quartz					
0·001	459 ± 2	698 ± 2	783 ± 2	1082 ± 3	
14·7	460 ± 2	700 ± 2	785 ± 2	1081 ± 3	
29·4	461 ± 2	702 ± 2	787 ± 2	1081 ± 3	
44·1	463 ± 2	704 ± 2	790 ± 3	1080 ± 3	
58·8	464 ± 2	707 ± 2	792 ± 3	1078 ± 3	
Fused silica					
0·001	475 ± 2		815 ± 3		
14·7	472 ± 2		818 ± 3		
29·4	472 ± 2		820 ± 3		
44·1	471 ± 2 (split at 461·5)		822 ± 3		
58·8	471 ± 2		825 ± 3		
Vycor					
0·001			814 ± 3	1100 ± 3	1384 ± 3
14·7			817 ± 3	1098 ± 3	1386 ± 3
29·4			820 ± 3	1096 ± 3	1387 ± 3
44·1			823 ± 3	1095 ± 3	1390 ± 3
58·8			827 ± 3	1093 ± 3	1392 ± 3
Pyrex					
0·001			812 ± 5		1390 ± 5
14·7			815 ± 5		1392 ± 5
29·4			818 ± 5		1395 ± 5
44·1			822 ± 5		1400 ± 5
58·8			828 ± 5		1405 ± 5

* Only vibrations showing pressure dependence are included.

Discussion

Pressure dependence of the infrared vibrations

The infrared active vibrations studied under pressure may be considered to be of two types, a stretching and a bending type. Among the stretching types, one main absorption band near 1 100 cm^{-1} is related to the Si–O stretching vibration within the tetrahedron (intratetrahedral), and the other band near 800 cm^{-1} is related to the Si stretching, ←SiOSi→, between the tetrahedra (intertetrahedral). Among the bending types, one mode is related to the Si–O–Si bending and the other to O–Si–O bending. The force constant, f_r, related to the intratetrahedral Si–O stretching type vibration is larger than that of either of the two bending types, f_α and f_β. One would, therefore, expect the Si–O bond within the tetrahedron to be comparatively less sensitive to pressure. Similar behaviour of this stretching vibration towards pressure has been found for other compounds involving tetrahedral structure, for example, sulphates and permanganates.[26] In the case of the bending vibration, both an intermolecular vibration, δ_{SiOSi} and an intramolecular vibration, δ_{OSiO}, are involved. The intermolecular mode involves a motion of the atoms during the vibration which is pseudolattice-like and should be sensitive to pressure, and the intramolecular mode should be insensitive to pressure. In a silicate glass the pressure dependences of the intermolecular vibrations are therefore closely related to the compressibility of the glass structure. The increase in frequency indicates a decrease in volume (increase in density) of the glass network, and a concurrent increase in the force constant. The intratetrahedral SiO vibrations are insensitive to pressure, and it is suggested that the individual SiO_4 tetrahedra are not significantly affected by pressure up to the pressures used, and thus the compression occurs along the network whereby the tetrahedra move in closer to one another. This is verified by the results which show that the intermolecular mode, ν_{SiOSi}, is sensitive to pressure. The small sensitivity to pressure of the absorption at 460 cm^{-1} may be due to the fact that both a mode sensitive to pressure (δ_{SiOSi}) and one which is not sensitive (δ_{OSiO}) are found beneath the broad envelope. The net result is to diminish the effect of pressure.

It is of interest to note that the frequency of the Si–O stretching vibration α-quartz decreases with pressure ($d\nu_i/dP = -0{\cdot}07$ cm^{-1}/kb) as given in Table 3. However, frequency changes with pressure could not be ascertained, within the experimental error, for fused silica and the Vycor and Pyrex glasses.

The Si stretching vibrations in α-quartz are represented by absorption bands at 698, 783, and 800 cm^{-1}, the latter two forming a doublet which disappears at pressures above 30 kb as shown in Figure 2. Corresponding Si stretching vibrational frequencies in fused silica and Vycor and Pyrex glasses at zero pressure are 815, 814, and 812 cm^{-1}, respectively. In all cases, there is a systematic increase in the Si stretching frequencies with pressure, the largest increase being in the case of Pyrex glass ($d\nu_i/dP = 0{\cdot}27$ cm^{-1}/kb). The results indicate that the compression of glass takes place along network chains, thus causing the tetrahedra to move closer to one another. This effect appears to follow the order Pyrex > Vycor > fused silica ~ α-quartz, and may be indicative of an ordering process occurring in these glasses under pressure. It is known that when one adds a modifier such as Na_2O to quartz, the frequency of the ν_{SiOSi} vibration at ~800 cm^{-1} is decreased.[4] To accommodate the sodium ions the tetrahedra must move further apart, weakening the force constants and causing a shift to lower frequency. The effects of pressure appear, as one would expect, to give opposite results.

The bending region, manifested by the broad infrared absorption near 460 cm^{-1}, involves motion within as well as between the tetrahedral groups, i.e. O–Si–O within the tetrahedra and Si–O–Si linking the tetrahedra. As the effect of pressure on the former mode is not expected to be very large, any pressure dependence noted for this frequency primarily reflects the change in the vibration of the Si–O–Si bending bond linking the tetrahedra. Borelli & Su[1] as well as other workers have noted that the corresponding Si–O–Si bending force constant, f_β, would be most affected by the degree of disorder in glass structure. One would, therefore, expect to find some interrelation among the three following parameters of glass structure the degree of disorder, the bond angle, β, and the molar volume. However, because of the overlap of two modes occurring at ~460 cm^{-1}, no definite conclusions can be drawn at this time.

As pressure would cause Si–O–Si bond angles in the glass structure to vary, the pressure dependency of the vibrational frequency of the Si–O–Si bending mode must principally reflect a change in the bond angle, β. In the present study the authors found that the 460 cm^{-1} mode shifted towards higher frequency for α-quartz ($d\nu_i/dP = 0{\cdot}09$ cm^{-1}/kb), towards lower frequency for fused silica ($d\nu_i/dP = -0{\cdot}07$ cm^{-1}/kb), and remained unchanged for Vycor and Pyrex glasses as shown in Table 3. These differences between the findings for fused silica and those for Vycor and Pyrex glasses were unexpected, and may be due to the presence of boron in the Vycor and Pyrex glasses.

Thermal expansion and the Grüneisen parameters

Fused silica and Pyrex have negative thermal expansion coefficients, α_V, below 200K but these are reduced by network filling agents such as B_2O_3, Al_2O_3, or Na_2O.[27] In order to explain negative coefficients of thermal expansion it has been suggested that the low frequency transverse vibration of the oxygen atom in the Si–O–Si network, which would be most easily excited at low temperatures, causes the lattice to contract.[28, 29]

The volume coefficient of thermal expansion, α_V, is related through lattice dynamics to specific heat at constant pressure. C_p, the adiabatic bulk modulus, K_s, and the density ρ

$$\alpha_V = \frac{\bar{\gamma}_{th} C_p \rho}{K_s} \qquad (1)$$

Table 3. *Grüneisen parameters calculated for the various glasses*

Mode	ν_i (cm^{-1})	$d\nu_i/dP$ (cm^{-1}/kb)	χ (kb^{-1})[31, 32]	Calculated γ_i
α-quartz				
$\delta_{SiOSi}+\delta_{OSiO}$	459	0·09	0·0026738	0·07
ν_{s} Si–O–Si ν_{as}	698	0·15		0·08
ν_{s} Si–O–Si ν_{as}	783	0·14		0·07
	800	no shift		—
ν_{s} Si–O ν_{as} Si–O–Si	1082	−0·07		−0·02
ν_{s} Si–O–Si	1168	no shift		—
Fused silica				
$\delta_{SiOSi}+\delta_{OSiO}$	475	−0·07	0·0030211	−0·05
ν_{s} Si–O–Si	815	0·17		0·07
ν_{s} Si–O ν_{as} Si	1095	no shift		—
Vycor				
$\delta_{SiOSi}+\delta_{OSiO}$	469	no shift	0·0038183	—
ν_{s} Si–O–Si ν_{as}	814	0·22		0·07
ν_{s} Si–O ν_{as} Si–O–Si	1095	no shift		—
ν_{BO}	1384	0·14		0·03
Pyrex				
$\delta_{SiOSi}+\delta_{OSiO}$	471	no shift(?)	0·002887	
ν_{s} Si–O–Si ν_{as}	812	0·27		0·12
ν_{s} Si–O ν_{as} Si–O–Si	1095	no shift		—
ν_{BO}	1390	0·26		0·06

The $\bar{\gamma}_{th}$ term derived from $\alpha\gamma$ measurements is, in turn, related to the average of the volume dependences of the acoustic and optical mode frequencies, ν_i, weighted by the contribution, C_{p_i}, that each vibrational mode makes to the total specific heat, C_p,

$$\bar{\gamma}_{th} = \frac{\sum_{i=1}^{3n} \gamma_i C_{p_i}}{\sum_{i=1}^{3n} C_{p_i}} \tag{2}$$

where the Grüneisen parameter, γ_i, is determined by

$$\gamma_i = -\frac{d\ln\nu_i}{d\ln V} = \frac{K_T}{\nu_i}\left(\frac{d\nu_i}{dP}\right)_T \tag{3}$$

where, K_T, is the isothermal bulk modulus.

The two limiting values of $\bar{\gamma}_{th}$ (high temperature gamma, γ_{HT}, and low temperature gamma, γ_{LT}) can also be calculated from the pressure derivatives of the elastic parameters,[30] assuming that only the acoustical modes contribute to γ

$$\gamma_{HT} = (\gamma_p + 2\gamma_s)/3 \tag{4}$$

$$\gamma_{LT} = \frac{(v_s/v_p)^3\gamma_p + 2\gamma_s}{2+(v_s/v_p)^3} \tag{5}$$

where

$$\gamma_s = 1/3 + K_T(\partial\ln v_s/\partial P)_T \tag{6}$$

and

$$\gamma_p = 1/3 + K_T(\partial\ln v_p/\partial P)_T. \tag{7}$$

Table 4. *Values of the Grüneisen parameters for α-quartz, fused quartz, and Vycor and Pyrex glasses*

	$\bar{\gamma}_{th}$	γ_{HT}	γ_{LT}
α-quartz	0·69*		
Fused quartz	0·04	2·40	2·32
Vycor	0·04	1·80	1·80
Pyrex	0·22	1·81	1·80

* From Reference 31.

Here γ_p and γ_s are the gamma contributions due to compressional and shear wave propagation and v_p and v_s represent compressional and shear velocities.

One of the unique aspects of glasses, fused silica in particular, is that the low temperature C_p is significantly greater than that calculated from the Debye theory and elastic modulus data. This is presumed to arise from the optical modes which are of lower frequency than the acoustic modes but which, nevertheless, produce a large contribution to low temperature C_p. There is, however, no direct evidence that optical frequencies are excited at such low temperatures.

Another unique characteristic of silica glasses is that their acoustical frequencies, as represented by the velocities of ultrasonic waves, decrease with hydrostatic pressure in both the transverse and the longitudinal modes. If one attempts to calculate the average $\bar{\gamma}$ from the acoustical γ_s and γ_p based on the volume dependence of the room temperature acoustic velocities as shown in Equations 4–7, it is found that the calculated high temperature liniting value, γ_{HT}, is considerably smaller than the, $\bar{\gamma}_{th}$, obtained from the αV, measurements at 298K for all glasses considered in the present paper. A comparison of the $\bar{\gamma}_{th}$ and γ_{HT} values for all three glasses is shown in Table 4. The γ_{HT} values are all in the range of −2 whereas the $\bar{\gamma}_{th}$ for fused silica and Vycor at 298K are slightly positive and the Pyrex $\bar{\gamma}_{th}$ is about +0·2. The conclusion from these calculations is that the optical γ_i must contribute a major part to $\bar{\gamma}_{th}$ at room temperatures and that the average optical mode, γ_i, is slightly positive for fused silica and Vycor glass and clearly positive for Pyrex glass. These conclusions are in good agreement with the values of the optical, γ_i, obtained from the present work and listed in Table 3.

As the present work and the measurement of the pressure derivatives of the ultrasonic velocities[32] were both carried out at room temperatures, the authors cannot make a direct contribution towards explaining

the negative $\bar{\gamma}_{th}$, in the silica glasses at lower temperatures. One conceivable model is that the freezing out of the optic modes with decreasing temperature increases the influence of the acoustic mode, γ_i's, and thus reduces, $\bar{\gamma}_{th}$, to negative values. This explanation presumes, then, that optical modes become less important below 200K and that they are then probably not responsible for the excess C_p. Measurements of the acoustic and optical mode, γ_i's, at low temperatures would be of great value in understanding the unique thermal properties of silica glasses.

Acknowledgement

The authors are grateful to E. S. Fisher of A.N.L. for critically reading the manuscript and making many helpful suggestions.

References

1. Borelli, N. F. & Su, G.-J. (1968). *Mater. Res. Bull.* **3**, 181. Su G.-J. Borelli, N. F. & Miller, A. R. (1962). *Physics Chem. Glasses* **3** (5), 167.
2. Gaskell, P. H. (1967). *Physics Chem. Glasses* **8** (1), 69.
3. Plendl, J. N., Mansur, L. C., Hadni, A., Brehat, F., Henry, P., Morlet, C., Naudin, F. & Strimer, P. (1967). *J. Physics Chem. Solids* **28**, 1589.
4. Hanna, R. (1965). *J. Am. Ceram. Soc.* **48**, 595. Hanna, R. & Su, G.-J. (1964). *J. Am. Ceram. Soc.* **47**, 597. Hanna, R. (1965). *J. phys. Chem.* **69**, 3846.
5. Saksena, B. D. (1961). *Trans. Faraday Soc.*, **57**, 242. Saksena, B. D. (1941). *Proc. Ind. Acad. Sci., Section A*, **12**, 93.
6. Simon, I. (1960). *Infrared studies of glasses in modern aspects of the vitreous state*, vol. 1, chapter 6. Edited by J. D. MacKenzie. Butterworths, London.
7. Lippencott, E. R., Van Valkenburg, A., Weir, C. E. & Bunting, E. N. (1958). *J. Res. natn. Bur. Stand.*, **61**, 61.
8. Lord, R. C. & Morrow, J. C. (1957). *J. chem. Phys.* **26**, 230.
9. Simon, I. & McMahon, H. (1953). *J. chem. Phys.* **21**, 23.
10. Matossi, R. (1949). *J. chem. Phys.* **17**, 679.
11. Barriol, J. (1946). *Phys. Radium* **7**, 209.
12. Krishnan, R. S. (1945). *Nature, Lond.* **155**, 452.
13. Barnes, R. B. (1932). *Phys. Rev.* **39**, 562.
14. Tobin, M. C. & Baak, T. (1968). *J. opt. Soc. Am.* **58**, 1459.
15. Shapiro, S. M., O'Shea, D. C. & Cummins, H. Z. (1967). *Phys. Rev. Lett.* **19**, 361.
16. Scott, J. F. & Porto, S. P. S. (1966). *Phys. Rev.* **161**, 903.
17. Nedungadi, T. M. K. (1940). *Proc. Ind. Acad. Sci., Section A*, **11**, 86.
18. Ansell, J. F. & Nicol, M. (1968). *J. chem. Phys.* **49**, 5395.
19. Angell, C. A., Wong, J. & Edgell, W. F. (1969). *J. chem. Phys.* **51**, 4519.
20. MacKenzie, J. D. & White, J. L. (1960). *J. Am. Ceram. Soc.* **43**, 170.
21. Bell, R. J. & Dean, P. (1966). *Nature, Lond.* **212**, 1354. Bell, R. J., Bird, W. F. & Dean, P. (1968). *J. Phys.* **1c** (2), 299.
22. Anderson, O. L. & Dienes, G. J. (1960). *Noncrystalline solids*, p. 449. John Wiley & Sons, Inc., New York.
23. Ferraro, J. R., Mitra, S. S. & Postmus, C. (1966). *Inorg. Nucl. Chem. Lett.* **2**, 269.
24. Postmus, C., Mitra, S. S., & Ferraro, J. R. (1968). *Inorg. Nucl. Chem. Lett.* **4**, 55.
25. Bragg, W. & Gibbs, R. E. (1925). *Proc. R. Soc.* **109**, 405.
26. Su, G.-J. & Bock, J. (1968). Office of Naval Research Contract Number 668 (19). Tech. Report, No. 3.
27. White, G. K. & Birch, J. A. (1965). *Physics Chem. Glasses* **6** (3), 85.
28. Smyth, H. T. (1955). *J. Am. Ceram. Soc.*, **38**, 140.
29. Leadbetter, A. J. (1968). *Physics Chem. Glasses* **9** (1), 1.
30. Schuele, D. E. & Smith, C. S. (1964). *J. Physics Chem. Solids* **25**, 801.
31. Soga, N. (1967). *J. geophys. Res.* **72**, 4227.
32. Manghnani, M. H. (1970). *Elastic parameters and infrared characteristics of glasses under high pressures and temperatures.* Final Report, O.N.R. Contract N00014-67-A-0387-0005, NR 032-515 H. G. Report 70-30, 37 pp.

INFRARED ABSORPTION SPECTRA OF SODIUM SILICATE GLASSES AT HIGH PRESSURES

By

John R. Ferraro and Murli H. Manghnani

(HIG Contribution No. 465)

Infrared absorption spectra of sodium silicate glasses at high pressures*

John R. Ferraro
Argonne National Laboratory, Argonne, Illinois 60439

Murli H. Manghnani
Hawaii Institute of Geophysics, University of Hawaii, Honolulu, Hawaii 96822
(Received 15 May 1972; in final form 13 July 1972)

Infrared absorption spectra of 12 sodium silicate glasses of varying composition (10 to 45 mole% Na_2O) are examined at varying pressures to 58.8 kbar. The pressure dependences of all the infrared absorption frequencies studied are found to be positive. Grüneisen γ's are evaluated from the pressure dependence of the infrared vibrations and elastic parameters. The results are compared with those obtained from previous high-pressure studies of α-quartz and several other silicate glasses.

INTRODUCTION

Physical properties such as elastic moduli and mechanical strength of silicate glasses are related to the density of the Si-O-Si bridges in the random-network structure of glasses.[1] The addition of Na_2O as a network modifier causes a breakdown of some of the Si-O-Si bridges and the formation of weaker Si-O-Na bridges and some terminal Si-O bonds—in proportion to the amount of Na_2O added. Further, some of the Si-O-Si bridges between the SiO_4 tetrahedra may be stretched to accommodate the sodium ion in the network. As a result, the elastic moduli and strength of Na_2O-SiO_2 glasses decrease with an increase in the Na_2O content.[1,2]

Several infrared investigations have been conducted on sodium silicate glasses.[3-9] Hanna and co-workers[3,4] have examined the infrared absorption spectra from 2500 to 50 cm^{-1} at ambient pressure, and others[5-9] have investigated the infrared reflectance spectra of the glasses. However, the pressure dependence of the infrared spectra of such glasses has not been investigated. This paper reports on a high-pressure study of the infrared spectra of 12 sodium silicate glasses from 1600 to 80 cm^{-1}. The mode Grüneisen parameters, γ_i, are calculated from the pressure dependence of all of the infrared vibration mode frequencies examined, and the values compared with the high-temperature limit of $\bar{\gamma}_{th}$, γ_{HT} arrived at from the pressure coefficients of the elastic parameters. The results are correlated with previous pressure studies on α-quartz and several other silicate glasses.[10]

EXPERIMENTAL METHODS

Eight sodium silicate glasses (K nomenclature) from the National Bureau of Standards and four (JRS nomenclature) from Sweet and White[9] at Pennsylvania State University were used in this study. Table I lists the chemical composition of the glasses in mole%.

The specimens were crushed in a ball mill finely powdered by extensive grinding in an agate mortar. The midinfrared absorption spectra at ambient conditions were obtained using KBr pellets and employing a Beckman IR-12 spectrophotometer. The spectra from 650 to 80 cm^{-1} were obtained with polyethylene pellets using a Perkin-Elmer Model No. 301 spectrophotometer. The region from 166 to 80 cm^{-1} was also checked with heavy concentrations of the glasses in Nujol. The instruments were calibrated in the midinfrared region with polystyrene film; and at frequencies <650 cm^{-1} with water vapor, the Hg emission lines and with low-frequency absorptions of solid HgO.

For the high-pressure measurements in regions of 333 to 80 cm^{-1} we used an opposed diamond cell linked with the Perkin-Elmer No. 301 spectrophotometer equipped with a 6× beam condenser.[11] Midinfrared studies at high pressures were made with a Beckman IR-12 spectrophotometer equipped with a 6× beam condenser.[12] The powdered sample was loaded in the cell, and the pressure alternately increased and decreased to distribute the material evenly between the anvils. During the pressure cycling, the sample was observed with a microscope. A description of the pressure cell and the method used in pressure calibration has been previously reported.[11-13]

HIG Contribution No. 465

TABLE I. Composition of Na_2O-SiO_2 glasses.

Sample No.	mole % SiO_2	mole % Na_2O	Ratio SiO_2/Na_2O
K-110	90	10	9.0
K-111	85	15	5.7
K-112	80	20	4.0
K-113	75	25	3.0
K-114	70	30	2.3
K-115	65	35	1.9
K-116	60	40	1.5
K-117	55	45	1.2
JRS-2	66.9	33.1	2.0
JRS-3	64.5	35.5	1.8
JRS-4	60.4	39.6	1.5
JRS-5	72.5	27.5	2.6

RESULTS AND DISCUSSION

A. Infrared absorption spectra at varying pressures

Table II lists the infrared absorption bands at ambient pressure for the sodium silicate glasses under study, and Fig. 1 displays several typical spectra. Figure 2 illustrates the effects of adding Na_2O to silica on the various absorptions between 1400—350 cm^{-1}. The increasing content of Na_2O causes a decrease in frequency of the three absorptions at ~1100, ~960, and ~790 cm^{-1}, and an increase for the ~460-cm^{-1} absorption. It is of interest to note that as the Na_2O content increases, the ~790-cm^{-1} band shifts toward a lower frequency than that found in α-quartz, and the intensity is considerably reduced. Since the number of Si-O-Si bridging units in the network decreases with an increase in the Na_2O content, it is expected that a decrease in intensity of this absorption would also occur. The low-frequency shift of the remaining Si-O-Si bridging units is consistent with a stretching of the Si-O bond as Na_2O enters the network. The ambient-pressure results are substantially in agreement with the reflectance work of Sweet and White[9] and the absorption studies of Hanna and Su.[3,4]

Although it is recognized that it may be incorrect to characterize an absorption band by a particular type of vibration in an amorphous material such as glass,[13] we find it convenient for purposes of the discussion in this paper to indicate that the four modes of vibration on interest may involve the following motions:

(a) ~1100 cm^{-1}, Si-O stretching within the tetrahedra;[6,14] (b) ~960 cm^{-1}, Si-O terminal, nonbridged stretching;[6] (c) ~790 cm^{-1}, Si-O-Si bridged stretching between tetrahedra; (d) ~460-cm^{-1}, bending modes involving Si-O-Si and O-Si-O. It should be emphasized that more definitive assignments for fused and crystalline silica have not been made.[13,15-18]

Under conditions of our experiments no significant absorptions were found lower than the broad band at ~460 cm^{-1}. Our measurements were carried out to 80 cm^{-1}. The pressure experiment is essentially a thin-film measurement, and under these conditions the glasses appeared to be transparent. When the glasses were measured in the far-infrared region as thick glasses, some weak absorptions were noted.

TABLE II. Sodium silicate glasses. Observed infrared absorptions at ambient pressure (cm^{-1}). Abbreviations: s = strong; m = medium; v = very; b = broad; w = weak

Glass (mole % Na_2O)	ν			
α quartz(0)	1082(vs)[a]		783(m) 800(m)	459(s)
Fused silica(0)	1087(vs)		815(m)	475(s)
(10)	1085[a](vs, b)		787(m)	460(s)
(15)	1075[b](vs, b)		785(m)	461(s)
(20)	1065(vs, b)	965(sh)	775(m)	462(s)
(25)	1065(vs)	975(vs)	765(m)	462(s)
(27.5)	1075(vs)	960(vs)	765(m)	458(s)
(30)	1070(vs)	960(vs)	760(m)	460(s)
(33.1)	1075(vs)	940(vs)	760(m)	460(s)
(35)	1070(vs)	940(vs)	755(m)	458(s)
(35.5)	1075(vs)	940(vs)	760(w)	458(s)
(39.6)	1060(vs)	930(vs)	745(w)	461(s)
(40)	1060(vs)	935(vs)	750(w)	460(s)
(45)	1040(vs)	935(vs)	730(w)	468(s)

[a] Asymmetric on high- and low-frequency sides of band.
[b] Very weak shoulder 980 cm^{-1}, 1220 cm^{-1}.

Table III presents the pressure dependence for the four main vibration modes, in terms of $d\nu_i/dP$, for the sodium silicate glasses. It is observed that $d\nu_i/dP$ values for all the absorption bands are higher than those for α-quartz and other silicate glasses.[10] Figure 3 presents typical infrared spectra (sample K-116) under high pressures. With an increase in pressure, frequencies of the three bands shift toward higher frequencies.

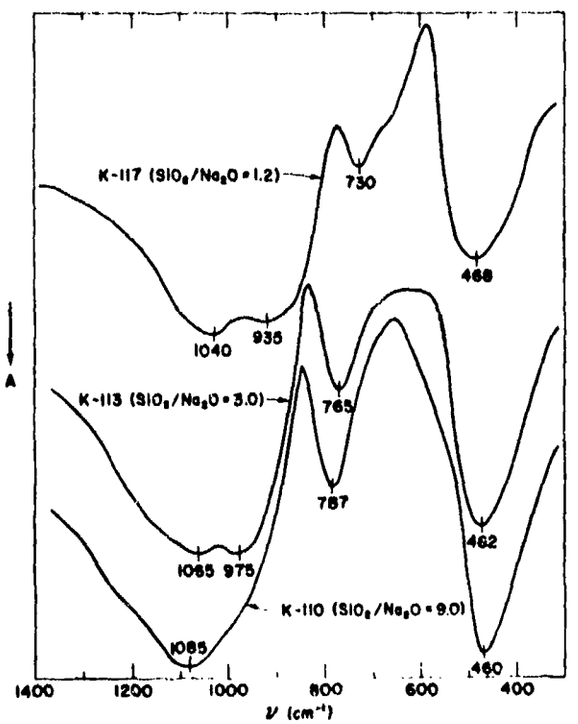

FIG. 1. Spectra (1400—350 cm^{-1}) of several sodium glasses at varying concentrations of SiO_2/Na_2O at ambient pressure.

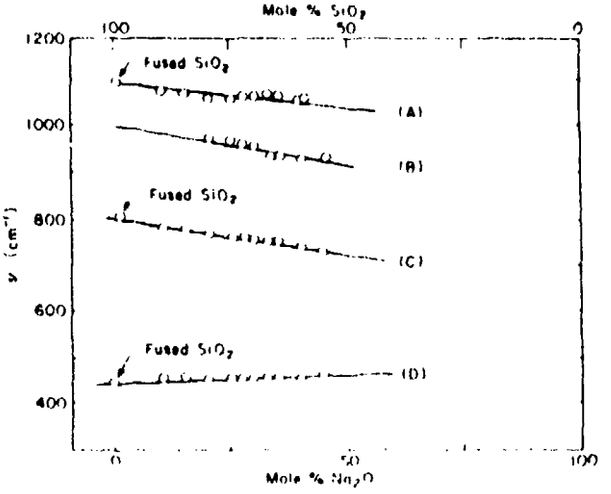

FIG. 2. (A) Plot of tetrahedra SiO stretching vibration vs mole% of Na_2O. (B) Plot of terminal SiO stretching vibration vs mole% of Na_2O. (C) Plot of SiOSi stretching vibration vs mole% of Na_2O. (D) Plot of bending vibrations vs mole% of Na_2O.

In pressure studies made on α-quartz, fused silica, Vycor, and Pyrex glasses, the pseudolatticelike Si stretching mode at ~800 cm^{-1} was found to be most pressure dependent.[10] For the sodium silicate glasses, all of the vibration modes studied are pressure sensitive, especially the tetrahedral Si-O stretching (~1100 cm^{-1}) and the bridging Si-O-Si stretching (~790 cm^{-1}) modes, and the terminal Si-O stretching (~960 cm^{-1}) mode. The effect of Na_2O on $d\nu_i/dP$ appears to be greater than the effect of B_2O_3 on $d\nu_i/dP$ in Vycor and Pyrex glasses. Differences between the effects of B_2O_3 and Na_2O on $d\nu_i/dP$ in silicate glasses are not unexpected since B_2O_3 is a glass former and strengthens the glass (e.g., elastic moduli increase as B_2O_3 increases),[1,2] whereas Na_2O is a glass modifier and weakens the glass.

The mode Grüneisen γ, γ_i, in Table III are evaluated from the relation

$$\gamma_i = \frac{K_T}{\nu_i}\left(\frac{d\nu_i}{dP}\right), \tag{1}$$

where K_T is the isothermal bulk modulus.

Whenever comparisons are possible, the sodium silicate glasses demonstrate γ_i values which are higher than those calculated for α-quartz and other silicate glasses,[10] and in every case are positive. The α-quartz and fused silica glass demonstrate negative γ_i values for some modes and also show anomalous thermal expansion and elastic behavior.[10,19] The positive γ_i values for the sodium silicate glasses are consistent with the effects of network filling agents such as Na_2O in diminishing these anomalies.[20] The higher ionic character of the sodium silicate glasses is also contributory to the higher sensitivity to pressure as opposed to the pure silicate glasses or those incorporating the more covalent boron atoms into the glass framework.[1,21,22]

Contrary to what was found for α-quartz and other silicate glasses,[10] even the modes involving the motions of the atoms within the SiO_4 tetrahedra in the sodium silicate glasses are significantly pressure sensitive. Thus, with an increase in pressure, the sodium silicate glasses demonstrate compression along the intertetrahedral linkages, but in addition some distortions of the individual tetrahedra[20] must occur. This difference from α-quartz and related nonmodified silicate glasses must relate to the insertion of the modifying sodium ions in the interstices of the glasses.

B. Thermal expansion and the Grüneisen parameters

The observed negative thermal expansion coefficients, α_v, at $T < 200$ °K for fused silica and Pyrex and the effects of diminishing this anomaly by the addition of a network filling agent such as Na_2O is of considerable interest.[23,24] The coefficient, α_v, is related to $\bar{\gamma}_{th}$ through the relation

$$\bar{\gamma}_{th} = \alpha_v K_T/\rho C_v, \tag{2}$$

where K_T is the ~~adiabatic~~ isothermal bulk modulus, ρ and C_v are density and specific heat at constant volume. $\bar{\gamma}_{th}$ is also related to γ_i and C_{v_i} by the relationship

$$\bar{\gamma}_{th} = \sum_{i=1}^{3n} \gamma_i C_{v_i} \Big/ \sum_{i=1}^{3n} C_{v_i}. \tag{3}$$

TABLE III. Mode Grüneisen parameters calculated for various sodium silicate glasses.

Glass (mole % Na_2O)	ν_i (cm^{-1})	$d\nu_i/dp$ (cm^{-1}/kbar)	χ ($kbar^{-1}$)	Calculated γ_i
α-quartz(0)	783 800	0.14	0.00267	0.07
Fused silica(0)	815	0.17	0.00302	0.07
Vycor(0)	814	0.22	0.00382	0.07
Pyrex(4)	812	0.27	0.00289	0.12
(10)	787	0.64	0.00295	0.28
(25)	765	0.50	0.00270	0.24
(35)	755	0.48	0.00252	0.25
(35.5)	760	0.50	0.00253	0.26
(40)	750	0.50	0.00251	0.27
(45)	730	0.56	0.00232	0.33
α-quartz(0)	1082	-0.07	0.00267	-0.02
(10)	1085	0.46	0.00295	0.14
(25)	1065	0.45	0.00270	0.16
(35)	1070	0.48	0.00252	0.18
(35.5)	1075	0.50	0.00253	0.18
(40)	1060	0.42	0.00251	0.16
(45)	1040	0.42	0.00232	0.17
(25)	975	0.45	0.00267	0.17
(35)	940	0.35	0.00252	0.15
(35.5)	940	0.50	0.00253	0.21
(40)	935	0.40	0.00251	0.17
(45)	935	0.45	0.00232	0.21
α-quartz(0)	459	0.09	0.00267	0.07
Fused silica(0)	475	-0.07	0.00302	-0.05
(10)	460	0.19	0.00295	0.14
(25)	462	0.13	0.00270	0.10
(35)	458	0.16	0.00252	0.14
(35.5)	458	0.21	0.00253	0.18
(40)	460	0.13	0.00251	0.11
(45)	468	0.19	0.00232	0.18

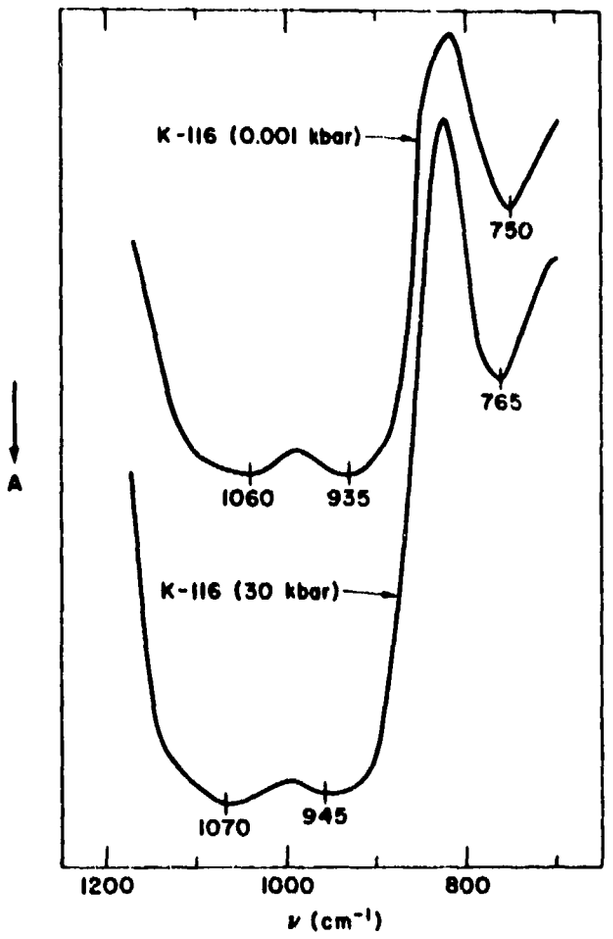

FIG. 3. Spectra of the K-116 glass at varying pressures from 1200—700 cm^{-1}.

where γ_i is defined by Eq. (1) and C_v is the specific-heat contribution for each vibrational mode to the total Einstein specific heat.

Since the thermal expansion data were obtained at room temperature and above, we will consider only the high-temperature limit of $\bar{\gamma}_{th}$ designated as γ_{HT}. γ_{HT} may be calculated from the pressure derivatives of the elastic parameters, assuming only the acoustic modes contributing to γ;

$$\gamma_{HT} = \tfrac{1}{3}(\gamma_p + 2\gamma_s), \tag{4}$$

where

$$\gamma_s = \frac{1}{3} + K_T\left(\frac{\partial \ln v_s}{\partial \ln P}\right)_T \tag{5}$$

and

$$\gamma_p = \frac{1}{3} + K_T\left(\frac{\partial \ln v_p}{\partial P}\right)_T. \tag{6}$$

Here γ_p and γ_s are the γ contributions to the compressional and shear-wave propagation, and v_p and v_s represent, respectively, compressional and shear acoustic wave velocities.[25,26]

Table IV shows a comparison of $\bar{\gamma}_{th}$ and γ_{HT} for the sodium silicate glasses at 298 °K. The values for α-quartz, fused silica, Vycor, and Pyrex are also included. We have no ready explanation for the observed differences in the $\bar{\gamma}_{th}$ and γ_{HT} values.

It is significant to note that as the Na_2O content increases, the optical γ_i values are observed to increase (Table III). The $\bar{\gamma}_{th}$ parameter increases slightly, but the γ_{HT} values increase significantly, and are much more sensitive to compositional changes occurring in the glasses. It may also be observed that the negative γ_{HT} values are related to the anomalous behavior in α-quartz and fused silica, for as Na_2O enters the glass, γ_{HT} becomes increasingly more positive and the anomaly decreases. Since Raman-active modes have not been examined under pressure, definite conclusions were not possible. However, the positive pressure dependences of the infrared-active modes examined, correlated with the absence of any negative thermal expansion observed for sodium silicate glasses.

SUMMARY

Infrared absorption spectra of sodium silicate glasses vary systematically with composition and pressure. The following findings are noteworthy:

(i) The strong broad band at ~1100 cm^{-1} due to Si-O stretching within the tetrahedron splits; the frequencies of both of the resultant bands decrease with substitution of Na_2O in the structure. With an increase in pressure these bands show a shift toward higher frequency.

(ii) The frequency and intensity of the bridging Si-O-Si stretching mode at ~790 cm^{-1} decreases with an increase in Na_2O content. The frequency was found to increase with pressure.

(iii) The low-frequency band, due to Si-O-Si and O-Si-O bending modes, slightly increases in frequency with Na_2O content, and with increasing pressure.

(iv) All values of $d\nu_i/dP$ for the four optical vibrational modes examined are positive.

TABLE IV. Thermal and elastic data and the Grüneisen parameter values for the Na_2O-SiO_2 glasses.

(mole % Na_2O)	$\bar{\gamma}_{th}$	γ_{HT}
(10)	0.003	−1.35
(15)	0.004	−0.84
(20)	0.006	−0.31
(25)	0.007	−0.17
(27.5)	0.008 (see erratum)	0.32
(30)	0.008	0.49
(33.1)	0.009	0.68
(35)	0.011	0.71
(35.5)	0.010	0.74
(39.6)	0.011	0.93
(40)	0.012	1.03
(45)	0.013	1.08
α-quartz(0)	0.69[a]	...
Fused silica(0)	0.04	−2.32
Vycor(0)	0.04	−1.80
Pyrex(4)	0.22	−1.80

[a] N. Soga, J. Geophys. Res. 72, 4227 (1967).

(v) The γ_i's calculated from $d\nu_i/dP$ are higher than those for α-quartz and high-silica glasses, reflecting the increase in ionic character of the glasses as the Na_2O content increases.

(vi) As the Na_2O content is increased in the sodium glasses, the value of γ_{HT} increases significantly, correlating with an absence of negative thermal expansion in these glasses.

ACKNOWLEDGMENT

The authors are grateful to G.W. Cleek, National Bureau of Standards and J.R. Sweet, The Pennsylvania State University, for providing the glass specimens. They thank E.S. Fisher, Argonne National Laboratory, for the critical reading of the manuscript and for his many helpful suggestions. One of the authors (M.H.M.) gratefully acknowledges the support for this work by the Office of Naval Research (Contract N00014-67-A-0387-0012, NR 032-527). Hawaii Institute of Geophysics Contribution No. 465.

*Based on work performed under the auspices of the U. S. Atomic Energy Commission
[1]R. J. Charles, *Progress in Ceramic Science* (Pergamon, New York, 1961), Vol 1.
[2]M. H. Manghnani (unpublished).
[3]R. Hanna, J. Phys. Chem. **69**, 3846 (1965).
[4]R Hanna and G.-J. Su, J. Amer. Ceram. Soc. **47**, 597 (1964).
[5]D Crozier and R. W. Douglas, Phys. Chem. Glasses **6**, 240 (1965).
[6]J. R. Sweet and W. B. White, Phys. Chem. Glasses **10**, 246 (1969)
[7]P E. Jellyman and J. P. Proctor, J. Soc. Glass Technol. **39**, 173 (1955)
[8]V A. Florinskaya, *The Structure of Glass* (Consultants Bureau, New York, 1960), p. 154.
[9]I. Simon and H. O. McMahon, J. Amer. Ceram. Soc. **36**, 160 (1953).
[10]J. R. Ferraro and M. H. Manghnani, J. Phys. Chem. Glasses (to be published).
[11]J R. Ferraro, S. S. Mitra, and C. Postmus, Inorg. Nucl. Chem. Lett. **2**, 269 (1966).
[12]C. Postmus, S. S. Mitra, and J. R. Ferraro, Inorg. Nucl. Chem. Lett. **4**, 55 (1966).
[13]N. F Borrelli and G.-J. Su, Mater. Res. Bull. **3**, 181 (1968).
[14]E. R. Lippincott, R. Van Valkenburg, A. Wier, and C. E. Bunting, J. Res Nat. Bur. Stand. **61**, 61 (1958).
[15]R. J. Bell, M. E. Bird, and P. Dean, Proc. Phys. Soc. Lond. **1**, 299 (1968)
[16]P. H. Gaskell, Phys. Chem. Glasses **8**, 69 (1967).
[17]J. Bock and G.-J. Su, J. Amer. Ceramic Soc. **53**, 69 (1970).
[18]M. Blackman, Proc. Phys. Soc. Lond. **70**, 827 (1957).
[19]A. Bienenstock and G. Burley, J. Phys. Chem. Solids **24**, 1271 (1963).
[20]H T. Smyth, J. Amer. Ceram. Soc. **42**, 276 (1959).
[21]J. Zarzycki, *Chemical and Mechanical Behavior of Inorganic Materials* edited by A W Searcy, D. V. Ragone, and V. Columbo (Interscience, New York, 1970), pp. 443–474.
[22]B E. Warren, J. Appl. Phys. **8**, 645 (1937).
[23]O. L. Anderson and G. J. Dienes, *Noncrystalline Solids* (Wiley, New York, 1960), p. 449.
[24]G. K. White, Cryogenics **4**, 2 (1964).
[25]T H. K. Barron, Phil. Mag. **46**, 720 (1955).
[26]D. E. Schuele and C. S. Smith, J. Phys Chem Solids **25**, 801 (1964).

Erratum: Infrared absorption spectra of sodium silicate glasses at high pressures [J. Appl. Phys. 43, 4595 (1972)]

John R. Ferraro

Argonne National Laboratory, Argonne, Illinois 60439

Murli H. Manghnani

Hawaii Institute of Geophysics, University of Hawaii, Honolulu, Hawaii 96822

In the manuscript on the high-pressure effects on the infrared absorption spectra of sodium silicate glasses, two errors appeared inadvertently. These are

1. Equation (5) on p. 4598 should read as follows:

$$\gamma_s = \frac{1}{3} + K_T\left(\frac{\partial \ln v_s}{\partial P}\right) \qquad (5)$$

2. Table IV should read as follows:

TABLE IV. Thermal and elastic data and the Grüneisen parameter values for the Na_2O-SiO_2 glasses.

(mole% Na_2O)	$\bar{\gamma}_{th}$ *	γ_{HT}
(10)	0.498	−1.35
(15)	0.854	−0.81
(20)	1.147	−0.35
(25)	1.334	−0.17
(27.5)	1.432	0.34
(30)	1.532	0.49
(33.1)	1.700	0.67
(35)	1.847	0.76
(35.5)	1.792	0.74
(39.6)	1.975	1.02
(40)	2.027	1.07
(45)	2.20	1.18
α-quartz (0)	0.694[a]	0.46
Fused silica (0)	0.04	−2.32
Vycor (0)	0.04	−1.80
Pyrex (4)	0.22	−1.80

[a] N. Soga, J. Geophys. Res. 73, 4227 (1968).

* The listed $\bar{\gamma}_{th}$ values should be divided by 3.

INFRARED ABSORPTION SPECTRA OF LITHIUM AND POTASSIUM SILICATE GLASSES AT HIGH PRESSURE

By

John R. Ferraro, Murli H. Manghnani, and Louis J. Basile

(HIG Contribution No. 544)

Infrared absorption spectra of lithium and potassium silicate glasses at high pressure*

John R. Ferraro

Argonne National Laboratory, Argonne, Illinois 60439

Murli H. Manghnani

Hawaii Institute of Geophysics, University of Hawaii, Honolulu, Hawaii 96822

Louis J. Basile

Argonne National Laboratory, Argonne, Illinois 60439

(Received 16 July 1973)

Infrared absorption spectra of five lithium silicate and six potassium silicate glasses of varying composition (20–35 mole% Li_2O and 15–40 mole% K_2O, respectively) are examined in the range 1500–100 cm^{-1}. The frequencies of the main absorption bands decrease with an increase of alkali-metal oxide (M_2O) content, with the exception of the ~960 cm^{-1} shoulder for the lithium silicate glasses. The pressure dependences to ~40 kbar, of all the main infrared absorption frequencies, which are pressure sensitive, are found to be positive. The values of $d\nu_i/dP$ are higher for potassium silicate glasses than for sodium and lithium silicate glasses. The effects of pressure are found to be opposite to the compositional effects. The Grüneisen mode γ's, γ_i, evaluated from the pressure dependence of the infrared absorption frequencies, are apparently related to the polarizing power of the alkali-metal ion. The results discussed in light of previous high-pressure infrared absorption studies of fused silica and sodium silicate glasses clearly indicate that γ_i, γ_{th}, and γ_{HT} generally increase with M_2O content in alkali silicate glasses.

I. INTRODUCTION

It has been demonstrated that the addition of an alkali-metal oxide, such as Na_2O, to the SiO_4 tetrahedral network in silicate glasses, in addition to effecting a minor role of network filling at low concentration, causes readjustment of the SiO_4 tetrahedra and, as a consequence, produces some structural distortion. These effects are accompanied by breakdown of the Si–O–Si bonds, and the formation of weaker, more ionic bonds with increasing alkali oxide content. The variations in the mechanical,[1] elastic,[2] and thermal properties,[3] and infrared absorption spectra of sodium silicate glasses,[4–14] having different composition, reflect such structural modification. In general, it is of interest to interpret the composition dependence of the various properties of alkali silicate (M_2O–SiO_2) glasses in light of the breakdown of Si–O–Si bonds, formation of weaker Si–O–M links and Si–O bonds, and the resultant changes in the Si–O–Si bond angles in the silicate glass structure. Such an evaluation is of particular value to better understanding of the anomalous thermal and optical properties of high-silica glasses.

The important conclusions reached in a recent paper concerning the composition and pressure dependence of the infrared absorption spectra of the sodium silicate glasses in the 1600–100-cm^{-1} frequency range were that first, except for the 460-cm^{-1} absorption band, frequencies of the other three major bands decreased with an increase in Na_2O content; second, the pressure dependence of the three major infrared vibrational modes ν_i was positive; and third, the values of mode Grüneisen gamma, γ_i, calculated from $d\nu_i/dP$, were larger than those found for fused silica and that γ_i for the ~800-cm^{-1} band appears to increase (outside experimental errors) with Na_2O content and ionic character of the glass.

This paper is an extension of an earlier study; its purpose is to report on the composition and pressure dependence of the infrared absorption spectra of five lithium silicate and six potassium silicate glasses in the range of 1500–100 cm^{-1} and to pressures of 40 kbar. The mode Grüneisen parameters, γ_i, calculated from the pressure dependence of the main infrared absorptions, are compared with $\bar{\gamma}_{th}$, and the high-temperature limit gamma value, γ_{HT}, obtained from the pressure coefficients of the elastic parameters. The results are correlated with previous studies on sodium silicate glasses[4] and fused silica.[14]

II. EXPERIMENTAL METHOD

Five lithium silicate glasses and six potassium silicate glasses, synthesized at the National Bureau of Standards, were used in this study; the glasses were annealed to 525 °C. Tables I and II list the chemical composition of the glasses in mole%. For obtaining the

TABLE I. Chemical composition of Li_2O–SiO_2 glasses.

Sample No.	mole% SiO_2	mole% Li_2O	SiO_2/Li_2O
1	80	20	4.00
2	75	25	3.00
3	70	30	2.33
4	68	32	2.13
5	65	35	1.86

TABLE II. Chemical composition of K_2O–SiO_2 glasses.

Sample No.	mole% SiO_2	mole% K_2O	SiO_2/K_2O	Remarks
1	85	15	5.7	
2	80	20	4.0	
3	75	25	3.0	
4	70	30	2.33	Phase separation
5	65	35	1.86	Phase separation
6	60	40	1.50	Phase separation

IIT Contribution No. [illegible]

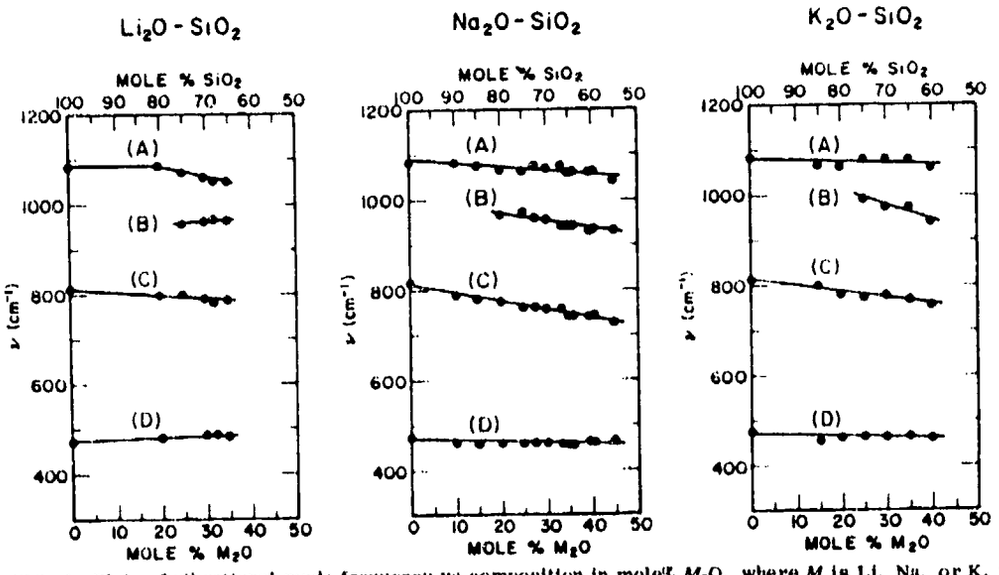

FIG. 1. Plots of vibrational mode frequency vs composition in mole% M_2O, where M is Li, Na, or K. Zero mole% M_2O is for fused silica. (A) Tetrahedral Si-O stretching vibration. (B) Terminal Si-O stretching vibration. (C) Si-O-Si bridged stretching vibration between tetrahedra. (D) Bending vibration involving Si-O-Si and O-Si-O.

infrared absorption spectra, small portions of the glasses were crushed and finely powdered by extensive grinding in an agate mortar. The procedures of sample grinding and preparation were conducted in a dry box flushed with dry nitrogen. The mid-infrared spectra from 1500 to 650 cm^{-1} were obtained by using a diamond anvil cell and Beckman IR-12 spectrophotometer. The spectra in the range < 650 to 300 cm^{-1} were obtained by using a diamond anvil cell and a Perkin-Elmer model No. 301 spectrophotometer. The instruments were calibrated in the mid-infrared region with polystyrene film, and at frequencies < 650 cm^{-1} with water vapor and Hg emission lines, and with the low-frequency absorptions of solid yellow HgO. For the high-pressure infrared absorption measurements < 650 cm^{-1}, the opposed diamond cell and the Perkin-Elmer 301 spectrophotometer equipped with a 6× beam condenser were used. Mid-infrared measurements at high pressures were made with a Beckman IR-12 spectrophotometer also equipped with a 6× beam condenser.[16] The powdered sample was loaded in the cell in a dry box, and the pressure applied in incremental steps. During the pressure cycling, the sample in the cell was observed with a microscope. A description of the pressure cell and the method used in pressure calibration have been previously reported.[15,16]

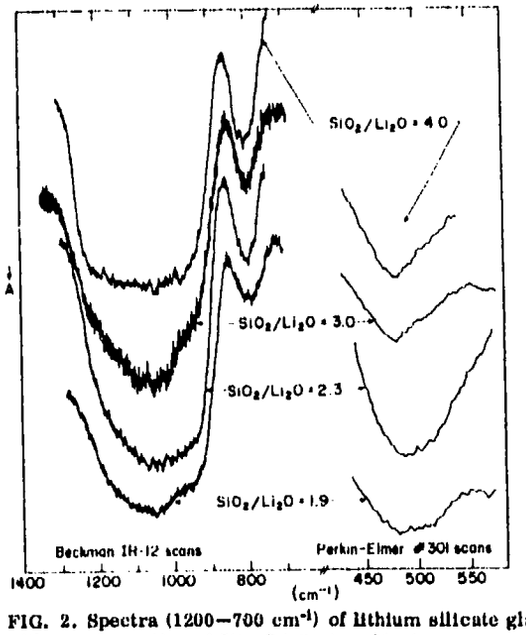

FIG. 2. Spectra (1200—700 cm^{-1}) of lithium silicate glasses with varying ratios of SiO_2/Li_2O at ambient pressure, observed by using a diamond cell with a Beckman IR-12 spectrophotometer. The spectra (600 to 300 cm^{-1}) of the same glasses, observed by using a diamond cell with a Perkin-Elmer No. 301 spectrophotometer, are also shown here.

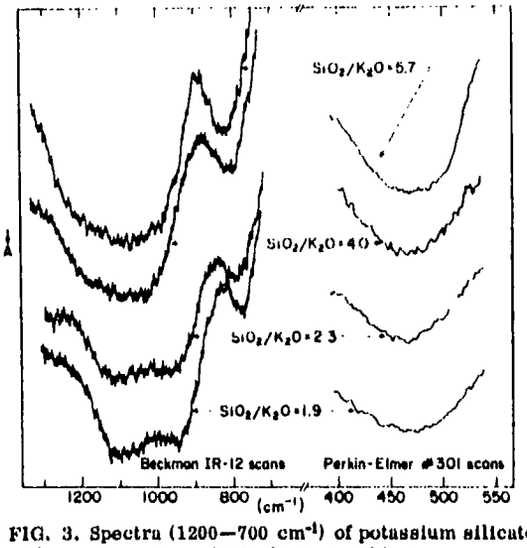

FIG. 3. Spectra (1200—700 cm^{-1}) of potassium silicate glasses with varying ratios of SiO_2/K_2O at ambient pressure, observed by using a diamond cell with a Beckman IR-12 spectrophotometer. The spectra (600 to 300 cm^{-1}) of the same glasses, observed by using a diamond cell with a Perkin-Elmer No. 301 spectrophotometer, are also shown here.

TABLE III. Lithium silicate glasses. Observed infrared absorptions at ambient pressure (cm^{-1}).

Glass (mole% Li_2O)	Absorptions [a] (1) [b]	(2) [c]	(3) [c]
20	1090 (vs, b)	800 (m)	480
25	1075 (vs, b); 960 (sh)	800 (m)	484
30	1060 (vs); 965 (sh)	790 (m)	488
32	1050 (vs); 970 (sh)	785 (m)	486
35	1050 (vs); 970 (sh)	790 (m)	488

[a] Abbreviations: v = very; s = strong; b = broad; m = medium; sh = shoulder.
[b] Limit of frequency measurement ± 5 cm^{-1}.
[c] Limit of frequency measurement ± 3 cm^{-1}.

TABLE IV. Potassium silicate glasses. Observed infrared absorptions at ambient pressure (cm^{-1}).

Glass (mole% K_2O)	Absorptions [a] (1) [b]	(2) [c]	(3) [c]
Fused silica (0)	1087 (vs)	815	475
15	1070 (vs, b) [d]	800	466
20	1065 (vs, b) [d]	780	469
25	1080 (vs); 995 (vs)	775	466
30	1080 (vs); 975 (vs)	780	469
35	1080 (vs); 975 (vs)	770	469
40	1065 (vs); 945 (vs)	755	464

[a] Abbreviations: v = very; s = strong; b = broad; m = medium.
[b] Limit of frequency measurement ± 5 cm^{-1}.
[c] Limit of frequency measurement ± 3 cm^{-1}.
[d] Asymmetric on high-frequency side of absorption band.

III. RESULTS AND DISCUSSION

A. Effects of compositional variation

Tables III and IV list the observed absorptions at ambient pressure for the glasses under study. The effects of increasing Li_2O or K_2O content in the glass composition are illustrated in Fig. 1, which also includes for comparison, the previously reported results of some sodium silicate glasses.[4] Typical spectra for the Li_2O-SiO_2 and K_2O-SiO_2 glasses studied here are displayed in Figs. 2 and 3, respectively. The frequency of the ~1100-cm^{-1} band, related to the Si-O stretching within the tetrahedral, decreases with an increase of alkali content in both glass types (see also Fig. 1), the effect being more marked in the lithium glasses. The relationship in the potassium glasses is not as well defined—the frequency increases slightly or remains invariant with the K_2O content. If we represent the composition dependence of frequency by $d\nu_i/dC$, where C is the mole% M_2O present in the glass, we have, from the least-squares analysis of the data, the values of $d\nu_i/dC$ for the ~1100-cm^{-1} band in the lithium, sodium, and potassium glasses as −2.87, −1.04, and ~0.11 cm^{-1}/mole% M_2O, respectively. This clearly indicates that the Si-O vibrational bond force constants may be weakened to a much greater extent in the lithium glasses than in the sodium glasses as a result of increased M_2O content; for the potassium glasses, there is no appreciable change.

The ~960-cm^{-1} absorption represents the nonbridging Si-O terminal stretching. Simon[14] has commented that this band appears in alkali silicate glasses at nearly the same frequency whenever the alkali metal oxide content reaches a value of 25 mole%. Our results are in agreement with the latter conclusion, but it is found that the frequency at which this band appears in the three types of alkali silicate glasses studied varies with the type of alkali metal present, being highest (~995 cm^{-1}) for a potassium glass (Fig. 3) and lowest (~960 cm^{-1}) for a lithium silicate glass (Fig. 2). This absorption band, which appeared as a shoulder in the sodium glasses containing 25 mole% Na_2O or more and which showed a definite separation from the ~1100-cm^{-1} band with increasing Na_2O content, appears as a small shoulder near ~960 cm^{-1} in the lithium glass containing 25 mole% Li_2O. It remains as a shoulder even at a higher concentration, 35 mole% Li_2O (Fig. 2). The value of $d\nu_i/dC$ estimated for this band in the lithium glasses is 1.08 cm^{-1}/mole%; this is only an approximate value in view of the failure to resolve the band. For the potassium glasses, this absorption is a very strong resolved band appearing at 995 cm^{-1} in the glass containing 25 mole% K_2O (Fig. 3). In contrast to the lithium glasses, the frequency of this band decreases with increase of potassium content, similar to that observed previously for the sodium system.[4] The value of $d\nu_i/dC$ is ~ −2.00 cm^{-1}/mole% which is the same as the value obtained for the sodium system. (For a comparison of the behavior of $d\nu_i/dC$ for the band, see Fig. 1 curves labeled B.) This clearly suggests that, as a result of increasing amounts of alkali-metal oxide, the Si-O bond is strengthened in Li_2O-SiO_2 glasses but is weakened in Na_2O-SiO_2 and K_2O-SiO_2 glasses. A similar effect is also found in a study of Young's moduli of these glasses[2]: the Young's modulus decreases in the Na_2O and K_2O-SiO_2 glasses but increases in Li_2O-SiO_2 glasses as the amount of alkali oxide increases.

The frequency of the ~800-cm^{-1} band which is related to the Si-O-Si bridged stretching between the tetrahedra, is observed to decrease with an increase in the M_2O content in all three glass types (plots C, Fig. 1), the decrease in the sodium and potassium glasses being larger than that in the lithium glasses.

The frequency of the ~460-cm^{-1} band, which represents the bending modes involving Si-O-Si and O-Si-O, does not appreciably vary with composition in all three cases (plots D, Fig. 1).

An examination of Fig. 2 shows that as the alkali oxide content of the lithium glasses increases, the intensity of the ~1100-cm^{-1} band decreases, a consequence of the decrease in the number of the Si-O-Si bridges that is also reflected by a very slight decrease in the intensity of the ~800-cm^{-1} band. Similar effects are observed in the potassium glasses (Fig. 3). However, the intensity of the ~800-cm^{-1} band decreases more appreciably with increasing K_2O content, and the intensity of the Si-O terminal nonbridging stretching absorption at ~960 cm^{-1} increases and becomes as strong as that of the ~1100-cm^{-1} band at a SiO_2/K_2O molar ratio of 3.0. Also seen in Fig. 3 is a decrease both in intensity and in frequency of the ~800-cm^{-1} band in the potassium glasses as the K_2O content increases. Similar effects of the absorption bands ~1100 and 800 cm^{-1}

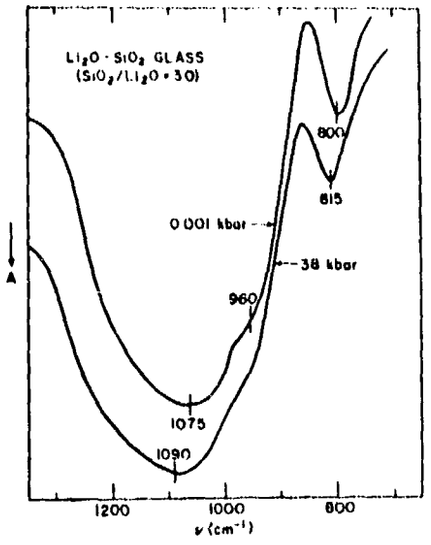

FIG. 4. Spectra of lithium silicate glass (25 mole% Li_2O) in the frequency range 1200—700 cm^{-1} at varying pressures.

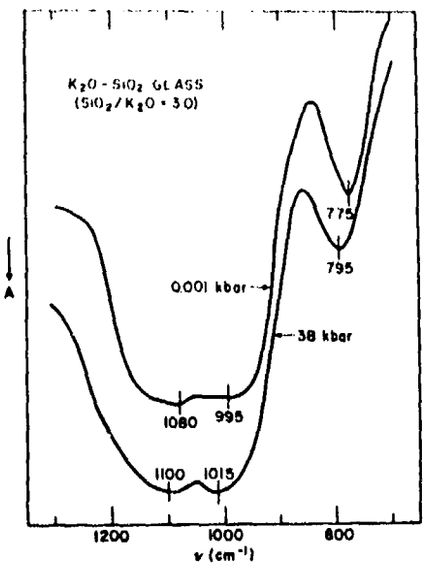

FIG. 5. Spectra of potassium silicate glass (25 mole% K_2O) in the frequency range 1200—700 cm^{-1} at varying pressures.

were also observed when the Na_2O content increased in sodium glasses.[4]

When all the results for the three types of glasses are compared, the compositional effect on the ~1100- and 960-cm^{-1} bands in the lithium glasses is more obvious than found in the other two glass types. On the other hand, the compositional effects on the ~800-cm^{-1} band are the least apparent in lithium glasses, probably due to the small size and large electronegativity of Li^+, which results in a less ionic Li-O bond. One might correlate the above-mentioned effects with the behavior of silicate glass under compression. To do so, let us consider the compressibility of vitreous silica, which is higher than in any other alkali silicate glass, and which decreases as alkali-metal oxide is added. The decrease in compressibility is in the order K > Na > Li silicate glasses.[17] Revesz[18] has commented upon the effect of electronegativity of the alkali metal of the oxide, added on the π bonding between Si and O, and its effect on the compressibility of silicate glass. According to this author, the lower the electronegativity of the alkali metal (the order of electronegativity being Li > Na > K), the larger is the π contribution to the $\equiv Si\text{-}O^-M^+ \equiv Si\text{-}O\text{-}Si \equiv$ bond. Thus, the higher electronegativity will result in the lower compressibility of an alkali silicate glass; the available experimental data on the compressibility of alkali silicate glasses support this conclusion.[2]

TABLE V. Comparison of the mode Grüneisen parameters γ_i with γ_{HT} and $\bar{\gamma}_{th}$ for various lithium silicate glasses. Note that the band at ~480 cm^{-1} shows no shift with pressure within experimental error.

Glass (mole% Li_2O)	ν_i (cm^{-1})	$d\nu_i/dP$ (cm^{-1}/kbar)	χ[a] ($Mbar^{-1}$)	γ_i	γ_{HT}[a]	$\bar{\gamma}_{th}$[a] *
20	800	0.26	2.446	0.13	−0.76	0.77
25	800	0.39	2.314	0.21	−0.40	0.99
30	790	0.39	2.174	0.23	0.23	1.22
32	785	0.39	2.092	0.24	0.43	1.36
35	790	0.39	2.027	0.24	0.71	1.46
20	1090[b]	0.26	2.446	0.10		
25	1075[b]	0.39	2.314	0.16		
30	1060[b]	0.26	2.174	0.11		
32	1050[b]	0.26	2.092	0.12		
35	1050[b]	0.26	2.027	0.12		

[a] Data from Ref. 2.
[b] Shoulder to this peak too weak to follow with pressure.

B. Pressure effects

Tables V and VI present the pressure dependence of the pressure-sensitive infrared absorption frequencies for the lithium and potassium glasses. Figures 4 and 5 depict typical spectra of some of these glasses under pressure. Except for the ~460-cm^{-1} band, which does

TABLE VI. Comparison of the mode Grüneisen parameters γ_i with γ_{HT} and $\bar{\gamma}_{th}$ for various potassium silicate glasses. Note that the band at ~470 cm^{-1} shows no shift with pressure within experimental error.

Glass (mole% K_2O)	ν_i (cm^{-1})	$d\nu_i/dP$ (cm^{-1}/kbar)	χ[a] ($Mbar^{-1}$)	γ_i	γ_{HT}[a]	$\bar{\gamma}_{th}$[a] *
15	800	0.26	3.212	0.10	−0.52	1.06
20	780	0.66	3.163	0.27	~0	1.34
25	775	0.52	3.095	0.22	0.39	1.69
30	780	0.52	...	...	...	...
35	770	0.52	...	...	...	...
40	755	0.52	...	...	...	...
15	1070	0.52	3.212	0.15		
20	1065	0.40	3.163	0.12		
25	1080	0.52	3.095	0.16		
30	1080	0.66	...	...		
35	1080	0.66	...	...		
40	1065	0.26	...	...		
25	995	0.52	3.095	0.17		
30	975	0.66	...	...		
35	975	0.52	...	...		
40	945	0.52	...	...		

[a] Data from Ref. 2.

* The listed $\bar{\gamma}_{th}$ values should be divided by 3.

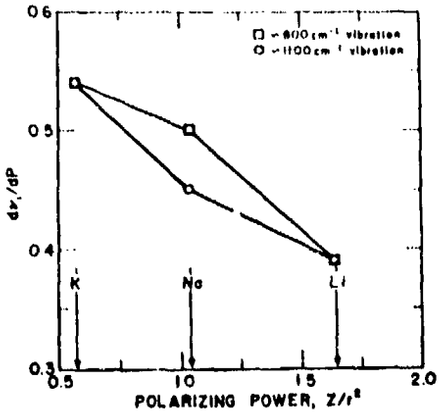

FIG. 6. Plot of $d\nu_i/dP$ vs polarizing power (Z/r^2) for M_2O-SiO_2 glasses, where M = Li, Na, or K. (Z = electronic change, and r = radius (Ref. 19) of the alkali ion.)

not appreciably vary with pressure, the $d\nu_i/dP$ values for the ~800- and ~1100-cm^{-1} absorptions are positive, as was found for the sodium silicate glasses.[4]

For a given molar content of alkali oxide, the $d\nu_i/dP$ values for the potassium silicate glasses are similar to those for sodium glasses and higher than those for lithium silicate glasses. The $d\nu_i/dP$ values for all the absorption bands considered appear to be more or less related to the type of alkali metal present rather than to the amount of alkali oxide in the glass. One explanation possibly lies in the difference in the polarizing power Z/r^2 (where Z is the electronic charge and r the ionic radius) of the three alkali metals involved in the composition of the glasses. Figure 6 shows a plot of $d\nu_i/dP$ versus the polarizing power (Z/r^2) of the three alkali-metal ions. It can be seen that as the Z/r^2 value of the alkali ion decreases, the $d\nu_i/dP$ value, for a given mode of vibration increases, the pressure dependencies being in the order of K > Na > Li silicate glasses.

The mode Grüneisen parameters γ_i, tabulated in Tables V and VI, are evaluated from the relation

$$\gamma_i = \frac{1}{\nu_i \chi}\left(\frac{d\nu_i}{dP}\right), \tag{1}$$

where χ is the isothermal compressibility of material. In all cases where comparisons are possible, the γ_i values for the alkali silicate glasses are higher than those for fused silica and reflect the more ionic character of the former. The results are consistent with the fact that the effects of adding alkali-metal oxide to silica will diminish both the anomalous thermal expansion and the elastic behavior of fused silica and high-silica glasses. In general, the higher sensitivity to pressure of the vibrational frequencies for the alkali silicate glasses, as compared to that for fused silica, and particularly the increasing $d\nu_i/dP$ values from lithium to potassium silicate glasses, is a consequence of the increasing ionic character of the glasses as one proceeds from fused silica to Li → Na → K silicate glasses. The previous study of sodium silicate glasses[4] and the present results indicate that the insertion of these oxides also makes the motion of the Si-O bond within the SiO_4 tetrahedra increasingly sensitive to pressure, and that addition of potassium ions causes the greatest change in the pressure dependence of this Si-O vibrational frequency bond.

C. Correlation of composition and pressure dependence of ν_i

The effects of composition and pressure on the vibrational frequencies are found to be opposite. For the alkali silicate glasses, almost all the infrared absorption frequencies decrease with increase in alkali oxide content, whereas pressure dependence is positive in all cases, except for the bond-bending vibrations at ~460 cm^{-1}, which does not show any appreciable change. Krüger,[3] in a study of the thermal properties of sodium silicate glasses at low temperatures, has considered that the introduction of Na_2O has two effects: (i) The joined SiO_4 tetrahedra readjust to a more ordered angular position and (ii) the network becomes increasingly disrupted. Our results are consistent with this consideration. Increase of the alkali-metal oxide content results in a decrease in the intensity of the ~800-cm^{-1} band, and the appearance of an absorption at ~960 cm^{-1}, which is due to the nonbridging Si-O$^-$ terminal vibration. As the number of the broken Si-O-Si links increases to accommodate the alkali metal, more new terminal bonds are created, thus causing the intensity of the ~960-cm^{-1} band to increase. The Si-O stretching bonds within the tetrahedra also change, and probably weaken slightly. In all cases the frequency decreases with an increase of alkali-metal oxide, except in the case of the bending vibration frequency (~460 cm^{-1}) which reflects little change. One would expect that the Si-O-Si and O-Si-O bond angles also change with the addition of alkali-metal oxide. However, no conclusions on the bond angles can be made from the present study of the infrared absorption frequency.

The pressure effects are opposite to the effects of composition. All frequencies shift back toward the position of the frequencies for fused silica, with the exception that the terminal Si-O$^-$ vibration remains invariant. The pressure effects may be considered to cause some ordering of structure, as was previously reported for quartz and fused silica.[13]

D. Thermal expansion and the Grüneisen parameters

The observed negative thermal expansion coefficients, α_V, at $T < 200$ °K for fused silica and a borosilicate glass, and the effects of diminishing this anomaly by the addition of a network-filling agent such as M_2O is of considerable interest.[20,21] The coefficient α_V is related to $\bar{\gamma}_{th}$ through the relation

$$\bar{\gamma}_{th} = \alpha_V K_S/\rho C_p = \alpha_V K_T/\rho C_V = \alpha_V/\rho C_V \chi \tag{2}$$

where K_S and K_T are the adiabatic and isothermal bulk moduli, ρ is density, and C_p and C_V are specific heats at constant pressure and volume, respectively. $\bar{\gamma}_{th}$ is also related to γ_i and C_V by the relationship

$$\bar{\gamma}_{th} = \sum_{i=1}^{3n} \gamma_i C_{V_i} \Big/ \sum_{i=1}^{3n} C_{V_i}, \tag{3}$$

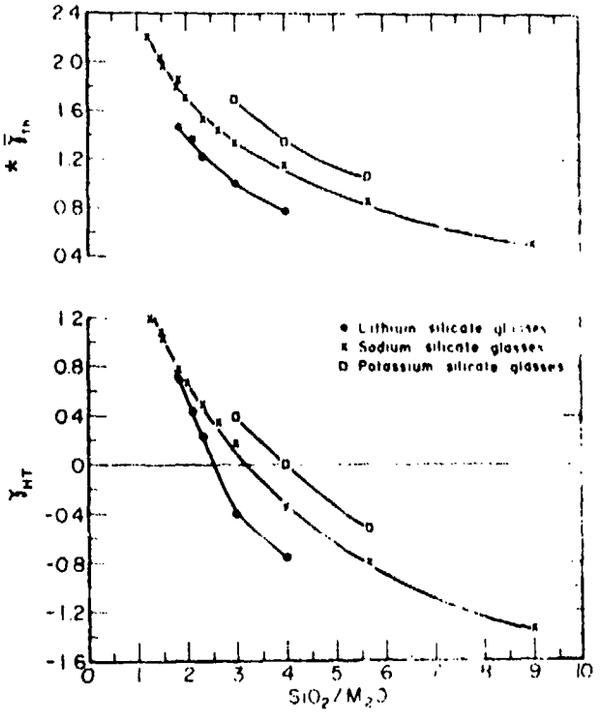

FIG. 7. Plots of $\bar{\gamma}_{th}$ and γ_{HT} vs SiO_2/M_2O ratio for the Li_2O-, Na_2O-, and K_2O-SiO_2 glasses (from Ref. 2).

where γ_i is defined by Eq. (1) and C_{v_i} is the specific heat contribution for each vibrational mode to the total Einstein specific heat

Since the thermal expansion data were obtained at room temperature and above, we will consider only the high-temperature limit of $\bar{\gamma}_{th}$ designated as γ_{HT}. γ_{HT} calculated from the pressure derivatives of the elastic parameters,[22,23] assuming that only the acoustic modes contribute to γ, are listed in Tables V and VI.

For the sodium silicate glasses, it was found that $\bar{\gamma}_{th}$ and γ_{HT} increase as more Na_2O enters the silica network. For the SiO_2/Na_2O ratio of 4 and larger, γ_{HT} was negative and this was correlated with the anomalous behavior found in fused silica and high-silica glasses. Tables V and VI show comparison of γ_i, γ_{HT}, and $\bar{\gamma}_{th}$ for the Li_2O and K_2O-SiO_2 glasses. Figure 7 shows plots of $\bar{\gamma}_{th}$ and γ_{HT} versus the SiO_2/M_2O ratio[2] for these and Na_2O-SiO_2 glasses. In both plots the $\bar{\gamma}_{th}$ and γ_{HT} values increase in the following order: K > Na > Li silicate glasses. At lower SiO_2/M_2O ratios, the γ_{HT} values appear to converge to 1.0. This trend then correlates with the decrease in the degree of anomalous (negative) thermal expansion due to the addition of alkali-metal oxide to fused SiO_2.

ACKNOWLEDGMENTS

The portion of the research work at the University of Hawaii was supported by the Office of Naval Research, Contract No. N00014-67-A-0387-0012, NR 032-527. The authors are grateful to T. Matui for making these glasses; to G.W. Cleek of the National Bureau of Standards for guidance in making these glasses; to E.S. Fisher of Argonne National Laboratory and J. Wong of G.E. Laboratory for a critical reading of the manuscript; and to Anthony Quattrochi of the U.S. Tobacco Co., Chicago, Illinois, for some preliminary experimental work accomplished. Hawaii Institute of Geophysics Contribution No. 544.

[a]Work performed under the auspices of the U.S. Atomic Energy Commission and the Office of Naval Research.
[1]R.J. Charles, *Progress in Ceramic Science* (Pergamon, New York, 1961), Vol. I.
[2]M.H. Manghnani (unpublished).
[3]J. Krüger, Phys. Chem. Glasses 13, 9 (1972).
[4]J.R. Ferraro and M.H. Manghnani, J. Appl. Phys. 43, 4595 (1972). Corrections to this paper appeared in J. Appl. Phys. 44, 2443 (1973).
[5]G.-J. Su, N.F. Borrelli, and A.R. Miller, Phys. Chem. Glasses 3, 167 (1962).
[6]R. Hanna and G.-J. Su, J. Am. Ceram. Soc. 47, 597 (1964).
[7]R. Hanna, J. Phys. Chem. 69, 3846 (1965).
[8]D. Crozier and R.W. Douglas, Phys. Chem. Glasses 6, 240 (1965).
[9]J.R. Sweet and W.B. White, Phys. Chem. Glasses 10, 246 (1969).
[10]P.E. Jellyman and J.B. Proctor, J. Soc. Glass Technol. 39, 173 (1955).
[11]V.A. Florinskaya, *The Structure of Glass* (Consultants Bureau, New York, 1960), p. 154.
[12]I. Simon and H.O. McMahon, J. Am. Ceram. Soc. 36, 160 (1953).
[13]J.R. Ferraro, M.H. Manghnani, and A. Quattrochi, Phys. Chem. Glasses 13, 116 (1972).
[14]I. Simon, in *Modern Aspects of the Vitreous State*, Vol. 1, edited by J.D. Mackenzie (Butterworths, London, 1960), Chap. 6, p. 120.
[15]J.R. Ferraro, S.S. Mitra, and C. Postmus, Inorg. Nucl. Chem. Lett. 2, 269 (1966).
[16]C. Postmus, S.S. Mitra, and J.R. Ferraro, Inorg. Nucl. Chem. Lett. 4, 55 (1966).
[17]S. Sakka and J.D. Mackenzie, J. Non-Cryst. Solids 1, 107 (1969).
[18]A.G. Revesz, J. Non-Cryst. Solids 7, 77 (1972).
[19]T. Moeller, *Inorganic Chemistry* (Wiley, New York, 1952), p. 140.
[20]O.L. Anderson and G.J. Dienes, *Non-Crystalline Solids* (Wiley, New York, 1969), p. 449.
[21]G.K. White, Cryogenics 4, 2 (1964).
[22]D.E. Schuele and C.S. Smith, J. Phys. Chem. Solids 25, 801 (1964).
[23]T.H.K. Barron, Phil. Mag. 46, 720 (1955).

* Consistent with the corrections made in Tables V and VI, the ordinate axis in the upper plot of Fig. 7 is now $3\bar{\gamma}_{th}$.

A STUDY OF Na_2O-TiO_2-SiO_2 GLASSES BY INFRARED SPECTROSCOPY

By

Murli H. Manghnani, John R. Ferraro, and L. J. Basile

(HIG Contribution No. 554)

A Study of Na_2O-TiO_2-SiO_2 Glasses by Infrared Spectroscopy*

Murli H. Manghnani

Hawaii Institute of Geophysics, University of Hawaii, Honolulu, Hawaii 96822

John R. Ferraro† and L. J. Basile

Argonne National Laboratory, Argonne, Illinois 60439

(Received 20 August 1973; revision received 29 October 1973)

The infrared absorption spectra of six Na_2O-TiO_2-SiO_2 glasses in the frequency range of 1600 to 200 cm^{-1} are reported. These glasses, having a SiO_2/Na_2O molar ratio of 1.67 to 3.84, and containing 20 or 25 mole % TiO_2, demonstrate two main absorptions at ~950 cm^{-1} and at ~450 cm^{-1}. A weak absorption at ~700 cm^{-1} becomes progressively weaker in intensity, and a weak shoulder at 1050 cm^{-1} appears with increasing Na_2O content. The frequency of the absorption band at ~950 cm^{-1} is found to decrease markedly and systematically with a decrease in the SiO_2/Na_2O molar ratio, whereas the frequency of the band at ~450 cm^{-1} shows a slight increase. The infrared results may be interpreted in terms of a lowering of symmetry occurring for the SiO_4 units. The effect of TiO_2 content on the relationship between vibrational frequency is discussed. The frequency composition curves for glasses containing 20 and 25 mole % of TiO_2 intersect at SiO_2/Na_2O ratio ~2. A reversal in the frequency vs SiO_2/Na_2O ratio relation was also found at SiO_2/Na_2O ~2 for the sodium silicate glasses.

INDEX HEADINGS: Infrared spectroscopy; Na_2O-TiO_2-SiO_2 glasses; Compositional effects.

INTRODUCTION

The glasses in the ternary Na_2O-TiO_2-SiO_2 system have been employed by several workers to demonstrate the effect of modifying ions, such as Ti^{4+} and Na^+, on the optical, thermal, electrical, and other physical properties[1-6] of silicate glasses. In most of these studies, the role of Ti^{4+} has been particularly emphasized.

Recently a study of the pressure and temperature dependence of the elastic properties of the Na_2O-TiO_2-SiO_2 glasses has been reported.[6] The purposes of this paper are to report the infrared absorption characteristics of the same Na_2O-TiO_2-SiO_2 glasses and to interpret the effects of composition on the structural state as revealed by the infrared absorption spectra.

In simple binary glasses, such as those in the system Na_2O-SiO_2, the various physical properties such as mechanical strength and elastic moduli are related to a number of the Si-O-Si links in the random network of silica tetrahedra.[7] The addition of Na_2O as a modifier causes the breakdown of these links and the formation of weaker Si-O-Na terminal links as reflected by the decrease in the Young's moduli of glasses in the binary Na_2O-SiO_2 glasses as the Na_2O content is increased.[7-9] It is of interest to understand how such a modification of the structure is affected in the presence of Ti^{4+} ions which occupy intratetrahedral positions at low concentration and the intertetrahedral positions at a high concentration of TiO_2.[3] We have carried out this study to shed some new light on the changing role of a modifying oxide (Na_2O) added to SiO_2 structure containing another network-forming oxide (TiO_2) in which the cation Ti^{4+} has different field strength,[8] Z/A^2, than that of Si^{4+}.

I. EXPERIMENTAL PROCEDURE

The six glasses employed in this study were obtained through the courtesy of G. W. Cleek, National Bureau of Standards, who has previously reported their physical and optical properties.[1] The pressure and temperature dependence of the elastic moduli of the same glasses has been recently reported.[6] Their chemical composition is given in Table I.

The mid-infrared absorption spectra of these glasses in the range of 1600 to 200 cm^{-1} were obtained with a Beckman IR-12 spectrophotometer, using the KBr pellet technique. The instrument was calibrated in the mid-infrared region with polystyrene film and CO gas, and in the low frequency region with H_2O vapor and solid yellow HgO.

II. RESULTS AND DISCUSSION

Figs. 1 and 2 show the infrared absorption spectra of the Na_2O-TiO_2-SiO_2 glasses containing 20 and 25 mole % TiO_2, respectively. Table I lists their composition and the vibrational frequency assignments for the two main absorption bands at ~950 and ~450 cm^{-1}.

A. Symmetry of SiO_4 Units in Na_2O-TiO_2-SiO_2 Glasses

As Na_2O and TiO_2 are added to the base silicate glass, the symmetry of the SiO_4 tetrahedra should decrease, and this will affect the vibrational spectra of the glass. Table II illustrates the correlation table for the symmetry T_d and the lower symmetries D_{2d}, C_{2v}, and C_{1v}. It may be observed that two F_2 infrared-active modes (stretching and bending) in T_d symmetry will

* Based on experimental work performed at Argonne National Laboratory under the auspices of the United States Atomic Energy Commission. Work at the University of Hawaii supported by the United States Office of Naval Research, Metallurgy Program, under Contract N00014-67-A-0387-0012, Nr 032-527. Hawaii Institute of Geophysics Contribution 554.

† To whom correspondence should be addressed.

TABLE I. Chemical composition and the infrared absorption frequency assignments for the ~950 and ~450 cm^{-1} vibration modes in Na_2O-TiO_2-SiO_2 glasses.

Glass serial No.	Mole % Na_2O	Mole % TiO_2	Mole % SiO_2	SiO_2:Na_2O ratio	Si-O-Si bending modes frequency (cm^{-1})	Si-O terminal stretching mode frequency (cm^{-1})
1	17.5	20.0	62.0	3.54	452 ± 3	900 ± 3
2	25.0	20.0	55.0	2.20	460 ± 5	985 ± 5
3	30.0	20.0	50.0	1.67	465 ± 5	920 ± 5
4	17.5	25.0	57.5	3.29	447 ± 5	905 ± 5
5	22.5	25.0	52.5	2.33	455 ± 5	902 ± 5
6	27.5	25.0	47.5	1.73	470 ± 5	945 ± 5

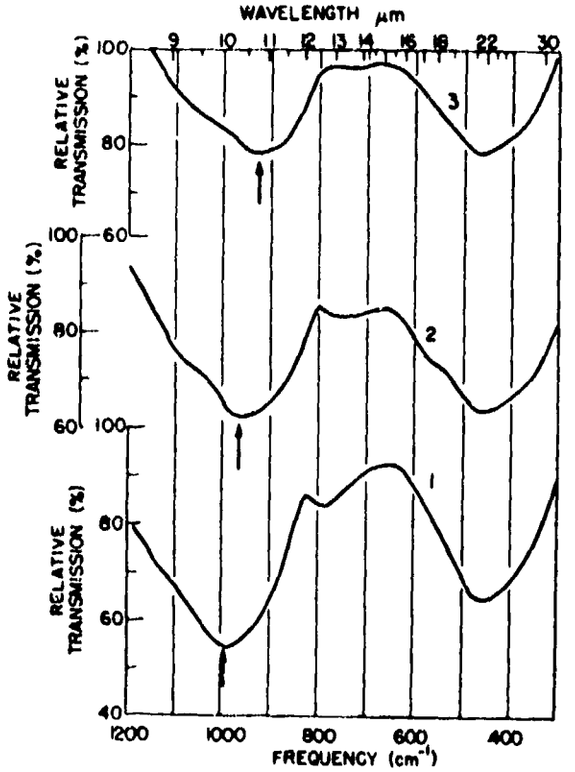

FIG. 1. Infrared absorption spectra of Na_2O-TiO_2-SiO_2 glasses containing 20 mole % TiO_2. Glass 1 contains 17.5 mole % Na_2O and 62.0 mole % SiO_2; glass 2 contains 25.0 mole % Na_2O and 55.0 mole % SiO_2; glass 3 contains 30 mole % Na_2O and 50.0 mole % SiO_2.

correlate to four infrared-active modes ($2B_2 + 2E$) in the D_{3d} symmetry. For C_{3v} symmetry the two F_2 modes correlate to six modes, active in the infrared and Raman. Three of these modes will be A_1 type and three will be E type. For C_{2v} symmetry eight modes will become active in the infrared and nine modes in the Raman. Thus, the infrared-active modes for the vibrations involving SiO_4 units, based on each symmetry, are as follows:

$$T_d \text{ symmetry} - \Gamma_{IR} = 2F_2$$
$$D_{3d} \text{ symmetry} - \Gamma_{IR} = 2B_2 + 2E$$
$$C_{3v} \text{ symmetry} - \Gamma_{IR} = 3A_1 + 3E$$
$$C_{2v} \text{ symmetry} - \Gamma_{IR} = 4A_1 + 2B_1 + 2B_2$$

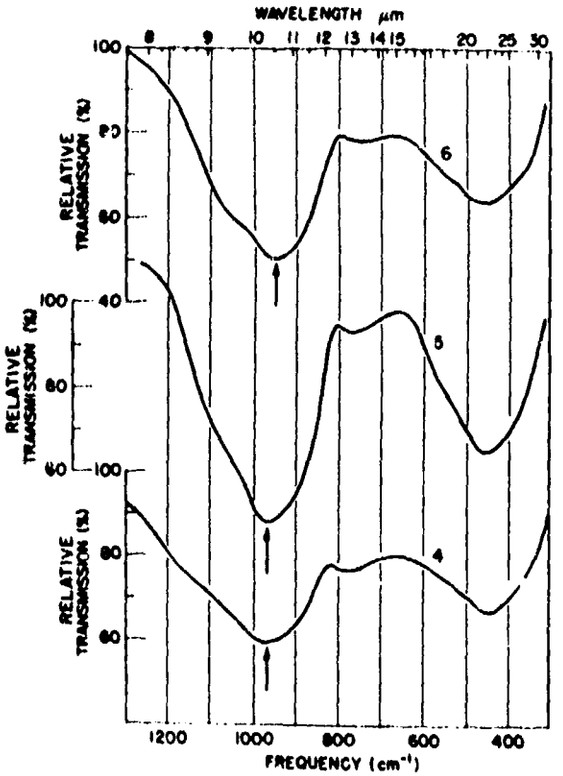

FIG. 2. Infrared absorption spectra of Na_2O-TiO_2 glasses containing 25 mole % TiO_2. Glass 4 contains 17.5 mole % Na_2O and 57.5 mole % SiO_2; glass 5 contains 22.5 mole % Na_2O and 52.5 mole % SiO_2; glass 6 contains 27.5 mole % Na_2O and 47.5 mole % SiO_2.

TABLE II. Correlation chart for T_d, D_{3d}, C_{3v} and C_{2v} symmetries.

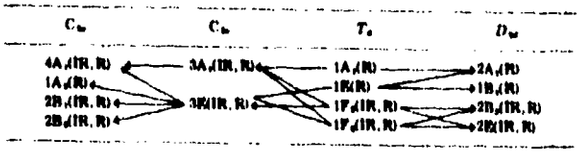

The infrared spectra of the Na_2O-TiO_2-SiO_2 glasses remain rather simple. Our experimental results provide evidence for a D_{2d} symmetry for the SiO_4 units, although the C_{3v} symmetry cannot be eliminated. No evidence for a C_{2v} symmetry is observed.

At least two stretching modes appear in the infrared spectrum: a shoulder at ~1050 cm^{-1} and a main absorption at 900 cm^{-1} (in the 20% TiO_2 glass, No. 1). The region is very broad. In the bending region, only a broad absorption appears at 452 cm^{-1} (in the 20% TiO_2 glass, No. 1). The broadness of the band is indicative of the overlapping of several modes, each having equivalent energy. This band was not resolvable at room temperature.

Table III summarizes the frequency assignments for the SiO_4 vibrations existing in a D_{2d} symmetry. No evidence was obtained for Ti-O vibrations in these glasses, scanning the infrared region to 200 cm^{-1}. Rutile[10] has strong bands at 695 and 608 cm^{-1} and weak

TABLE III. Infrared assignments for the SiO_4 tetrahedron vibrations in D_{2d} symmetry.

D_{2d}	Assignment	Approximate frequency position (cm^{-1})
B_2	SiO terminal stretch	~950
B_1	SiO_2 bending	~450
E	SiO stretch	~1050 (sh)
E	SiO_2 bending	~450

bands at 423 and 352 cm^{-1}, while the Ba_2TiO_4[11] shows infrared absorptions at 770 and 371 cm^{-1}. The region of 600 to 700 cm^{-1} in Na_2O-TiO_2-SiO_2 glasses is free of absorption. The lower frequency region at ~450 cm^{-1} is obscured because of the broad absorption occurring in the region.

B. Assignments for the Intermolecular Vibrations

The weak vibration at ~790 cm^{-1} has been assigned to the ←Si(O)Si→ stretching mode between the SiO_4 tetrahedra.[12-14] The bending mode Si-O-Si has been assigned in the energy region of the broad envelope occurring at ~450 cm^{-1}.[12-15]

C. Relation of Vibrational Frequencies with Composition in Na_2O-TiO_2-SiO_2 Glasses

Referring to Figs. 1 and 2 and Table III, the absorption at ~950 cm^{-1} is attributed to the Si-O terminal nonbridged vibration, and the ~450 cm^{-1} absorption is attributed to the vibrations involving Si-O-Si and O-Si-O bending modes, referred to and discussed in an earlier paper.[14,15] The shoulder at ~1050 cm^{-1}, appearing as the Na_2O content increases, is assigned to the Si-O stretch within the SiO_4 unit. Absorption at ~790 cm^{-1}, due to Si-O-Si bridged stretching between tetrahedra, which is strong in glasses (3 and 6) containing low Na_2O content, becomes weaker as the Na_2O content is increased (compare the spectra of glasses 1 → 3 and of 4 → 6 in Figs. 1 and 2, respectively).

Fig. 3 illustrates the effect of the SiO_2/Na_2O ratio on the two main absorption frequencies (~950 and ~450 cm^{-1}), respectively, for the Na_2-TiO_2-SiO_2 glasses. The previous results for the sodium silicate glasses[14] are also included for comparison. As seen, the frequency of the ~950 cm^{-1} absorption band decreases systematically and nonlinearly as the Na_2O content is increased (i.e., as the SiO_2/Na_2O ratio decreases). The frequency-composition curves for the two types of Na_2O-TiO_2-SiO_2 glasses, one containing 20 and the other 25 mole % TiO_2, intersect at SiO_2/Na_2O ratio ~2, corresponding to ~28 molar % of Na_2O. The effect of increasing Na_2O content on the ~450 cm^{-1} absorption is opposite and less marked—the frequency increases slightly with a decrease in SiO_2/Na_2O ratio. Here again, the two curves for the 20 and 25 mole % TiO_2 composition intersect at SiO_2/Na_2O ratio of ~2. It is of interest to note from Fig. 3 that the relation of frequency vs SiO_2/Na_2O for sodium silicate glasses inverts at SiO_2/Na_2O ratio value slightly less than 2 (~18 mole % Na_2O). The inversion effect for the sodium silicate

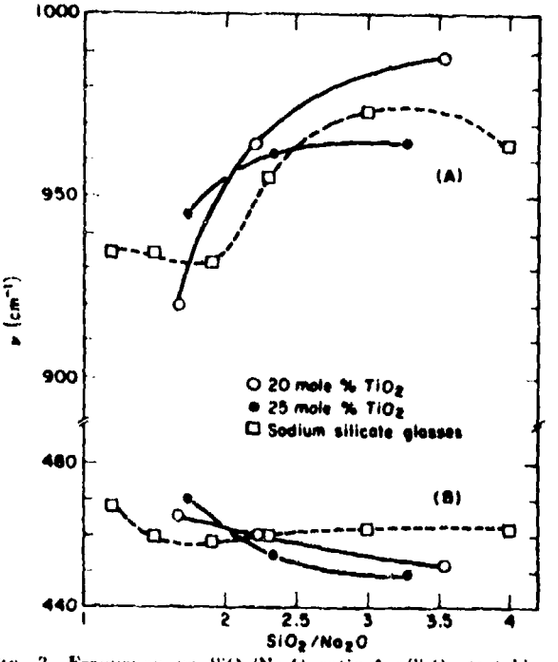

FIG. 3. Frequency vs SiO_2/Na_2O ratio for Si-O stretching (~950 cm^{-1}) and for the SiO_2 bending modes (~450 cm^{-1}).

glasses corresponds to Na_2O content of 35 mole %, the structure parameter $y = (6 - 200/p)$, where p is mole % SiO_2,[14] being equal to ~3. Whether the causes of the two observations at $SiO_2/Na_2O \sim 2$ for the Na_2O-TiO_2-SiO_2 and Na_2O-SiO_2 glasses are related is not established. On comparing the results of parts A and B in Fig. 3, it is found that the role of TiO_2 content in enhancing and diminishing the composition dependence of the vibration frequencies of the ~950 and ~450 cm^{-1} absorption bands, respectively, is not similar. Increase of TiO_2 content diminishes the effect on the ~950 cm^{-1} absorption frequency and enhances it for the ~460 cm^{-1} frequency.

III. SUMMARY

1. Data are presented to indicate that the symmetry of the SiO_4 units in Na_2O-TiO_2-SiO_2 glasses has lowered from T_d to D_{2d} (or C_{2v} symmetry).

2. The two main absorptions at ~950 cm^{-1} and ~450 cm^{-1} occur at lower frequency than in the Na_2O-SiO_2 glasses and fused silica. Significant shifts toward lower frequency occur as the Na_2O content is increased.

3. Frequency of the terminal Si-O stretching mode (~950 cm^{-1}) is more sensitive to added Na_2O than the SiO_2 bending modes are.

4. The effect of adding Na_2O on the Si-O terminal stretching mode (~950 cm^{-1}) is opposite to that found for the SiOSi and O-Si-O bending modes—decreasing frequency occurring for the stretching mode as the Na_2O content increases, and increasing frequency for the bending modes with an increase in Na_2O content.

5. For each absorption (20 and 25% TiO_4), the frequency vs SiO_2/Na_2O ratio curves intersect at ~2.

6. No evidence for TiO vibrations was obtained in this work.[17]

ACKNOWLEDGMENT

The authors acknowledge with thanks the technical assistance of Mr. Anthony Quattrochi of the United States Tobacco Company, 4325 N. Fifth Avenue, Chicago, Illinois.

1. E. H. Hamilton and G. W. Cleek, J. Res. Nat. Bur. Stand. **61**, No. 2, 89 (1958).
2. G. Bayer and W. Hoffmann, Glass Technol. **7**, No. 3, 94 (1966).
3. R. C. Turnbull and W. C. Lawrence, J. Am. Ceram. Soc. **35**, No. 2, 48 (1952).
4. M. D. Beals and J. H. Strimple, Glass Ind. **44**, 679 (1963).
5. C. Hirayama and D. Berg, Phys. Chem. Glasses **2**, No. 5, 145 (1961).
6. M. H. Manghnani, J. Am. Ceram. Soc. **55**, 360 (1972).
7. R. J. Charles, in *Progress in Ceramic Science*, J. E. Burke, Ed. (Pergamon Press, Elmsford, N. Y., 1961), Vol. 1, p. 1.
8. R. R. Shaw and D. R. Uhlmann, J. Non-Crystalline Solids **5**, 237 (1971).
9. M. H. Manghnani, to be submitted.
10. J. R. Ferraro, *Low Frequency Vibrations of Inorganic and Coordination Compounds* (Plenum Press, New York, 1971).
11. F. Gonzalez-Vilchez and W. P. Griffiths, J. Chem. Soc. Dalton 1416 (1972).
12. E. R. Lippincott, A. Van Valkenburg, C. E. Weir, and E. N. Bunting, J. Res. Nat. Bur. Stand. **61**, 61 (1958).
13. J. R. Ferraro, M. H. Manghnani, and A. Quattrochi, Phys. Chem. Glasses **13**, 116 (1972).
14. J. R. Ferraro and M. H. Manghnani, J. Appl. Phys. **43**, 4395 (1972).
15. J. R. Ferraro, L. J. Basile, and M. H. Manghnani, J. Appl. Phys. submitted for publication.
16. H. J. L. Trap and J. M. Stevels, Phys. Chem. Glasses **1**, No. 4, 107 (1968).
17. One of the referees of this paper commented on the recent Raman study [see M. C. Tobin and T. Baak, J. Opt. Soc. Am. **58**, 1459 (1968)], in which a related glass containing 10% titanium exhibited vibrations assigned to TiO motions. The reasons for the differences are not immediately apparent, but our glasses contain more Na_2O, and vibrations due to the latter effects could obscure any TiO vibrations.

EFFECTS OF COMPOSITION, PRESSURE, AND TEMPERATURE ON THE ELASTIC, THERMAL, AND ULTRASONIC ATTENUATION PROPERTIES OF SODIUM SILICATE GLASSES

By

Murli H. Manghnani

(HIG Contribution No. 598)

(To be published in: M. Kunigi, M. Tashiro, and N. Soga (eds.), Proceedings of the Xth International Congress on Glass, July 1974, Kyoto University, Kyoto, Japan.)

EFFECTS OF COMPOSITION, PRESSURE, AND TEMPERATURE ON THE ELASTIC, THERMAL, AND ULTRASONIC ATTENUATION PROPERTIES OF SODIUM SILICATE GLASSES

MANGHNANI, M.H., SINGH, B.K.
Hawaii Institute of Geophysics, University of Hawaii
Honolulu, Hawaii 96822 USA

INTRODUCTION

In the course of reviewing various thermal and elastic properties of glasses, it has been clearly shown (refs. 1-2) that two types of anomalous behavior exist in the vibrational properties of inorganic glasses. The first is related to abnormally low-frequency vibrational modes for which volume dependence of frequency (i.e., $d\omega/dV$) is positive, and includes anomalous properties such as negative thermal expansion coefficient, positive temperature derivative of elastic moduli and negative pressure derivative of elastic moduli, all of which are characteristic of the tetrahedral glasses like fused silica. The second type depends solely upon the low-frequency vibrational modes and includes properties such as large acoustic loss, excess specific heat, and low-frequency Raman scattering, all of which are characteristic of glassy state, in general. This paper reports on the elastic moduli, thermal expansion and acoustic loss in fused silica, and in seven sodium silicate glasses, as the function of composition, pressure, and temperature. Although several investigations on the elastic and thermal properties of alkali silicate glasses have been carried out (e.g., refs. 1, 3-6), virtually no data exist on ultrasonic attenuation in such glasses, except for some lower frequency, high-temperature data (ref. 22).

The elastic properties of simple silicate glasses in general depend on the density of the Si-O-Si bonds in the random network of silica. The addition of a network-modifier such as Na_2O results in a breakdown of some of those bonds and the formation of relatively weaker Si-O-Na bonds in proportion to the Na_2O added. In this manner, Charles (ref. 7) has shown that Young's modulus in the Na_2O-SiO_2 glass system decreases systematically with increase in Na_2O content.

It is of interest to study the changes in the anomalous behavior of tetrahedral silica-like glasses as they are progressively modified by the addition of Na_2O. The purpose of this study is to investigate the elastic, thermal, and ultrasonic attenuation properties of the glasses in the Na_2O-SiO_2 glass system in an effort to elucidate the structural changes in the random silica-based network, and the mechanism involved.

(*From:* Preprints, Tenth International Congress on Glass, No. 11, Strength (II) and Hardness. Viscoelasticity and Elasticity.)

HIG Contribution No. 598

EXPERIMENTAL TECHNIQUES

Fused silica (CGW code 7940), obtained from the Corning Glass Works, Corning, New York, and seven sodium silicate glasses, synthesized at the National Bureau of Standards, Washington, D.C., were used in this study. The chemical composition and annealing temperatures of the sodium silicate glasses are given in Table 1. Right circular cylinders, 1.25 cm long, were prepared from the glass samples for the velocity measurements as function of pressure (to 5 kbar at 298° K) and temperature (298-498° K at 1 bar); cylinders of approximately the same length but larger diameter (~2 cm) were used for the low-temperature (80-298° K) attenuation and velocity measurements, in order to minimize the errors of the side-wall effects in attenuation work. The end-faces of cylindrical specimens were paralleled to within 1 part in 10^4 parts, and polished flat to ±1/2 wavelength of sodium light.

The pulse superposition technique (ref. 8) was employed for studying the pressure and temperature dependence of ultrasonic velocities and, hence, of the moduli. X- and Y-cut quartz transducers, 0.65 cm diameter, having 20 MHz natural resonant frequency were used to generate compressional and shear waves in the specimen; 30 MHz transducers were used for attenuation measurement. The bonding materials between the specimen and transducer were: Dow-Corning 276-V9 resin for the pressure measurements at high pressure; HT-424 epoxy (manufactured by American Cyanamid Co.) at high temperatures (298-498° K); and 'Nonaq' stopcock grease (Fisher Scientific Co.) for the low-temperature velocity and attenuation measurements. The details of the ultrasonic equipment, the high-pressure and high-temperature apparatus, and the procedure for evaluating the pressure and temperature velocity data have been described previously (ref. 9). The basic experimental measurement was the pulse repetition frequency (PRF) of the carrier rf wave applied to the transducer attached to one plane-paralleled faces of the specimen. At the 'resonant' condition, ignoring the effects of the bond, the velocity is given by $v = 2f\ell$ where f is PRF rate (i.e., reciprocal of a round-trip delay time) and ℓ is length of the specimen. For evaluating velocities and moduli at high and low temperatures (above and below 298° K, respectively), corrections were applied for path-length changes, using the measured expansivity data (in the 298-498° range). The results, to be discussed later, are shown in Fig. 4.

The "modified" pulse-echo-overlap (ref. 10) was employed for making the low-temperature measurements of ultrasonic velocities and attenuation simultaneously, and liquid-N_2 dewer and the electronic equipment similar

to that given in ref. 10. The method allowed a continuous recording of attenuation with temperature, the resolution of measured attenuation values being 0.04 dB or better. The accuracy of the measured velocity is estimated to be .03% or better.

DISCUSSION OF RESULTS

1. Elastic Moduli at Ambient Conditions. The elastic parameter measurements for fused silica and the Na_2O-SiO_2 glasses at 20 MHz are listed in Table 1. The density of the Na_2O-SiO_2 glasses continuously increases

Table 1

Composition, and elastic and thermal properties of fused silica and Na_2O-SiO_2 glasses at ambient conditions

Glass No.	Composition, mole % SiO_2	Composition, mole % Na_2O	Annealing temp., °C	$\bar{M}$, g	ρ, g/cm³	V_p, km/sec	V_s, km/sec	θ_D, °K	C_v, cal/g.deg	$\gamma_{vol} \times 10^5$, deg⁻¹	K_S, kbar	γ_{th}	γ_{RT}
Fused silica (7940)	100	0	1,020	20.02	2.202	5.941	3.764	498.7	0.2597	0.183	361.2	0.019	-2.37
K110	90	10	575	20.08	2.288	5.565	3.478	467.0	0.2632	1.236	338.8	0.166	-1.35
K111	85	15	540	20.11	2.316	5.457	3.355	453.9	0.2643	2.139	344.6	0.285	-0.81
K112	80	20	520	20.14	2.383	5.382	3.251	443.2	0.2654	2.863	354.5	0.382	-0.35
K113	75	25	510	20.18	2.431	5.347	3.159	434.3	0.2660	3.248	370.5	0.445	0.17
K114	70	30	495	20.21	2.474	5.348	3.101	429.4	0.2664	3.638	389.6	0.511	0.49
K115	65	35	475	20.24	2.495	5.361	3.038	422.4	0.2665	4.191	410.0	0.616	0.77
K116	60	40	450	20.27	2.520	5.401	2.993	418.1	0.2666	4.393	430.6	0.676	1.07

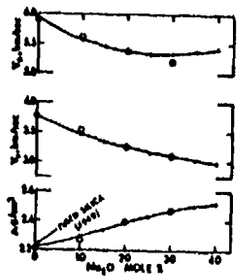

Fig. 1 Density, V_s and V_p as function of Na_2O content. Open circles represent unpublished data of Kurkjian and Krause.

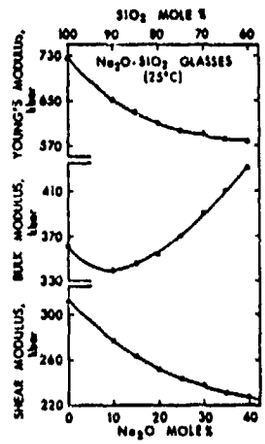

Fig. 2

Composition dependence of the elastic moduli.

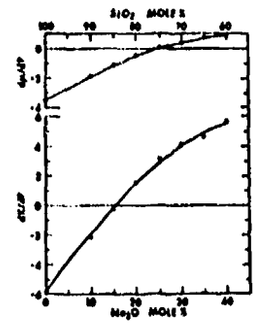

Fig. 3

dK/dP and dμ/dP versus Na_2O content.

with increasing Na_2O content, however, the velocities of both the compressional (V_p) and shear (V_s) waves decrease. Good agreement is found with the unpublished velocity data of Krause and Kurkjian (personal communication, 1974), as seen in Fig. 1. The present data indicate a minimum in V_p near 25 mole % Na_2O composition; thereafter V_p seems to increase with increasing Na_2O content. Fig. 2 shows the composition dependence of shear (μ), bulk (K), and Young's (E) moduli. Both μ and E decrease nonlinearly but systematically with increasing Na_2O content; K modulus in fused silica appears at first to decrease when Na_2O is added but, above 10-12 mole % Na_2O), it continuously increases. These results show that the role of added Na^+ is twofold: (1) the ions fill-in the void space in silica structure; and (2) they modify the Si-O-Si bonds, forming weaker Si-O-Na bonds in proportion to the amount of Na_2O added and causing moduli to decrease (ref. 7).

2. Pressure and Temperature Dependence of Elastic Moduli. The pressure dependence of the elastic moduli of Na_2O-SiO_2 glasses is found to be linear, within experimental error, in the pressure range of this study (5 kbar). Lower soda-content glasses appear more anomalous (i.e., dK/dP and $d\mu/dP$ are both more negative); the anomalous behavior systematically decreases (i.e., becomes less negative) with increase in Na_2O content (fig. 3). At lower Na_2O content ($\leq$ 20 mole %), the values of dK/dP and $d\mu/dP$ change more rapidly with composition than at higher content (> 20 mole %). From Fig. 3, dK/dP and $d\mu/dP$ are zero for glasses containing approximately 16 and 25 mole % Na_2O, respectively.

The results of the temperature dependence of fractional velocities, $(V_p)_T/(V_p)_{298}$ and $(V_s)_T/(V_s)_{298}$, and of shear modulus are shown in Figs. 4 and 5, respectively. Except for glasses K110 and K111 (containing

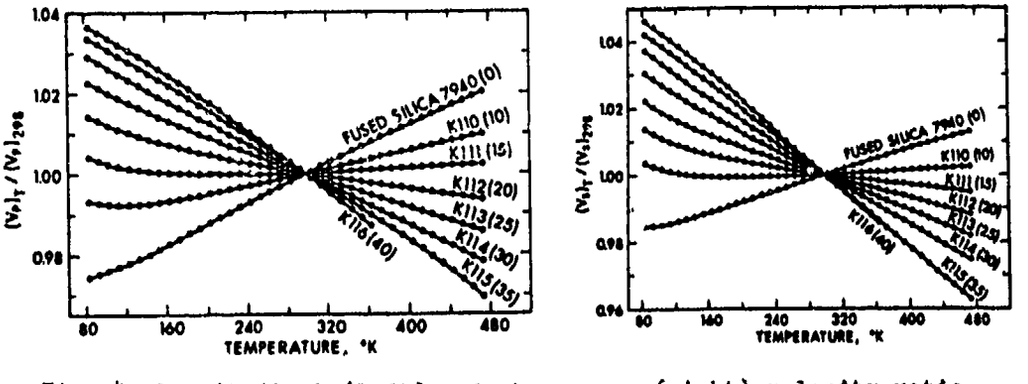

Fig. 4 Longitudinal- (left) and shear-wave (right) velocity ratio versus temperature. The values in parentheses represent Na_2O mole %.

10 and 15 mole % Na_2O, respectively), the temperature dependence of V_p (above 298° K) in all of the others is normal (i.e., negative temperature derivatives); for V_s, only K110 shows anomalous behavior (i.e., positive temperature derivative). The values of dK/dT and dμ/dT from both the high- and low-temperature measurements at 298° K are in good agreement (Fig. 6).

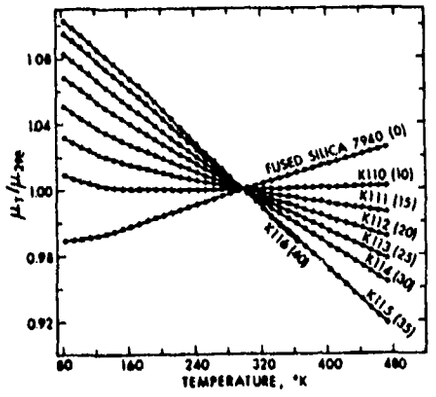

Fig. 5 Shear modulus ratio versus temperature.

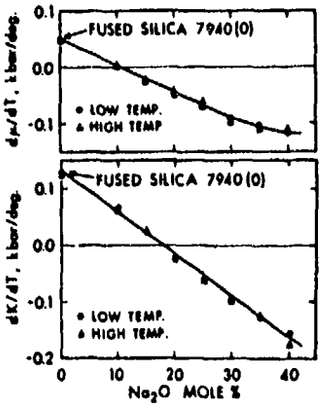

Fig. 6 dK/dT and dμ/dT versus Na_2O content.

Here it is again noted that the degree of anomalous behavior (positive dK/dT and dμ/dT) decreases with addition of Na_2O. The composition dependence of dK/dT is linear; but that of dμ/dT is somewhat nonlinear, at least for higher Na_2O content.

In the course of a study of the acoustic spectra of Na_2O-GeO_2 glasses (ref. 11), it was pointed out that a 30% Na_2O-70% GeO_2 glass shows low-temperature thermal relaxation at ∿125° K. The low-temperature results in Figs. 4 and 5, showing reversals in the anomalous behavior of fused silica and the K111 and K112 glasses, also indicate such thermal relaxation. The minima in the velocity and modulus (around ∿120° K), caused by the thermal relaxation, is seen to shift to higher temperatures with increase in the Na_2O content; also, the magnitude of thermal relaxation decreases, as indicated by increasing linearity of the curves, with increasing Na_2O content.

3. Grüneisen Parameters. The thermal Grüneisen parameters, $\gamma_{th} = \alpha_V K_s/\rho C_p = \alpha_V K_T/\rho C_v$, were evaluated using measured α_V, K_s and ρ values, and calculated C_v values; the latter were obtained from the Debye theory (ref. 12). Values of Debye temperature (θ_D), C_v, and γ_{th} are given in Table 1. The γ_{th} values systematically increase with increase in Na_2O

content (fig. 7) which systematic increase is also reflected in the

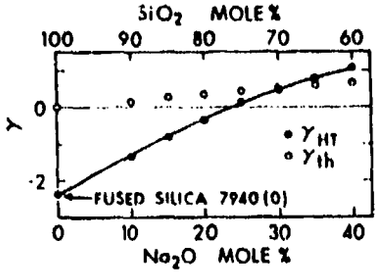

Fig. 7 γ_{th} and γ_{HT} as functions of Na_2O content.

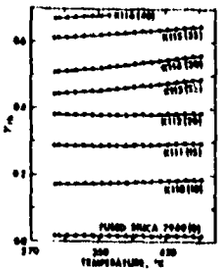

Fig. 8 γ_{th} as function of temperature.

pressure and temperature derivative values. The high-temperature limiting values of mode Grüneisen parameter, γ_{HT}, can be evaluated from pressure dependence of velocities (ref. 13). The values of γ_{HT} increase more rapidly than γ_{th} does with increasing Na_2O content (fig. 7). Although the γ_{HT} values are negative and larger than the γ_{th} values, both Grüneisen parameters increase when Na_2O is added to the silica structure.

Temperature dependence of γ_{th} in the range of 298-498° K is shown in Fig. 8. In fused silica and the lower soda-content glasses, the γ_{th} value is more or less temperature-invariant. For higher soda-content glasses, γ_{th} increases more rapidly with temperature.

4. Ultrasonic Attenuation. Large ultrasonic attenuation occurs in simple inorganic oxide glasses such as SiO_2, GeO_2, B_2O_3, and As_2O_3 at various temperatures in the range from ∿50° to ∿250° K (refs. 14-21). Anderson and Bömmel (ref. 14) proposed a structural relaxation mechanism to explain the attenuation spectrum for fused silica at low temperatures. According to them, thermally activated lateral shifting of an oxygen atom between two equivalent equilibrium positions, perpendicular to the Si-O-Si bond, is a source of structural relaxation which also explains the negative thermal expansion and excess specific heat anomalies at low temperatures in fused silica. An alternate mechanism, which involves the movement of the oxygen atom in the direction of the Si-O-Si bond rather than perpendicular to it, has been proposed in a two-bond-length model (refs. 15-16).

Compared to the amount of work on fused silica, very little work has been done on the study of relaxational processes in sodium silicate glasses except at low frequencies (.01 and 10 Hz) where the attenuation occurs due to ionic migration of Na^+ (refs. 17, 22) and possibly oxygen ions (refs. 22-24). The Na^+-migration relaxation is a stress-induced phenomenon, resolvable at frequencies of the order of KHz.

Figures 9 and 10 show the composition dependence of longitudinal and

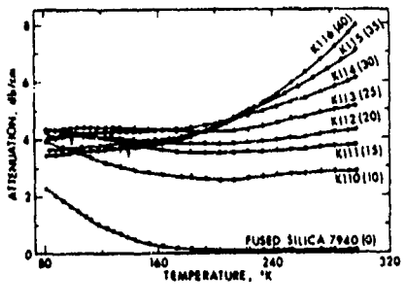

Fig. 9
Temperature dependence of attenuation (longitudinal mode).

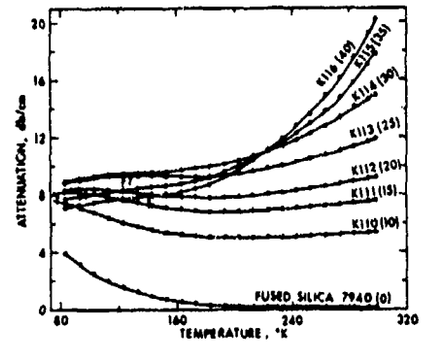

Fig. 10
Temperature dependence of attenuation (shear mode).

shear attenuation at 30 MHz, respectively, for the Na_2O-SiO_2 glasses at ambient conditions. As seen, the attenuation due to shear-wave propagation is approximately twice that due to longitudinal-wave propagation, which supports the previous conclusion (ref. 19) that the loss is in large part sensitive to shear distortion. The temperature dependence of longitudinal and shear ultrasonic attenuation are plotted in Fig. 11. The

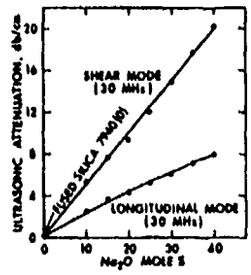

Fig. 11 Ultrasonic attenuation as function of Na_2O content.

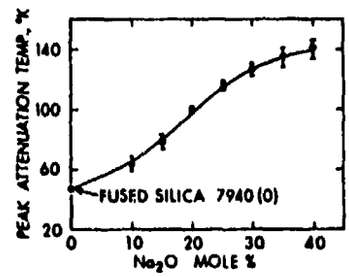

Fig. 12 Peak attenuation temperature versus Na_2O content.

present 30 MHz attenuation data for fused silica are in good qualitative agreement with previous 20 MHz data (ref. 14, 16, 21) with respect to the shape of the attenuation-temperature curve, although our attenuation values at 30 MHz are larger. Figures 9 and 10 show increasing broadening of the attenuation peaks with increasing concentration of Na_2O. This is probably due either to thermal broadening (ref. 14) or to a wider distribution of activation energy; the width of the loss peak (e.g., in fused silica; refs. 14, 16) has been interpreted in light of the distribution of activation energy. Alternately, the broadening could also be due to the superposition of the high temperature Na^+-migration relaxation on the structural relaxation, at least, for the low-silica glasses.

One of the most interesting findings of this study is the shifting of the peak attenuation temperature (in the low-temperature range) with increasing Na_2O content; the peak attenuation temperature for each glass is indicated by an arrow (figs. 9 and 10). Because of the broadness of the attenuation curves, there is significant uncertainty in determining the peak temperatures. Also, since the peak attenuation temperatures for glasses K110 and K111 would fall below 80° K--outside the temperature range of this study--the peak attenuation temperatures for these glasses were estimated by extrapolating the attenuation versus temperature curves (Figs. 9 and 10); hence the relationship shown in Fig. 12 is subject to further uncertainty.

However, compared to the peak attenuation temperature of 47° K for fused silica (refs. 14, 16), the peaks for the Na_2O-SiO_2 glasses certainly appear to be composition-dependent. Since the peak attenuation temperature increases with increase in the Na_2O content, the effect of adding Na_2O to SiO_2 is opposite that of adding Na_2O to GeO_2 (ref. 11), although there are structural similarities between fused SiO_2 and GeO_2 (both glasses have tetrahedral structures).

For the low-temperature structural relaxation mechanism, such as that present in fused silica (ref. 14) and presumably also in the Na_2O-SiO_2 glasses, it would be of interest to compute from the frequency-dependence of the peak attenuation temperatures the most probable activation energies for different concentrations of Na_2O. However, as attenuation data at different frequencies are not yet available for these glasses, no attempt can be made to calculate the activation energies for these glasses (for fused silica, activation energy is ∿1030 cal/mole; ref. 14). However, from the shift of the peaks to higher temperatures (Fig. 12), it is suggested that in some systematic fashion the activation energy increases with Na_2O, contrary to that found for the Na_2O-GeO_2 system (ref. 11). Although the high-temperature Na^+ relaxation (>250° K) seems to obscure the low-temperature side of the attenuation curve, at least, for higher Na_2O content glasses, it is clearly inferred from the magnitudes of attenuation curves of the Na_2O-SiO_2 glasses (figs. 9 and 10) that the magnitude of attenuation, and thereby relaxation strength, decreases with increasing Na_2O. As a phenomenon, this behavior can be interpreted on the basis of a structural model in which the Na_2O molecule modifies the existing Si-O-Si bonding sites. This modification may result in the formation of a weaker Si-O-Na bond or an unbridged Si-O- bond. The former would impede the movement of the oxygen atoms, and since movement of the oxygen atom is the cause of attenuation this would result in decrease in the attenuation, accompanied by the increase in the activation energy as revealed by the

shifting of the attenuation peak to higher temperatures. The latter modification would, however, make no contribution to attenuation. In other words, a loosening of structure occurs with the addition of soda, which is in agreement with the low frequency internal friction work (ref. 22).

In high-soda glasses, at 30 MHz, one would expect to find Na^+ relaxation at temperatures above room temperature. Near room temperature (Figs. 10 and 11), the temperature-dependence of both longitudinal and shear attenuation increases with increasing Na_2O. The effect of composition on the internal friction at much lower frequencies (.01-Hz) for Na_2O-SiO_2 glasses studied by Forry (ref. 22) shows a decrease both in intensity and peak temperature as Na_2O content increases. In light of this and our results, it may be concluded that the expected high-temperature attenuation peak is shifting toward lower temperatures with increasing Na_2O. A similar shift in Na^+ relaxation temperatures has also been observed in the Na_2O-GeO_2 glasses (ref. 11). This type of high-temperature relaxation requires large activation energy compared to low-temperature structural relaxation. It is desirable to investigate further the composition dependence of Na^+ relaxation at high temperatures and low frequencies in other types of glasses.

5. Summary

a. Elastic moduli of Na_2O-SiO_2 glasses and their pressure and temperature derivatives vary systematically with composition. Increasing Na_2O content results in decrease of μ and E moduli. K modulus first decreases ($\sim$10% Na_2O) and then increases with increase in Na_2O. Low-soda glasses exhibit anomalous behavior under pressure and temperature. The degree of anomalous behavior decreases with increasing Na_2O, i.e., the pressure derivatives of moduli increase and the temperature derivatives decrease with increase in Na_2O.

b. The Grüneisen parameters γ_{th} and γ_{HT} increase with Na_2O. The disparity between the γ_{th} and γ_{HT} values decreases as Na_2O increases; at 70 mole % Na_2O glass composition, the two values are the same. γ_{th} increases with temperature; the temperature dependence of γ_{th} increases with increase in Na_2O.

c. At room temperature, shear-wave attenuation at 30 MHz is larger ($\sim$2 times) than the longitudinal-wave attenuation; both types of losses, however, increase with Na_2O.

d. The low-temperature attenuation peak (due to structural relaxation) observed in fused silica at $\sim$47° K is also found in Na_2O-SiO_2 glasses. The peak attenuation temperature is found to increase with increase in Na_2O,

indicating that the activation energy is increasing with Na_2O, contrary to what has been previously reported for Na_2O-GeO_2 glasses (ref. 11). The attenuation-temperature curves at these low temperatures show a reversed relationship compared to that found at room temperature, i.e., the attenuation peak height decreases with increasing Na_2O. Explanation is offered in terms of the formation of Si-O-Na bonds, which are weaker than Si-O-Si bonds.

6. Acknowledgments

The authors are greatly indebted to Drs. Krause and Kurkjian of Bell Laboratories, Murray Hill, New Jersey, for their unpublished results, and for many helpful suggestions on this study. Thanks are due Dr. G.W. Cleek for the help and advice in making the glasses. The support for this research was provided by the Office of Naval Research, contract N00014-67-A-0387-0012, NR 032-527. Hawaii Institute of Geophysics Contribution 598.

REFERENCES

1. Kurkjian, C.R., Krause, J.T., J. Am. Ceram. Soc., 54, 226 (1968).
2. Kurkjian, C.R., Krause, J.T., McSkimin, H.J., Andreatch, P., Bateman, T.B., in Amorphous Materials, edited by R.W. Douglas and B. Ellis, 463-473. Wiley-Interscience, New York, 1972.
3. Shaw, R.R., Uhlmann, D.R., J. Non-Cryst. Solids, 5, 237 (1971).
4. Krüger, J., Phys. Chem. Glasses, 13, 9 (1972).
5. Manghnani, M.H., Rai, C.S., Bull. Amer. Ceram. Soc., 52, 390 (1973).
6. Ferraro, J.R., Manghnani, M.H., J. Appl. Phys., 43, 4595 (1972).
7. Charles, R.J., in Progress in Ceramic Science, 1, 1-38, edited by J.E. Burke. Pergamon Press, New York, 1961.
8. McSkimin, H.J., J. Acoust. Soc. Amer., 33, 12 (1961).
9. Manghnani, M.H., J. Amer. Ceram. Soc., 55, 360 (1972).
10. Chung, D.H., Silversmith, D.J., Chick, B.B., Rev. Sci. Instr., 40, 718 (1969).
11. Kurkjian, C.R., Krause, J.T., J. Amer. Ceram Soc., 49, 134 (1966).
12. Anderson, O.L., J. Phys. Chem. Solids, 12, 41 (1959).
13. Schuele, D.E., Smith, C.S., J. Phys. Chem. Solids, 25, 801 (1964).
14. Anderson, O.L., Bömmel, H.E., J. Amer. Ceram. Soc., 38, 125 (1955).
15. Strakna, R.E., Phys. Rev., 121, 2020 (1961).
16. Strakna, R.E., Savage, H.T., J. Appl. Phys., 35, 1445 (1964).
17. Marx, J.W., Silversten, J.M., J. Appl. Phys., 24, 81 (1953).
18. Fine, M.E., Van Duyne, H., Kenney, N.T., J. Appl. Phys., 25, 402 (1954).
19. McSkimin, H.J., J. Appl. Phys., 24, 988 (1953).

20. Krause, J.T., Kurkjian, C.R., J. Amer. Ceram. Soc., 51, 226 (1968).
21. Krause, J.T., J. Appl. Phys., 42, 3035 (1971).
22. Forry, K.E., J. Amer. Ceram. Soc., 40, 90 (1957).
23. Hopkins, I.L., Kurkjian, C.R., in Physical Acoustics, 2B, 91-163, edited by W.P. Mason. Academic Press, New York (1965).
24. Mohyuddin, I., Douglas, R.W., Phys. Chem. Glasses, 1, 71 (1960).

Unclassified

SECURITY CLASSIFICATION OF THIS PAGE (When Data Entered)

REPORT DOCUMENTATION PAGE

READ INSTRUCTIONS BEFORE COMPLETING FORM

1. REPORT NUMBER	2. GOVT ACCESSION NO. / 3. RECIPIENT'S CATALOG NUMBER
4. TITLE (and Subtitle): Pressure and Temperature Studies of Glass Properties Related to Vibrational Spectra	5. TYPE OF REPORT & PERIOD COVERED: Final Report, 1 Feb. 1971 to 31 Dec. 1974
	6. PERFORMING ORG. REPORT NUMBER: HIG-74-11
7. AUTHOR(s): Murli H. Manghnani	8. CONTRACT OR GRANT NUMBER(s): N00014-67-A-0387-0012
9. PERFORMING ORGANIZATION NAME AND ADDRESS: University of Hawaii, Hawaii Institute of Geophysics, Honolulu, Hawaii 96822	10. PROGRAM ELEMENT, PROJECT, TASK AREA & WORK UNIT NUMBERS: NR 032-527
11. CONTROLLING OFFICE NAME AND ADDRESS	12. REPORT DATE: December 1974
	13. NUMBER OF PAGES
14. MONITORING AGENCY NAME & ADDRESS(if different from Controlling Office): Department of the Navy (Code 471), Office of Naval Research, Metallurgy Program, 800 Quincy Street, Arlington, Virginia 22217	15. SECURITY CLASS. (of this report): Unclassified
	15a. DECLASSIFICATION/DOWNGRADING SCHEDULE

16. DISTRIBUTION STATEMENT (of this Report)

17. DISTRIBUTION STATEMENT (of the abstract entered in Block 20, if different from Report)

Distribution of this document is unlimited.
Reproduction in whole or in part is permitted for any purpose of the United States government.

18. SUPPLEMENTARY NOTES

19. KEY WORDS (Continue on reverse side if necessary and identify each number)

Glasses
Elasticity
Infrared Absorption
Pressure Effects
Temperature Effects
Vibrational Spectra

20. ABSTRACT (Continue on reverse side if necessary and identify by block number)

This report concerns the $M_2^{I}O$-SiO_2^{IV} and SiO_2-TiO_2 glass systems.

Elastic, thermal and infrared absorption characteristics of nineteen simple binary $M_2^{I}O$-SiO_2 glasses, where M is Li, Na or K, have been studied at ambient conditions as well as function of pressure and temperature. M_2O content of these glasses ranges from 10 to 45 mole %. Elastic moduli were investigated to 5 kbar and to 300°C, thermal expansivity to 300°C, and infrared absorption to 58.8 kbar. (cont'd.)

DD FORM 1 JAN 73 1473 EDITION OF 1 NOV 65 IS OBSOLETE
S/N 0102-014-6601

Unclassified

SECURITY CLASSIFICATION OF THIS PAGE (When Data Entered)

20. ABSTRACT (cont'd.) (p 1473A)

The elastic properties of the M_2O-SiO_2 glasses vary systematically with composition. Addition of M_2O to SiO_2 structure causes increase in bulk modulus (K) of all the glasses, decrease in shear (μ) and Young's moduli (E) of all but the Li_2O-SiO_2 glasses, and increase in Poisson's ratio. Low M_2O glasses show anomalous elastic behavior under pressure, that is, dM/dP, where M is any modulus, is negative. The values of dM/dP increase linearly with M_2O content. Likewise dM/dT for the M_2O-SiO_2 glasses decreases with M_2O content.

Effect of phase separation on the elastic properties is not significant; however, their temperature dependence is sensitive to phase separation.

Ultrasonic longitudinal (α_p) and shear (α_s) wave attenuation are found to be linearly proportional to frequency. Both α_p and α_s increase with M_2O content; α_p/α_s ratio varies from 2 to 2.6.

The low-temperature attenuation peak found in fused silica at (approximately) 47°K broadens and shifts to higher temperature with increase in M_2O content. Implication of this is discussed in terms of transverse oxygen vibrations.

Coefficient of the thermal expansion (α_ℓ) of M_2O-SiO_2 glasses increases in the order: K_2O-SiO_2 > Na_2O-SiO_2 > Li_2O-SiO_2 glasses, and increases with increase in M_2O content. The α_ℓ is found to vary quadratically with temperature.

Elastic properties of SiO_2-TiO_2 glasses containing up to ~10% TiO_2, investigated to 5 kbar and 300°C, show that annealing causes density and V_s to increase, and V_p to decrease. The elastic properties of the annealed glasses vary systematically and more or less linearly with composition. Due to the weakening of structure, all the moduli decrease. Addition of TiO_2 also causes the glasses to become more anomalous under pressure and temperature (dM/dP and dM/dT become more negative and more positive, respectively). This behavior, consistent with the thermal expansion data, appears to be caused by increasing openness of the structure.

1473B

DISTRIBUTION LIST

Organization

Office of Naval Research
Department of the Navy
Attn: Code 471
Arlington, Virginia 22217

Director
Office of Naval Research
Branch Office
495 Summer Street
Boston, Massachusetts 02210

Commanding Officer
Office of Naval Research
New York Area Office
207 West 24th Street
New York, New York 10011

Director
Office of Naval Research
Branch Office
219 South Dearborn Street
Chicago, Illinois 60604

Director
Office of Naval Research
Branch Office
1030 East Green Street
Pasadena, California 91101

Commanding Officer
Office of Naval Research
San Francisco Area Office
50 Fell Street
San Francisco, California 94102

Commanding Officer
Naval Weapons Laboratory
Attn: Research Division
Dahlgren, Virginia 22448

Organization

Director
Naval Research Laboratory
Attn: Technical Information Officer
Code 2000
Washington, D. C. 20390

Director
Naval Research Laboratory
Attn: Technical Information Officer
Code 2020
Washington, D. C. 20390

Director
Naval Research Laboratory
Attn: Technical Information Officer
Code 6000
Washington, D. C. 20390

Director
Naval Research Laboratory
Attn: Technical Information Officer
Code 6100
Washington, D. C. 20390

Director
Naval Research Laboratory
Attn: Technical Information Officer
Code 6300
Washington, D. C. 20390

Director
Naval Research Laboratory
Attn: Technical Information Officer
Code 6400
Washington, D. C. 20390

Director
Naval Research Laboratory
Attn: Library
Code 2029 (ONRL)
Washington, D. C. 20390

Commander
Naval Air Systems Command
Department of the Navy
Attn: Code AIR 320A
Washington, D. C. 20360

Commander
Naval Air Systems Command
Department of the Navy
Attn: Code AIR 5203
Washington, D. C. 20360

Commander
Naval Ordnance Systems Command
Department of the Navy
Attn: Code ORD 033
Washington, D. C. 20360

Commanding Officer
Naval Air Development Center
Aeronautical Materials Div.
Johnsville
Attn: Code MAM
Warminster, Pa. 18974

Commanding Officer
Naval Ordnance Laboratory
Attn: Code 210
White Oak
Silver Spring, Maryland 20910

Commander
Naval Ship Systems Command
Department of the Navy
Attn: Code 0342
Washington, D. C. 20360

Commanding Officer
Naval Civil Engineering Laboratory
Attn: Code L70
Port Hueneme, California 93041

Commander
Naval Ship Engineering Center
Department of the Navy
Attn: Code 6101
Washington, D. C. 20360

Naval Ships R&D Laboratory
Annapolis Division
Attn: Code A800
Annapolis, Maryland 21402

Commanding Officer
Naval Ships R&D Center
Attn: Code 747
Washington, D. C. 20007

U. S. Naval Postgraduate School
Attn: Department of Chemistry
and Material Science
Monterey, California 93940

Commander
Naval Weapons Center
Attn: Code 5560
China Lake, California 93555

Commander
Naval Underseas Warfare Center
Pasadena, California 92152

Scientific Advisor
Commandant of the Marine Corps
Attn: Code AX
Washington, D. C. 20380

Commanding Officer
Army Research Office, Durham
Box CM, Duke Station
Attn: Metallurgy & Ceramics Div.
Durham, North Carolina 27706

Office of Scientific Research
Department of the Air Force
Attn: Solid State Div. (SRPS)
Washington, D. C. 20333

Defense Documentation Center
Cameron Station
Alexandria, Virginia 22314

National Bureau of Standards
Attn: Metallurgy Division
Washington, D. C. 20234

National Bureau of Standards
Attn: Inorganic Materials Div.
Washington, D. C. 20234

Atomic Energy Commission
Attn: Metals & Materials Branch
Washington, D. C. 20545

Argonne National Laboratory
Metallurgy Division
P. O. Box 299
Lemont, Illinois 60439

Brookhaven National Laboratory
Technical Information Division
Attn: Research Library
Upton, Long Island, New York 11973

Library
Bldg. 50, Room 134
Lawrence Radiation Laboratory
Berkeley, California 94720

Los Alamos Scientific Laboratory
P. O. Box 1663
Attn: Report Librarian
Los Alamos, New Mexico 87544

Commanding Officer
Army Materials and Mechanics
Research Center
Attn: Res. Programs Office (AMXMR-P)
Watertown, Massachusetts 02172

Director
Metals & Ceramics Division
Oak Ridge National Laboratory
P. O. Box X
Oak Ridge, Tennessee 37830

Commanding Officer
Naval Underwater Systems Center
Newport, Rhode Island 02844

Aerospace Research Laboratories
Wright-Patterson AFB
Building 450
Dayton, Ohio 45433

Defense Metals Information Center
Battelle Memorial Institute
505 King Avenue
Columbus, Ohio 43201

Army Electronics Command
Evans Signal Laboratory
Solid State Devices Branch
c/o Senior Navy Liaison Officer
Fort Monmouth, New Jersey 07703

Commanding General
Department of the Army
Frankford Arsenal
Attn: ORDBA-1320, 64-4
Philadelphia, Pennsylvania 19137

Executive Director
Materials Advisory Board
National Academy of Sciences
2101 Constitution Avenue, N. W.
Washington, D. C. 20418

NASA Headquarters
Attn: Code RRM
Washington, D. C. 20546

Air Force Materials Lab
Wright-Patterson AFB
Attn: MAMC
Dayton, Ohio 45433

Air Force Materials Lab
Wright-Patterson AFB
Attn: MAAM
Dayton, Ohio 45433

Deep Submergence Systems Project
Attn: DSSP-00111
Washington, D. C. 20360

Advanced Research Projects Agency
Attn: Director, Materials Sciences
Washington, D. C. 20301

Army Research Office
Attn: Dr. T. E. Sullivan
3045 Columbia Pike
Arlington, Virginia 22204

Department of the Interior
Bureau of Mines
Attn: Science & Engineering Advisor
Washington, D. C. 20240

Defense Ceramics Information Center
Battelle Memorial Institute
505 King Avenue
Columbus, Ohio 43201

National Aeronautics & Space Adm.
Lewis Research Center
Attn: Librarian
21000 Brookpark Rd.
Cleveland, Ohio 44135

Naval Missile Center
Materials Consultant
Code 3312-1
Point Mugu, California 93041

Commanding Officer
Naval Weapons Center Corona Labs.
Corona, California 91720

Commander
Naval Air Test Center
Weapons Systems Test Div. (Code 01A)
Patuxent River, Maryland 20670

Director
Ordnance Research Laboratory
P. O. Box 30
State College, Pennsylvania 16801

Director
Applied Physics Laboratory
Johns Hopkins University
8621 Georgia Avenue
Silver Spring, Maryland 20901

Director
Applied Physics Laboratory
1013 Northeast Fortieth St.
Seattle, Washington 98105

Materials Sciences Group
Code S130.1
271 Catalina Boulevard
Navy Electronics Laboratory
San Diego, California 92152

Dr. Waldo K. Lyon
Director, Arctic Submarine Laboratory
Code 90, Building 371
Naval Undersea R&D Center
San Diego, California 92132

Dr. R. Nathan Katz
Ceramics Division
U.S. Army Materials & Mechanics
Research Center
Watertown, Mass. 02172

SUPPLEMENTARY DISTRIBUTION LIST

Professor R. Roy
Materials Research Laboratory
Pennsylvania State University
University Park, Pennsylvania 16802

Professor D. H. Whitmore
Department of Metallurgy
Northwestern University
Evanston, Illinois 60201

Professor J. A. Pask
Department of Mineral Technology
University of California
Berkeley, California 94720

Professor D. Turnbull
Div. of Engineering and Applied Science
Harvard University
Pierce Hall
Cambridge, Massachusetts 02100

Dr. T. Vasilos
AVCO Corporation
Research and Advanced Development Div.
201 Lowell Street
Wilmington, Massachusetts 01887

Dr. H. A. Perry
Naval Ordnance Laboratory
Code 230
Silver Spring, Maryland 20910

Dr. Paul Smith
Crystals Branch, Code 6430
Naval Research Laboratory
Washington, D. C. 20390

Dr. A. R. C. Westwood
RIAS Division
Martin-Marietta Corporation
1450 South Rolling Road
Baltimore, Maryland 21227

Prof. M. H. Manghnani
University of Hawaii
Hawaii Institute of Geophysics
2525 Correa Road
Honolulu, Hawaii 96822

Dr. R. H. Doremus
General Electric Corporation
Metallurgy and Ceramics Lab.
Schenectady, New York 12301

Professor G. R. Miller
Department of Ceramic Engineering
University of Utah
Salt Lake City, Utah 84112

Dr. Philip L. Farnsworth
Materials Department
Battelle Northwest
P. O. Box 999
Richland, Washington 99352

Mr. G. H. Haertling
Ceramic Division
Sandia Corporation
Albuquerque, New Mexico 87101

Mr. I. Berman
Army Materials and Mechanics
Research Center
Watertown, Massachusetts 02171

Dr. F. F. Lange
Westinghouse Electric Corporation
Research Laboratories
Pittsburgh, Pennsylvania 15235

Professor H. A. McKinstry
Pennsylvania State University
Materials Research Laboratory
University Park, Pa. 16802

Professor T. A. Litovitz
Physics Department
Catholic University of America
Washington, D. C. 20017

Dr. R. J. Stokes
Honeywell Corporate Research Center
10701 Lyndale Avenue South
Bloomington, Minnesota 55420

Dr. W. Haller
Chief, Inorganic Glass Section
National Bureau of Standards
Washington, D.C. 20234

Dr. Harold Liebowitz
Dean of Engineering
George Washington University
Washington, D. C. 20006

Dr. H. Kirchner
Ceramic Finishing Company
P. O. Box 498
State College, Pennsylvania 16801

Professor A. H. Heuer
Case Western Reserve University
University Circle
Cleveland, Ohio 44106

Dr. D. E. Niesz
Battelle Memorial Institute
505 King Avenue
Columbus, Ohio 43201

Dr. F. A. Kroger
University of Southern California
University Park
Los Angeles, California 90007

Dr. Sheldon M. Wiederhorn
National Bureau of Standards
Inorganic Materials Division
Washington, D.C. 20234

Dr. C. O. Hulse
United Aircraft Research Labs
United Aircraft Corporation
East Hartford, Connecticut 06108

Dr. Stephen Malkin
Department of Mechanical Engineering
University of Texas
Austin, Texas 78712

Prof. H. E. Wilhelm
Department of Mechanical Engineering
Colorado State University
Fort Collins, Colorado 80521

Stanford University
Dept. of Materials Sciences
Stanford, California 94305

Dr. R. K. MacCrone
Department of Materials Engineering
Rensselaer Polytechnic Institute
Troy, New York 12181

Dr. D. C. Mattis
Belfer Graduate School of Science
Yeshiva University
New York, New York 10033

Professor R. B. Williamson
College of Engineering
University of California
Berkeley, California 94720

Professor R. W. Gould
Department of Metallurgical
and Materials Engineering
College of Engineering
University of Florida
Gainesville, Florida 32601

Professor V. S. Stubican
Department of Materials Science
Ceramic Science Section
Pennsylvania State University
University Park, Pennsylvania 16802

Dr. R. C. Anderson
General Electric R and D Center
P. O. Box 8
Schenectady, New York 12301

Dr. Bert Zauderer
MHD Program, Advanced Studies
Room L-9513 - VFSC
General Electric Company
P. O. Box 8555
Philadelphia, Penna. 19101

Prof. C. F. Fisher, Jr.
Department of Mechanical and Aero-
space Engineering
University of Tennessee
Knoxville, Tennessee 37916